LOW PRESSURE MEASUREMENT TECHNIQUES

HERBERT A. PAINTER

FOREWORD

This development project was performed by Electro-Optical Systems, Inc., Pasadena, California, under USAF Contract No. AF 33(615)-1838. The work was supervised and this report was prepared by Herbert A. Painter, Project Engineer. The contract was initiated under Project 1469, "Vehicle Loads Validation," Task No. 146907, "Advanced Technology for Data Sensing." The work described in this document was authorized by and completed under the auspices of the Air Force Flight Dynamics Laboratory, Research and Technology Division, with Mr. Lawrence A. Moorman as Project Engineer.

This report covers work conducted from June 1964 to December 1965.

This Manuscript was released by the authors in January 1966 for publication as a RTD Technical Report.

This technical report has been reviewed and is approved.

James C. Horsley Jr.

JAMES C. HORSLEY, JR.
Major, USAF
Chief, Experimental Mechanics Branch

ABSTRACT

This project was initiated to develop four prototype pressure transducers in the range of 0.0 to 0.1 psia for the AF Flight Dynamics Laboratory. The design selected makes use of a convoluted diaphragm force collector to drive a cantilever beam. A semiconductor strain gage bridge bonded to the beam converts the force to an electrical signal which is amplified to provide a 0 to 5V dc output. The results presented demonstrate achievement of essentially all requirements, save high-temperature transient performance. It is apparent from the results of this project that an accurate 0.0 to 0.1 psia transducer of low weight and reasonably high natural frequency can be produced. Achievement of higher operating temperature and natural frequency is possible. Further work to accomplish this is recommended.

CONTENTS

CONTENTS (contd)

ILLUSTRATIONS

ILLUSTRATIONS (contd)

TABLES

1. INTRODUCTION

This project was initiated to design and produce a transducer capable of measurements in the range of 0.0 to 0.1 psia (see Fig. 1). Discussion concerns the design and development of four prototypes and is divided into two sections: Technical Discussion, and Materials and Processes. Additionally, supporting information including test data is provided in the appendixes.

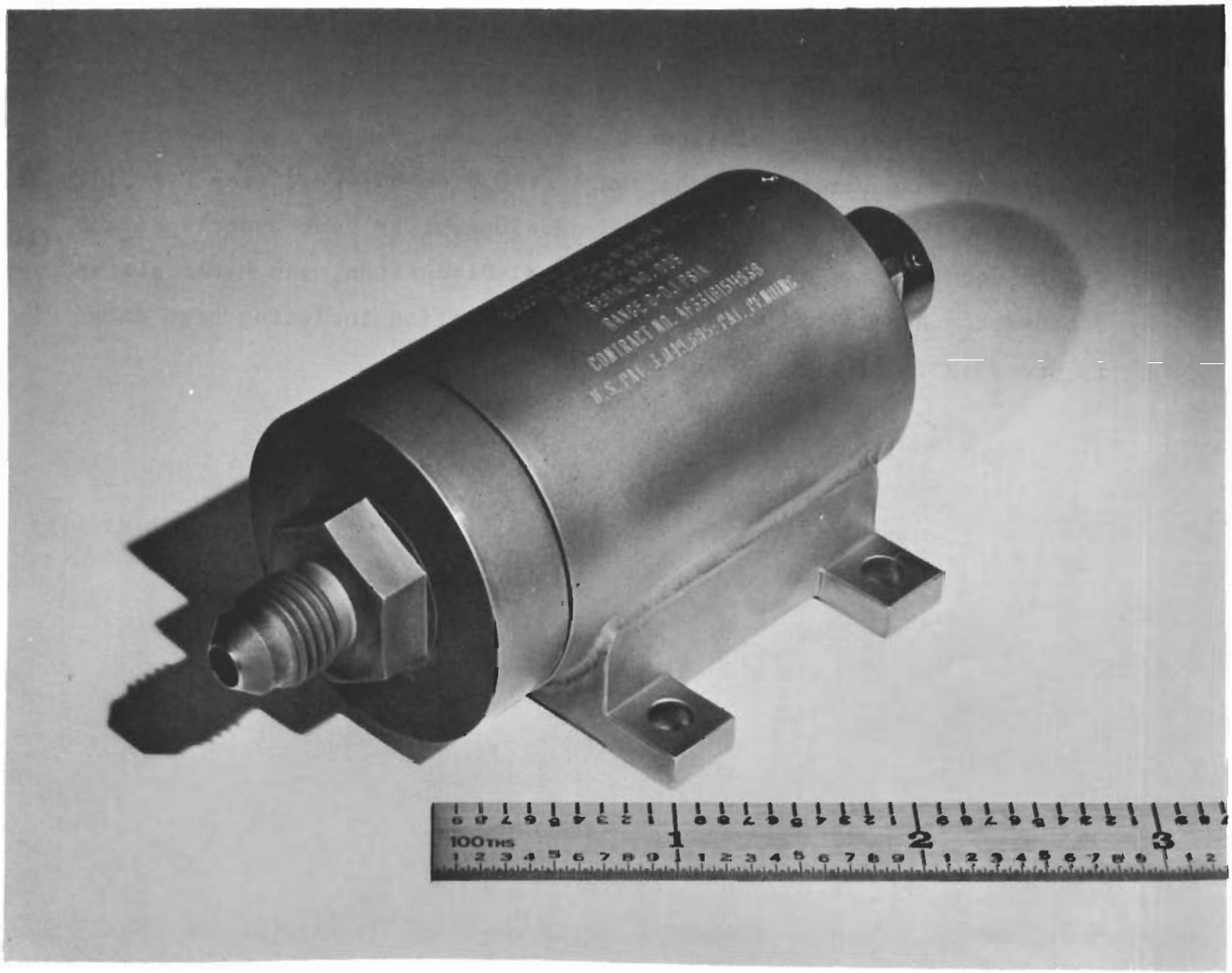

FIG. 1 TRANSDUCER MODEL 5431-1

2. TECHNICAL DISCUSSION

2.1 Specification

The specification controlling this project was a target specification, subject to modification during the progress of the project.

2.1.1 Initial Specification

The initial specification at the commencement of the project is shown below:

1. Range (full scale) - 0.0 to 0.1 psia
2. Accuracy - plus or minus 1 percent of full scale, including linearity, hysteresis, repeatability, and environmental effects
3. Full scale output - 5 volts dc
4. Resolution - 0.1 percent full scale
5. Size - 10 cubic inches (max)
6. Weight - 16 ounces (max)
7. Low end point - 1 percent of full scale
8. Frequency response - dc to 20 cps
9. Noise or output ripple - 0.2 percent full scale
10. The sensing device and all electronics for each model shall be assembled in one package

2.1.2 Environmental Requirements

In the evaluation of the most promising techniques, consideration must be given to the following environmental conditions:

1. Temperature - 0 to 500^{o}F (transient and steady state)
2. Acceleration - plus and minus 10 g each axis
3. Overpressures - up to 1 atmosphere
4. Vibration - 5 to 2400 cps plus and minus 3 to plus and minus 10 g, respectively
5. Shock - 50 g 10 milliseconds, all axes

6. Acoustic noise - 140 dB above 0.0002 dynes per square cm
7. Exposure to corrosive atmosphere

2.1.3 Final Specification

The agreed specification against which the prototypes were shipped is shown below:

1. Range - 0.0 to 0.1 psia
2. Static error band - ±1 percent of full scale
3. Size - 10 cubic inches (max)
4. Weight - 16 ounces (max)
5. Zero setting - 0 ±1 percent of full scale
6. Compensated temperature range - 0° to $+250^{\circ}$F
7. Temperature error - ±3 percent full scale (max)
8. Acceleration - ±10 g in three mutual axes
9. Vibration - 5 to 2400 cps up to 10 g (For actual amplitude see test procedure in Appendix VII.)
10. Overpressure - 15 psia or 1 atmosphere

2.2 Design

After considering various possible approaches, the diaphragm/cantilever design was selected as offering the best possibility of success.

2.2.1 Flat Diaphragm Model

An experimental model using a flat diaphragm (Fig. 2) was constructed with the object of ascertaining the necessary diaphragm effective area. This design is shown in Figs. 2 and 3. The test data indicated (with the test equipment available) that such a design would probably meet the requirements of sensitivity, linearity, and hysteresis. Test data is contained in Appendix I and reflects results of:

Sensitivity	-	81.4 mV/0.1 psia
Linearity	-	1.03 percent full scale
Hysteresis	-	0.61 percent full scale

The calculations covering the design dimensions are contained in Appendix II.

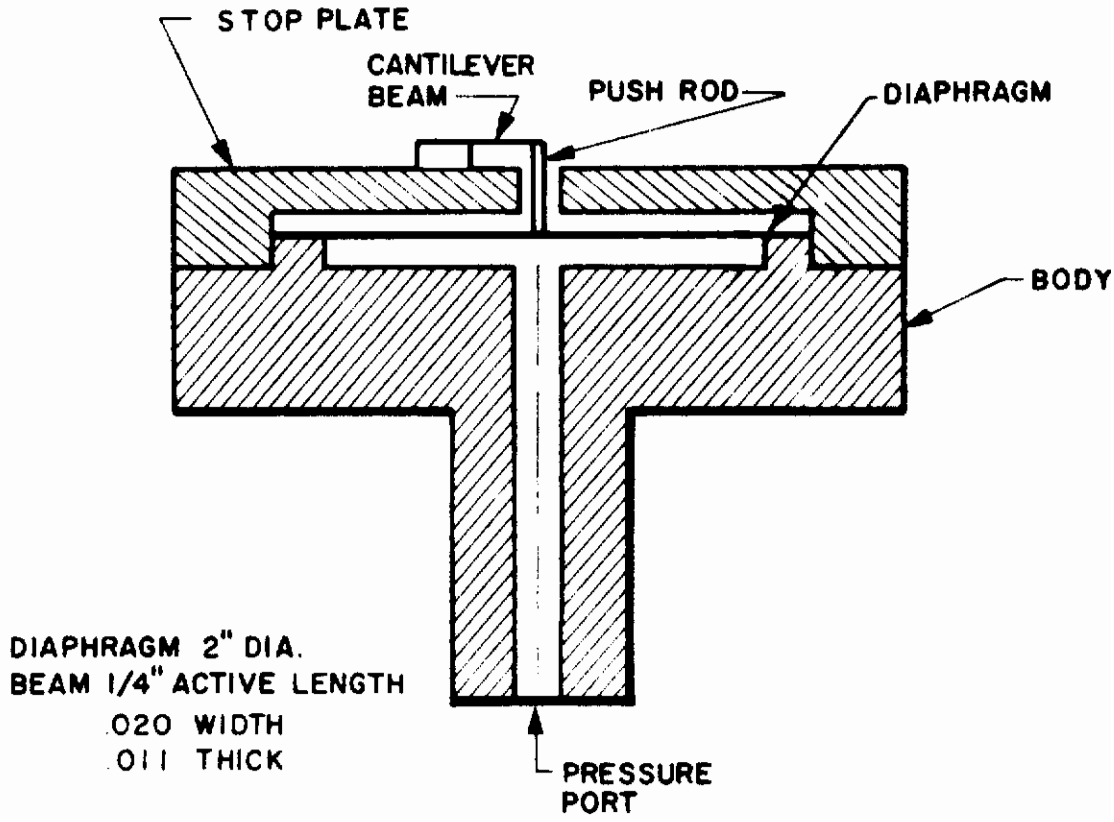

NOTE: DRAWING NOT TO SCALE

FIG. 2 TRANSDUCER PRELIMINARY LAYOUT

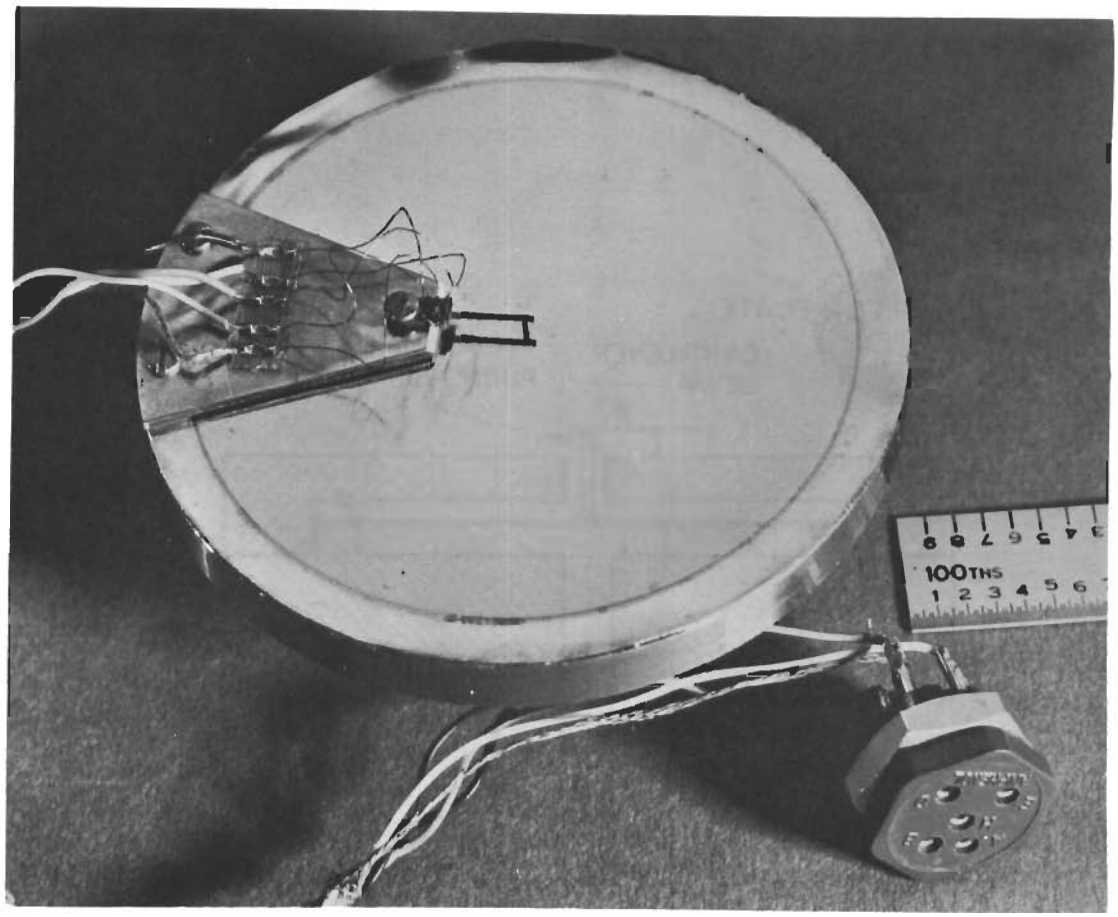

FIG. 3 LABORATORY TEST MODEL TRANSDUCER

2.2.2 Convoluted Diaphragm Design

To maintain the required effective area of diaphragm while keeping the transducer configuration within that outlined in the specification, a model incorporating a convoluted diaphragm was designed. Such a diaphragm, in its test fixture, is shown in Fig. 4. The diaphragm was formed by high-energy rate-forming (HERF) using a die as shown in Fig. 5. The beam used with this diaphragm is shown in Fig. 6. It should be noted that the pushrod welded to the center of the diaphragm was not welded to the cantilever beam, but was merely pushing on the end of the beam. Some reduction in output would be expected when the beam and pushrod are welded together. The calculations used to determine the beam and diaphragm configurations are shown in Appendix III. Typical results obtained are summarized below and are contained in Appendix IV.

Sensitivity: 130 MV/3 inch H_2O

Nonlinearity: Ranging from 0.5 percent to 0.9 percent

(NOTE: It should be noted that the work to this point was being done with average test equipment and, hence, results should be looked upon as approximate. It is reasonable to presume, however, that the value for nonlinearity is in reality better than the test data obtained.)

2.2.3 Initial Prototype

The encouraging results obtained with the convoluted diaphragm models indicated that the next useful step was to incorporate such a diaphragm/beam system into a complete transducer conforming to the required external configuration.

It was realized that the two major problems encountered would be: (1) the necessity to provide an efficient overload protection system so that the instrument would not suffer damage during its shelf life, and (2) ensuring a true leak-free reference cavity for stable zero setting throughout the life of the instrument.

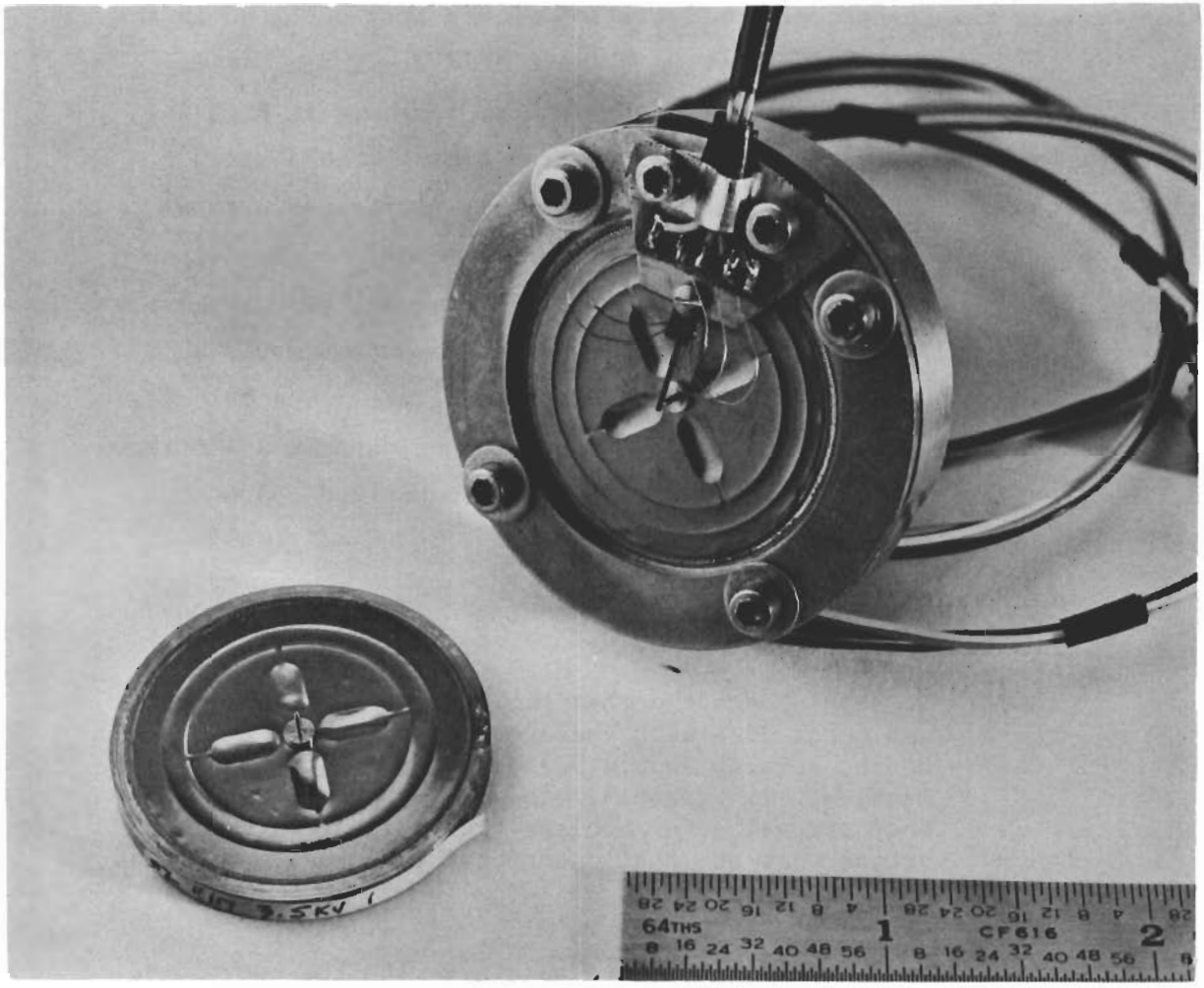

FIG. 4 DIAPHRAGM TEST FIXTURE

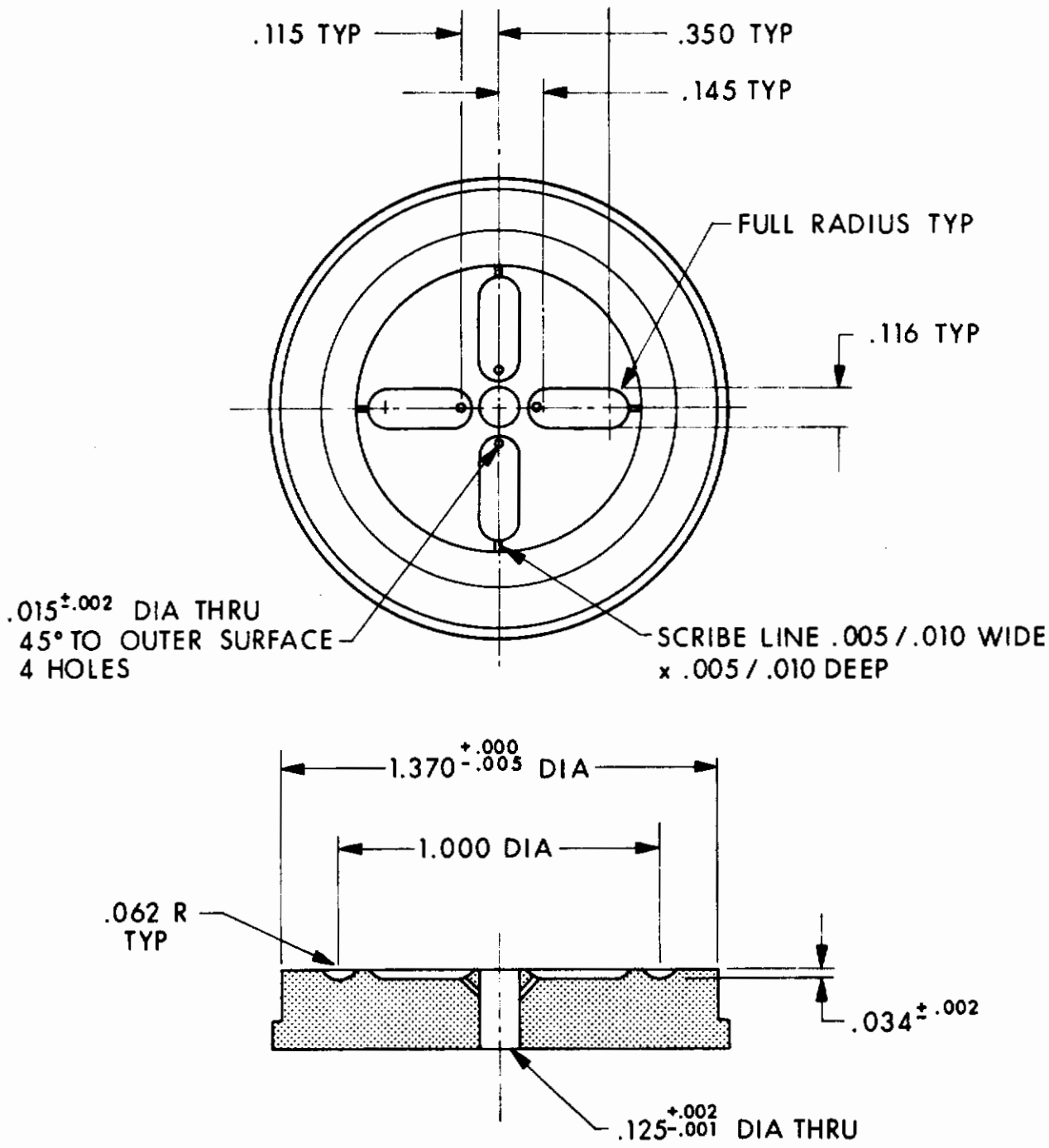

FIG. 5 FORMING DIE

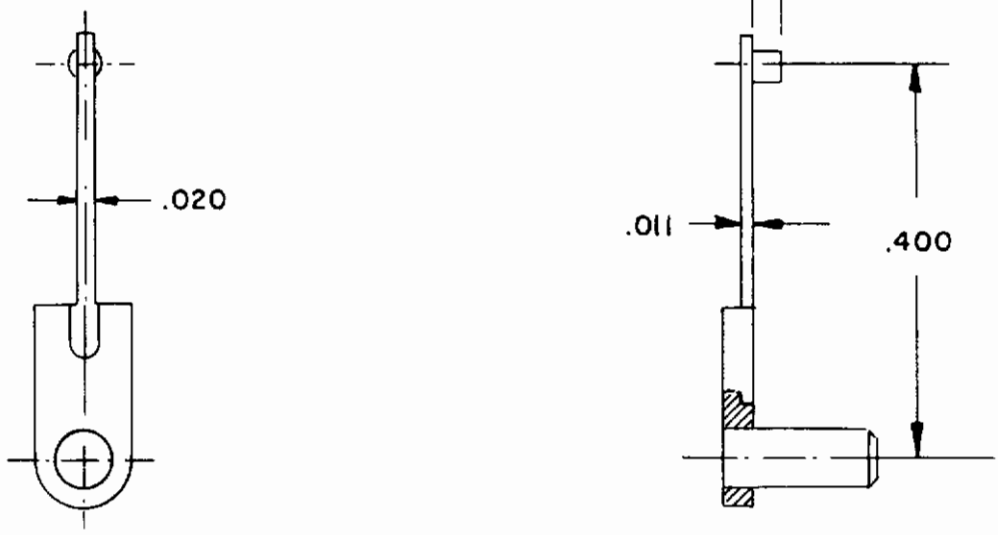

FIG. 6 STANDARD LOW-PRESSURE BEAM

Overload Stop

To avoid a permanent set occurring in the diaphragm and beam, it was felt to be necessary to stop the system at about 2 to 3 times overpressure and to support the diaphragm over its entire surface area while the system was stopped out. The difficulty of machining a stop to match the diaphragm shape and then locating the diaphragm to the stop needs no explanation. In this particular instrument, the difficulty was anticipated by using each individual stop-plate as the forming die for its corresponding diaphragm. Under these circumstances, the best method of forming appeared to be high-energy, rate-forming (HERF). The familiar process of exploding a wire under water was used to generate the necessary energy. The wire was exploded by discharging a capacitor bank through it. After some experimentation, a satisfactory procedure was established, and this method was adopted for the manufacture of the transducers required.

Sealed Reference Cavity

To establish a stable zero in a low absolute pressure transducer, it is essential that a leak-free reference cavity be supplied, and that materials used do not outgas to any marked degree. The probable leak areas are (a) the weld of the diaphragm to the case, (b) the seals in the header, and (c) the weld of the header to the case.

To ensure a high degree of integrity in these areas the following precautions were taken: Seam welding was used to attach the diaphragm to the case. This method has been proven by experience both in the transducer and other fields to afford an extremely reliable leak-free weld when made correctly. (To decrease the risk of leaks, two concentric seam welds were used, separated by a diametral distance of 1/8 inch.) Experience has also indicated that, for good glass-to-metal seals and to avoid damage in assembly, it is preferable to use solid feed-through pins as opposed to hollow pins and to keep the glass seals as remote as possible from the join weld. To this end, as large a diameter header as possible was used, together with

solid feed-through pins. (The disadvantage of these solid pins is that they make for a more difficult assembly operation, but they do avoid the necessity of using the high temperature solder for sealing hollow pins with its consequent risk of cracking the insulating glass seal.) By carefully designing the join and using electron-beam welding a deep and reliable join of header to body was obtained. Careful leak checking at each stage of the operation ensured confidence in the integrity of the various seals discussed. To guard against outgassing, no organics other than the gage adhesive and the wire insulation were used, and these were chosen to keep outgassing at an insignificant minimum at the specified operating temperatures. To ensure a completed outgassed assembly, the pickup was baked at 350°F in a hard vacuum for a minimum of 16 hours immediately prior to sealing.

Overall Design

The design of the first prototype is shown in Fig. 7. It consists of a convoluted diaphragm coupled to a simple cantilever beam to which was bonded four semiconductor strain gages at the point of maximum strain. These strain gages (two compression and two tension) were connected as a four-arm bridge. The output from this bridge was amplified to achieve the 0 to 5V dc output required. The electronic package used was a standard item manufactured by Micro Systems, Inc. (MSI) and is fully described in Appendix IV.

Temperature Stability

To avoid variations in zero setting and sensitivity of this transducer when the environmental temperature is varied through the specified range, certain precautions must be taken. Firstly, the semiconductor strain gages were selected so that, when connected as a four-arm bridge, they balanced; i.e., the resistance of the gages used was carefully selected so that each arm of the bridge was equal and, hence, as the ambient temperature varied, the output from the bridge remained constant. Secondly, prior to sealing the reference cavity, the transducer (excluding electronics) was temperature-soaked

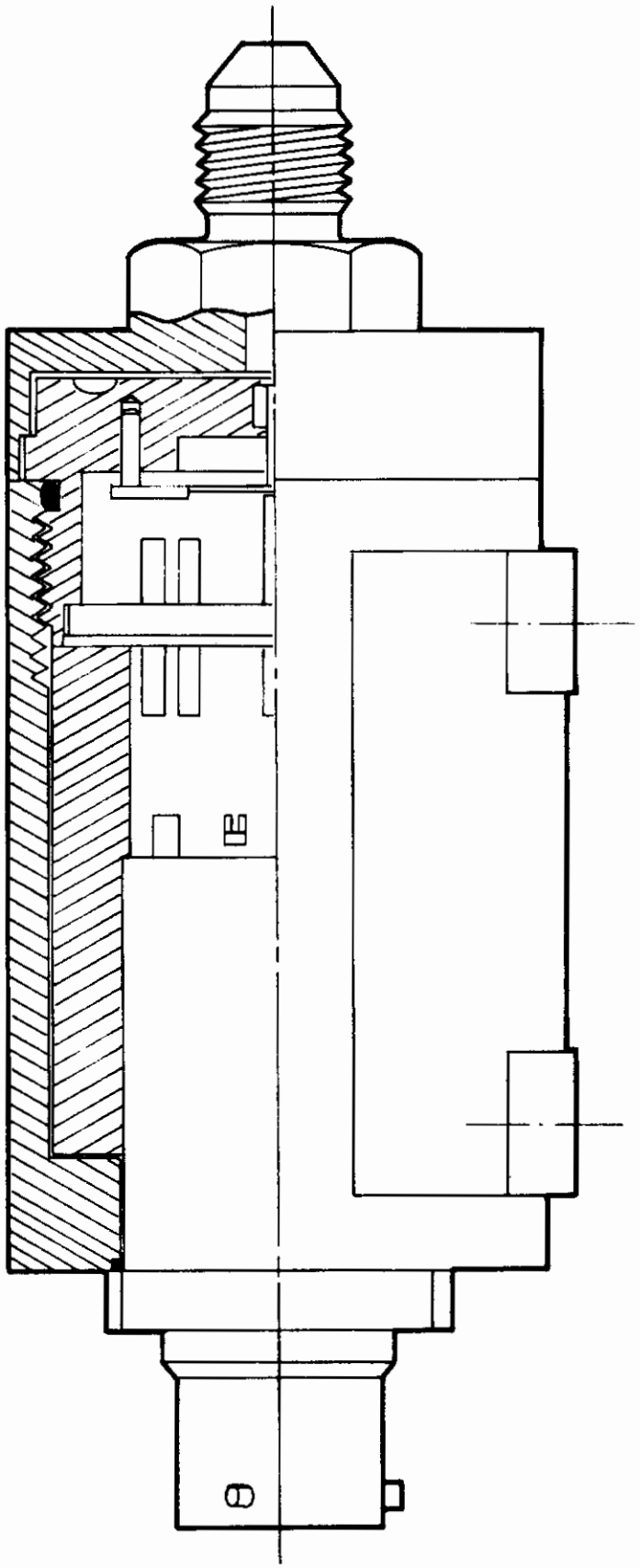

FIG. 7 PROTOTYPE DESIGN, SECTIONAL VIEW

at 350°F in a hard vacuum. This ensured proper gassing-off of the component parts in the evacuated cavity. After this cure cycle, the evacuated cavity was flushed with dry helium three times and sealed at 5Ω. With only dry helium in the reference cavity, the problems involved with unclean atmosphere (outgassing, condensation expansion, etc.) were avoided. Despite these precautions, variations in zero and sensitivity through the environmental range were unavoidable, mainly because of stresses built in during manufacture. To overcome these problems, a system of temperature compensation was employed.

2.3 Temperature Compensation

2.3.1 General

Under operational conditions, the response of a pressure transducer to a change in temperature is indistinguishable from that due to a change in the measured pressure. Consequently, some form of temperature compensation must be built into each transducer. Standard EOS compensation techniques were found to be adequate for reducing thermal zero and sensitivity shifts of the 0.0 to 0.1 psia pressure transducers, to acceptable levels.

Two temperature effects must be compensated in order to have a transducer maintain accuracy over a wide temperature range. These are: the no-load, bridge output change with temperature or thermal zero shift; and, the change of bridge full scale output (sensitivity) with temperature.

2.3.2 Thermal Zero Shift Compensation

Thermal zero shift results from mismatch of total resistance, gage factor, and coefficient of resistance among the four silicon bridge elements. Additionally, mismatch of expansion coefficients between the silicon elements, force collectors, and sensing diaphragm provides additional bridge unbalance for wide temperature excursions. The approach normally taken and found applicable to these transducers is as follows: Resistance temperature coefficients of the

gages are precisely measured prior to selecting a set of four for installation in the transducer. Typically, a group of 20 to 30 gages is tested at +20°C and +170°C, and the unit resistance change values tabulated. Sensors with like resistance changes from +20°C to +170°C are grouped as adjacent bridge arms. It must be recognized that, regardless of the matching obtained, there remains some bridge unbalance for the ΔT experienced and a temperature compensating element must, therefore, be placed in that bridge arm with the lowest temperature coefficient of resistance.

Thermal zero shift compensation by this technique is a fairly simple procedure. The bridge is connected as a five-wire system as shown in Fig. 8. The bridge is externally balanced at room temperature with a decade box. The transducer is then placed in an environmental chamber and the output with temperature noted. The amount of Balco wire resistance required for compensation is computed from the following equation:

$$R_{Balco} = \frac{0.02 \times \lambda_o \times R_b}{E_{in}}$$

where:

R_{Balco} = resistance of compensating Balco wire, ohms

λ_o = output shift, mV/100°F

R_b = input impedance of bridge at room temperature, ohms

E_{in} = input voltage to bridge at room temperature, volts

The calculated amount of Balco is wound and placed in the appropriate bridge arm. The resistor is inserted in series with a compression arm if the output shift for increasing temperature is positive, and into a tension arm if it is negative. Another temperature run is made and the Balco adjusted if necessary. This step is repeated until the desired results are obtained. The unit is then balanced with the decade resistance box, at room temperature; the balance resistance is

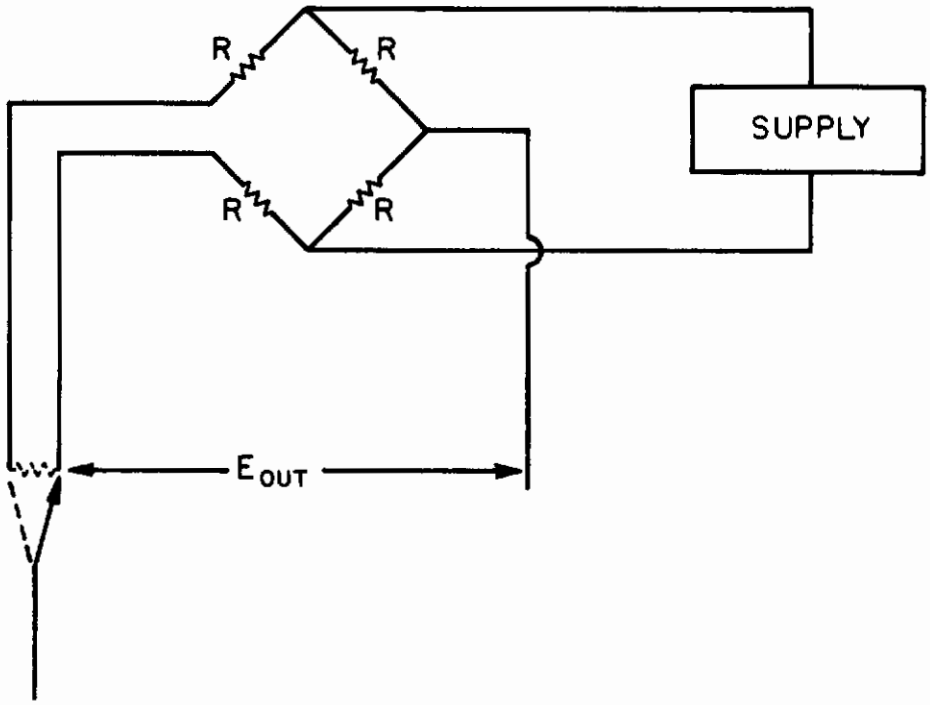

FIG. 8 THERMAL ZERO SHIFT COMPENSATION

noted and a resistor of this value wound with Evanohm wire is placed in the correct arm of the bridge. The bridge can then be closed to the conventional four-wire system.

2.3.3 Sensitivity Compensation

For semiconductor strain gage bridges, either constant voltage or constant current excitation can be used. With constant voltage excitation, the uncompensated bridge typically shows a sensitivity loss of between 12 to 20 percent/100°F; even in the heaviest dopant levels this value is typically 3 to 5 percent/100°F.

The gage factor versus temperature for a typical silicon element is shown in Table I. The severe reduction in gage factor with increasing temperature is quite apparent. Therefore, constant current excitation is used since, with constant current excitation, the change of sensitivity with temperature is proportional to ΔR rather than $\Delta R/R$.

The following equations are pertinent to this discussion:

$$\text{since} \quad GF = \frac{\frac{\Delta R}{R}}{\mu\epsilon}$$

$$\text{then since} \quad E_{in} = I_{in} R$$

$$E_o = E_{in} \times GF \times \mu\epsilon$$

$$E_o = E_{in} \times \frac{\Delta R}{R}$$

$$E_o = \frac{IR\Delta R}{R} = I\Delta R$$

where

E_o = bridge output, in volts

R = gage resistance at zero balance

ΔR = incremental resistance change due to applied pressure

GF = gage factor

$\mu\epsilon$ = full scale operating strain in/in x 10^{-6}, assuming four active gages, two in tension, two in compression. The ΔR for a given

TABLE I SPECIMEN OF P-TYPE Si WITH STRESS APPLIED PARALLEL TO [111] $N_A = 3 \times 10^{18}$

Temp. (°C)	Resistance (ohms) Forward	Reverse	Tensile Load (gm)	Gage Factor	ΔR Forward	Reverse
25	172.6	173.0	0	135	2.7	2.7
	175.3	175.7	20			
250	271.4	268.4	0	83	2.6	2.6
	274.0	271.0	20			
500	402.9	402.5	0	54	2.5	2.5
	405.4	405.0	20			

strain, at several different temperatures, is shown in Table I, and it can be seen that this is relatively constant. If a constant current excitation is provided to the bridge, slightly increasing sensitivity versus temperature might be expected since there is interaction between the effect of ΔR versus temperature and the decrease in Young's modulus with temperature. Typically, a constant current excitation coupled with an input shunt resistor will give relatively flat temperature performance as shown in Figs. 9 and 10.

2.4 Test Equipment

In a program of this sort, establishing a suitable test setup and selecting suitable test equipment is of major importance. When one considers that the full scale of this instrument is 0.039 inch of mercury, it is possible to appreciate the difficulties involved in measuring these pressures to a sufficient degree of accuracy. Furthermore, to generate incremental pressures of 0.01 psi absolute without overshoot is fraught with innumerable difficulties.

2.4.1 Water Manometer

In the initial stages of investigation a 30-inch "U" tube, water manometer was used. Although this instrument is very inaccurate, it did give satisfactory information as regards sensitivity and approximate linearity. It was also used during the production of the four delivered instruments for preassembly checking at gage pressures.

2.4.2 Micromanometer

The writer visited the National Bureau of Standards in Washington where the various test equipments in use there were demonstrated. They were particularly enthusiastic about a micromanometer which had been designed at NBS and obligingly supplied EOS with drawings of such an instrument. A modified version of this micromanometer was manufactured at EOS and is fully described in

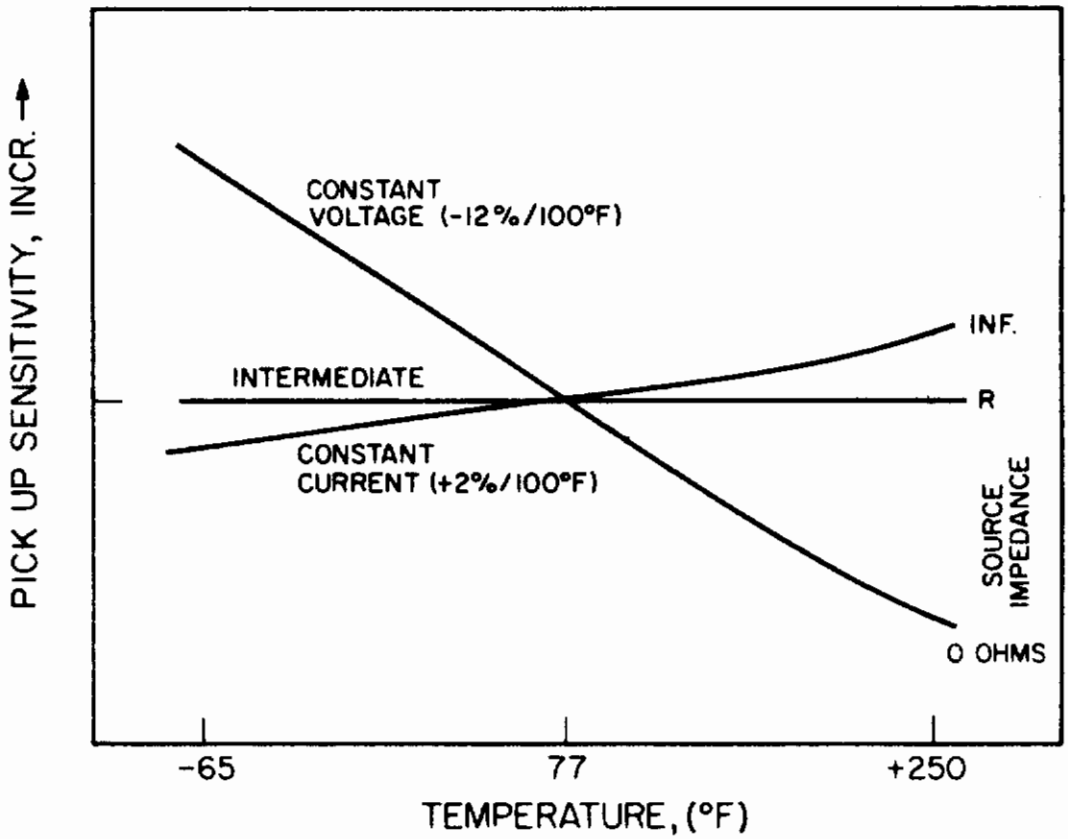

FIG. 9 TYPICAL SENSOR SENSITIVITY VERSUS TEMPERATURE CHARACTERISTIC FOR SILICON STRAIN GAGE ELEMENTS

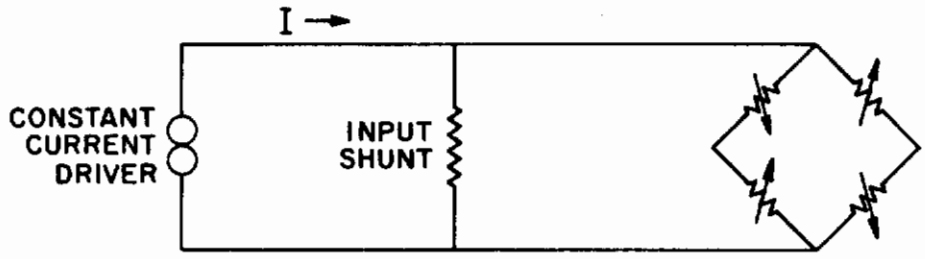

FIG. 10 SHUNT COMPENSATION WITH CONSTANT CURRENT EXCITATION

Appendix VI. The manometer was simple to operate and read and was used to test transducers at gage pressure and to calibrate the test console which was subsequently built.

The micromanometer had a number of disadvantages which can be divided into two classes: (1) those inherent in this type of instrument and (2) the defects in this particular instrument. The fact that the requirement here is for very low absolute pressure makes any manometer type of instrument difficult to use. Because mercury tends to vaporize at relatively low pressure, even at room temperature, it is necessary to avoid pumping to excessively low pressure on the reference side of the manometer. It is also advisable to install cold-traps, both to condense any possible evaporated mercury and to catch solid mercury in the event of accidental vacuum "dumping". There also remains the problem of metering small increments without overshoot at this level of vacuum. It is also essential to have a system free from leaks. The test setup actually used with the micromanometer is shown in Fig. 11.

The major problem with this particular manometer was leakage past the seals at the micrometer shafts and between the glass tubes and end plates. The leakage at the glass tubes was rectified by obtaining new tubes, but redesigning the micrometer seals failed to cure leaks at this point, and so this micromanometer was never really successful as an absolute test instrument. With better quality micrometers and a different seal design, this test instrument could be useful.

2.4.3 The Volumetrics Test Gear

This test equipment was manufactured to EOS requirements by Volumetrics Inc. Basically, it uses the Knudsen system of volume ratios to obtain small linear increments of pressure. This equipment is fully described in Appendix VI.

It has the advantage that it does actually generate very small absolute pressure of accurately predetermined quantity without overshoot. Being semiautomatic, it is not subject to human

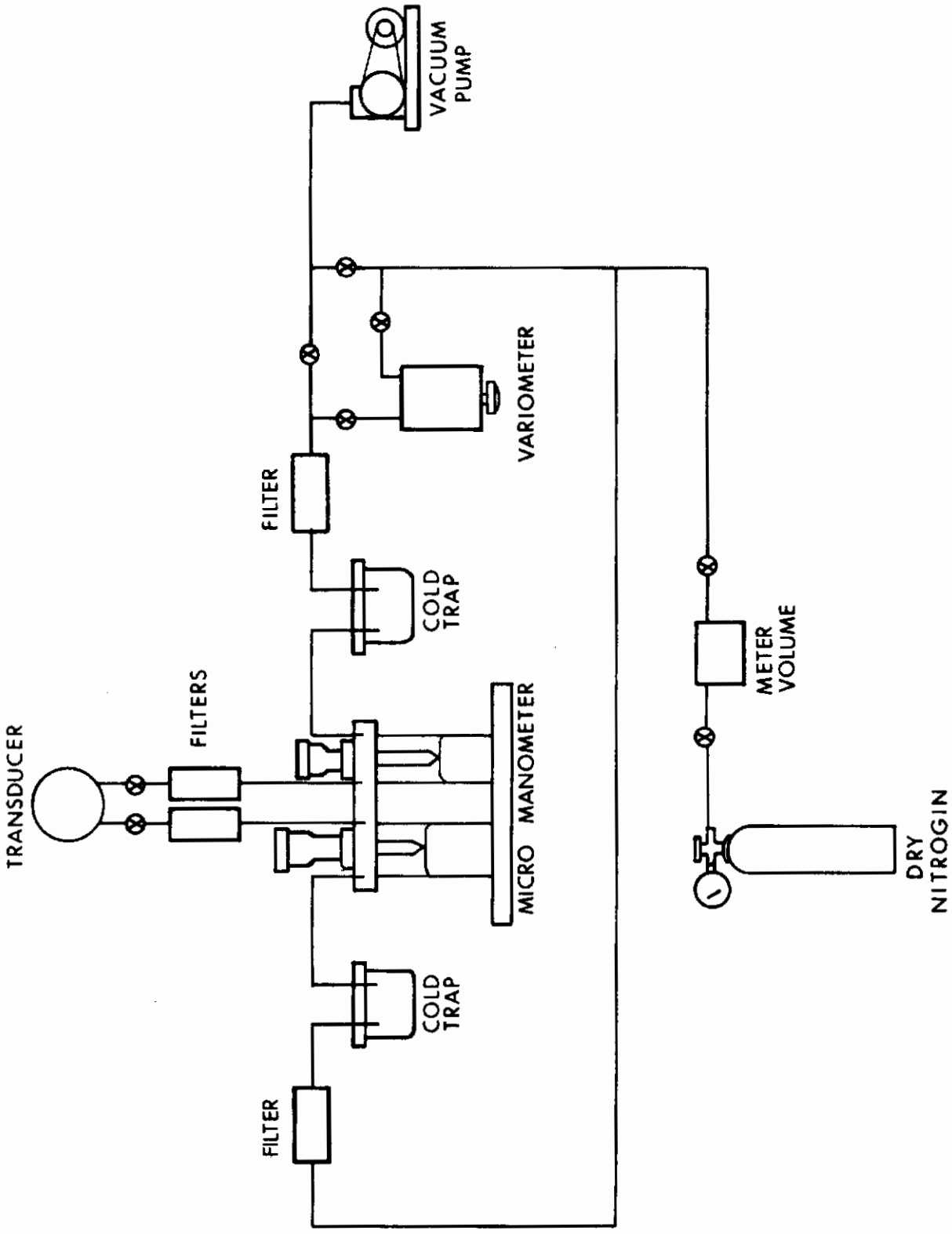

FIG. 11 MICROMANOMETER TEST SETUP

error in reading and manipulation. Since this is a dead-ended system, absolute freedom from leaks is essential for accurate operation, but it is possible to ensure noncontamination of the transducer under test. This test equipment was checked against the micromanometer and a Texas Instruments Company precision gage in addition to the manufacturer's calibration. (All of the transducers shipped under this contract were acceptance tested with this equipment.)

2.4.4 Testing of Transducers

The transducers were tested to the requirements of the test procedure contained in Appendix VII. The test results are summarized in Table II and shown in full in Appendix VII. (The test setup used in final testing is shown in Fig. 12).

2.4.5 Conclusions

From the results, it can be concluded that this design for a 0.0 to 0.1 psia transducer is very satisfactory. The linearity, repeatability, and hysteresis are excellent for an absolute transducer having such a low pressure range. The stop system works efficiently enabling the transducer to withstand overpressures far in excess of its rated range without degradation of calibration. With the signal conditioner specified it was possible to compensate the transducer satisfactorily for environmental temperature variations over the range 0 to 250^{o}F. The transducer had a natural frequency which was quite high for such a low pressure range. Because of the epoxy bonding cement used for attaching the semiconductor strain gages to the cantilever beam, it is not considered safe to subject this transducer to ambient temperatures as high as 400^{o}F.

TABLE II

SUMMARY OF TEST RESULTS

Serial No.	Linearity	Hysteresis	Nonrepeatability	Temp. Zero Shift max.	Temp. Sens. Shift max.	Natural Frequency
002	0.07% FS	0.4% FS	0.05% FS	3.9% FS	2.4% FS	1420 cps
003	0.88% FS	0.38% FS	0% FS	1.35% FS	1.73% FS	1380 cps
004	0.33% FS	0.08% FS	0.10% FS	1.79% FS	1.85% FS	1690 cps
005	0.46% FS	0.04% FS	0.04% FS	2.22% FS	2.64% FS	1310 cps

Note: The temperature range is 0 to +250°F

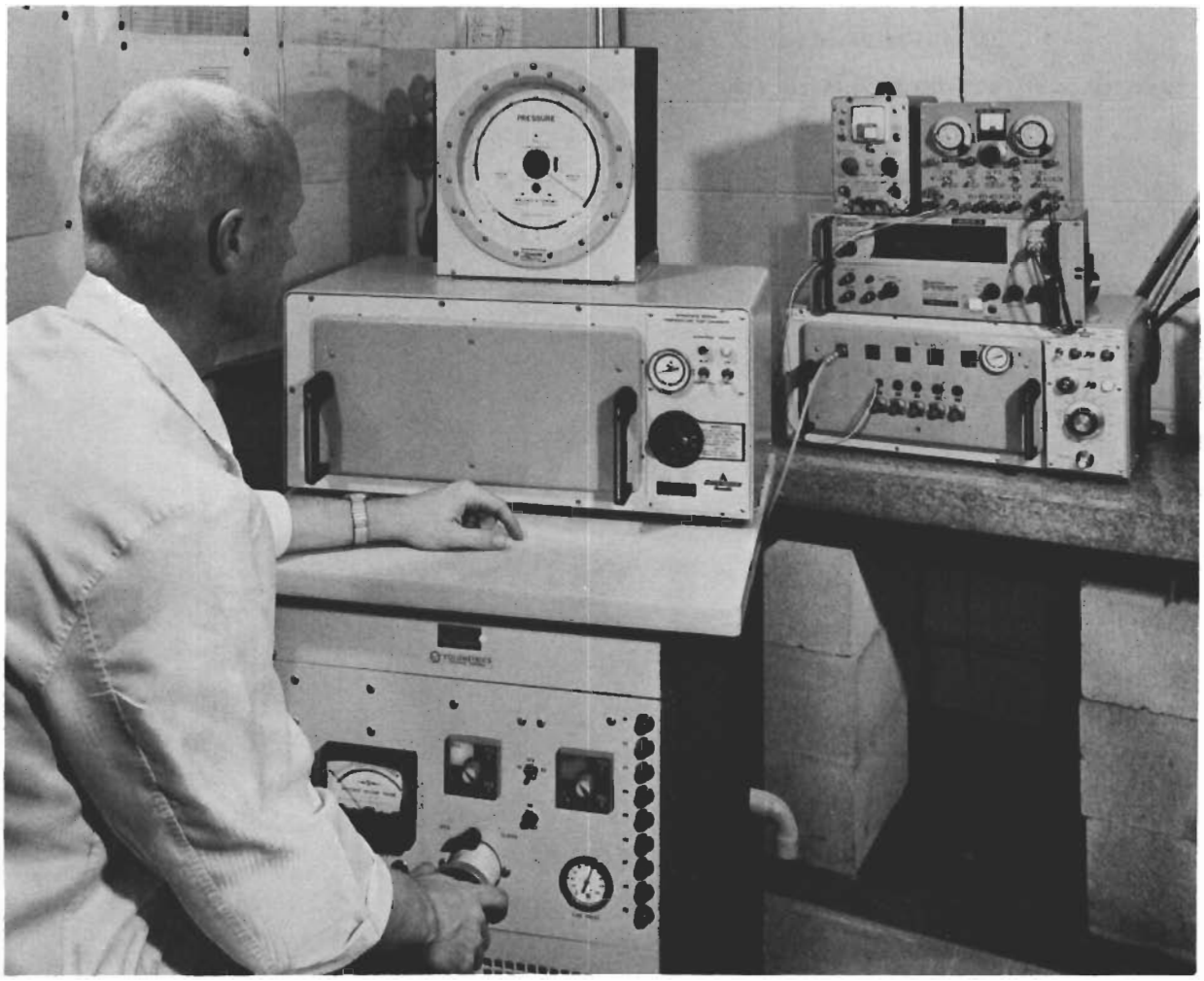

FIG. 12 TRANSDUCER TEST SETUP

2.4.6 Recommendations

It is recommended that work be carried out to further develop this transducer to operate up to 600°F by adapting various new techniques.

Whereas 1500 cps is gratifyingly high for such a transducer, efforts should now be made to raise this natural frequency above 2000 cps or artificially dampen it out.

The steady-state acceleration sensitivity of this instrument should also be improved, possibly by dynamic balancing.

The overall weight of the instrument should also be reduced.

3. MATERIALS AND PROCESSES

3.1 Experimental Silicon Beam

This report discusses the results of the evaluation of SP5B silicon cantilever bending beam, lot No. 7, 14, and 18, dopant concentration 5×10^{19}. (See Fig. 13 for beam configuration.)

3.1.1 Test Objectives

The object of this evaluation is to determine the strain gage, temperature sensor, and p-n junction characteristic with temperatures up to $500^{\circ}F$.

3.1.2 Test Method

Ten SP5B beams were subjected to the following tests:

The resistance of each element, breakdown voltage between sensor and gage, and leakage current at 5V between sensor and gage at room temperature were measured. Then four (7-1, 3, 6, and 10) of the 10 beams were temperature-cycled from $-108^{\circ}F$ (dry ice) to $+500^{\circ}F$, 10 times. After temperature cycling the beams (both temperature-cycled and nontemperature-cycled) were tested according to the referenced memo. Temperature measurements were made with a copper constantan thermocouple.

3.1.3 Test Results

The test results are presented in Figs. 14 through 21. From Fig. 14 it can be seen that the resistance of temperature sensors increases until $350^{\circ}F$, then it decreases rapidly due to p-n junction breakdown.

Figure 15 shows the resistance change of strain gages with temperature. Also it can be seen that the resistance of gages decreases rapidly after $350^{\circ}F$ and higher temperature.

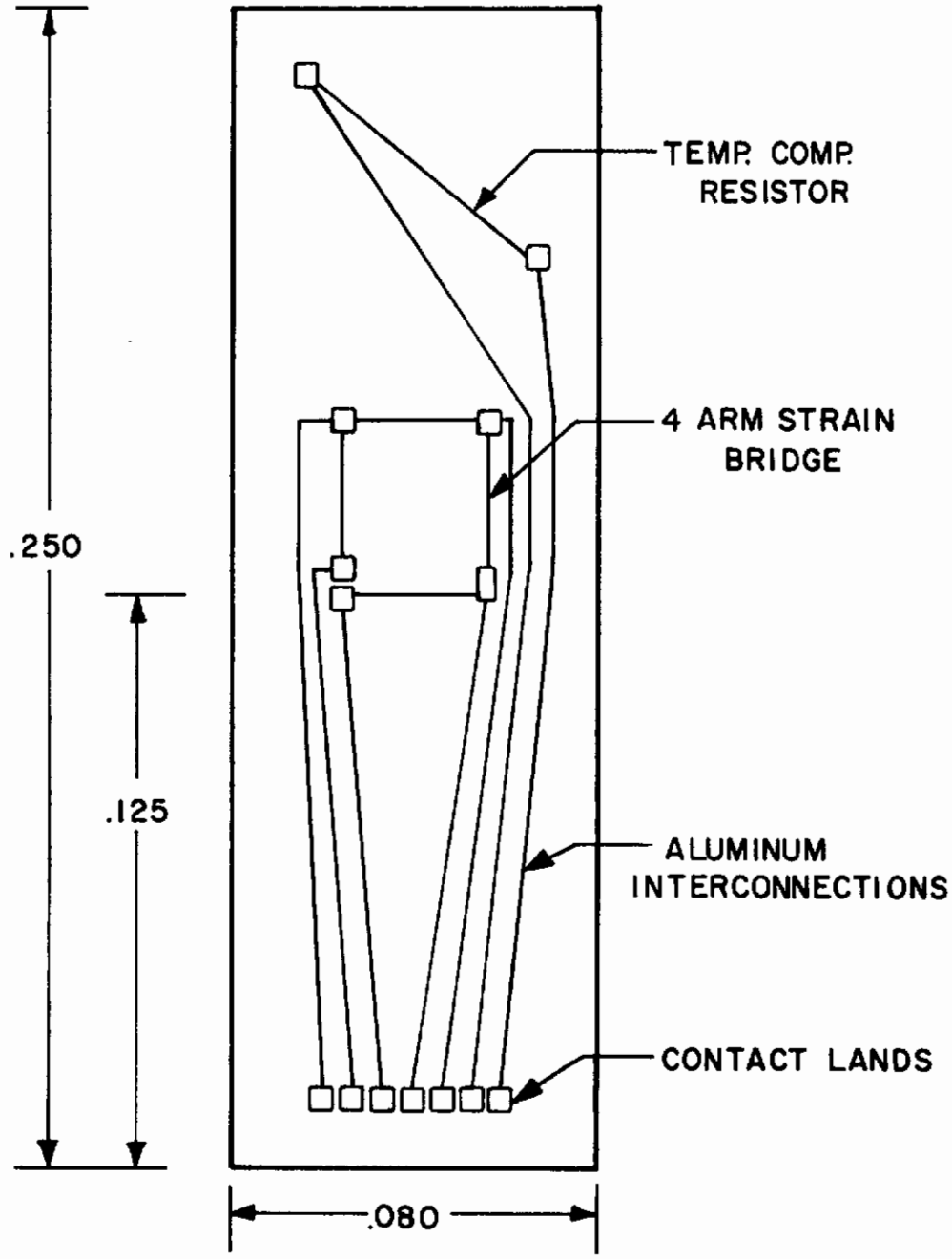

FIG. 13 FOUR ACTIVE ARM CANTILEVER BEAM

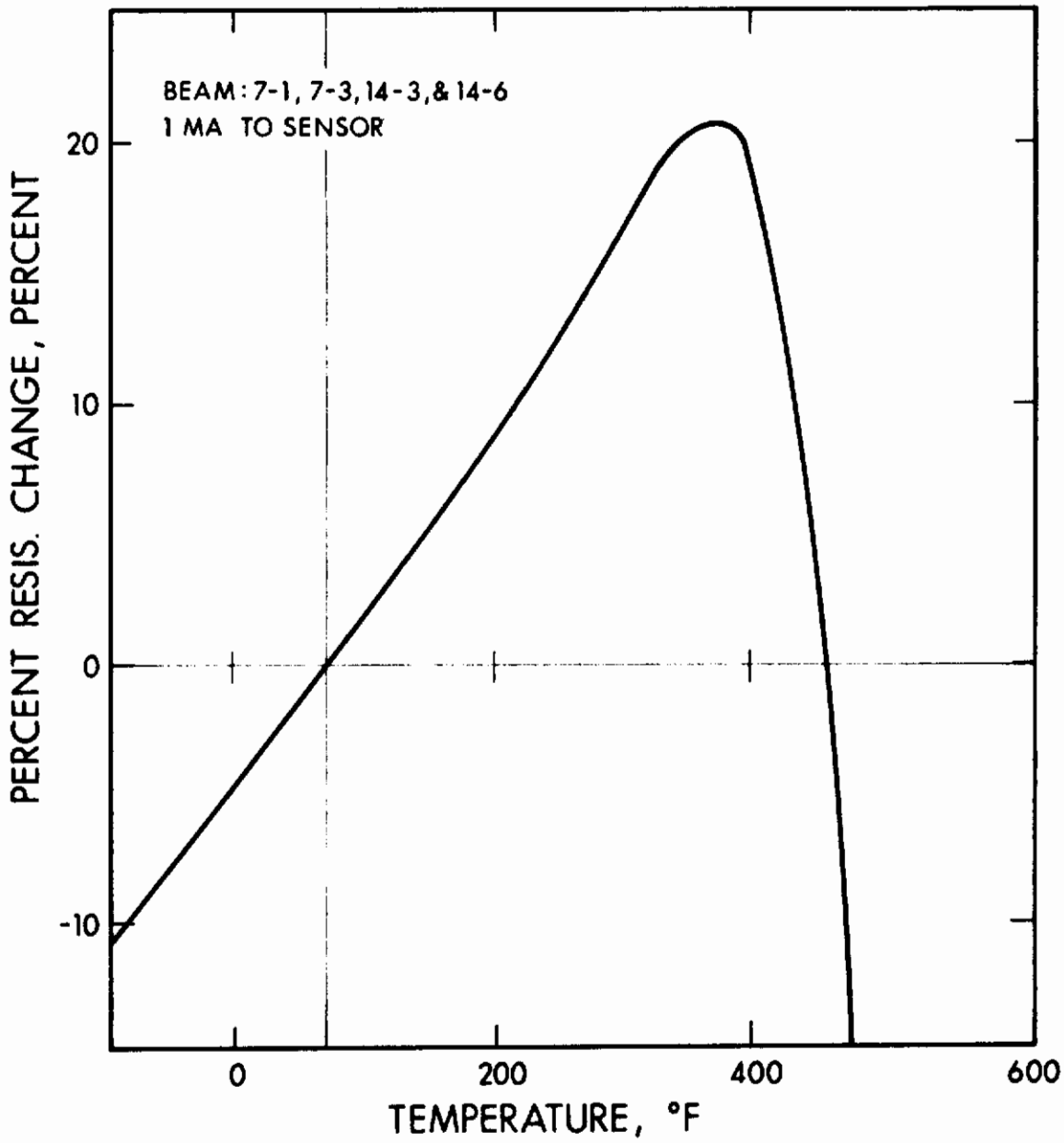

FIG. 14 RELATIVE RESISTANCE CHANGE VERSUS TEMPERATURE (SP5B Temperature Sensor)

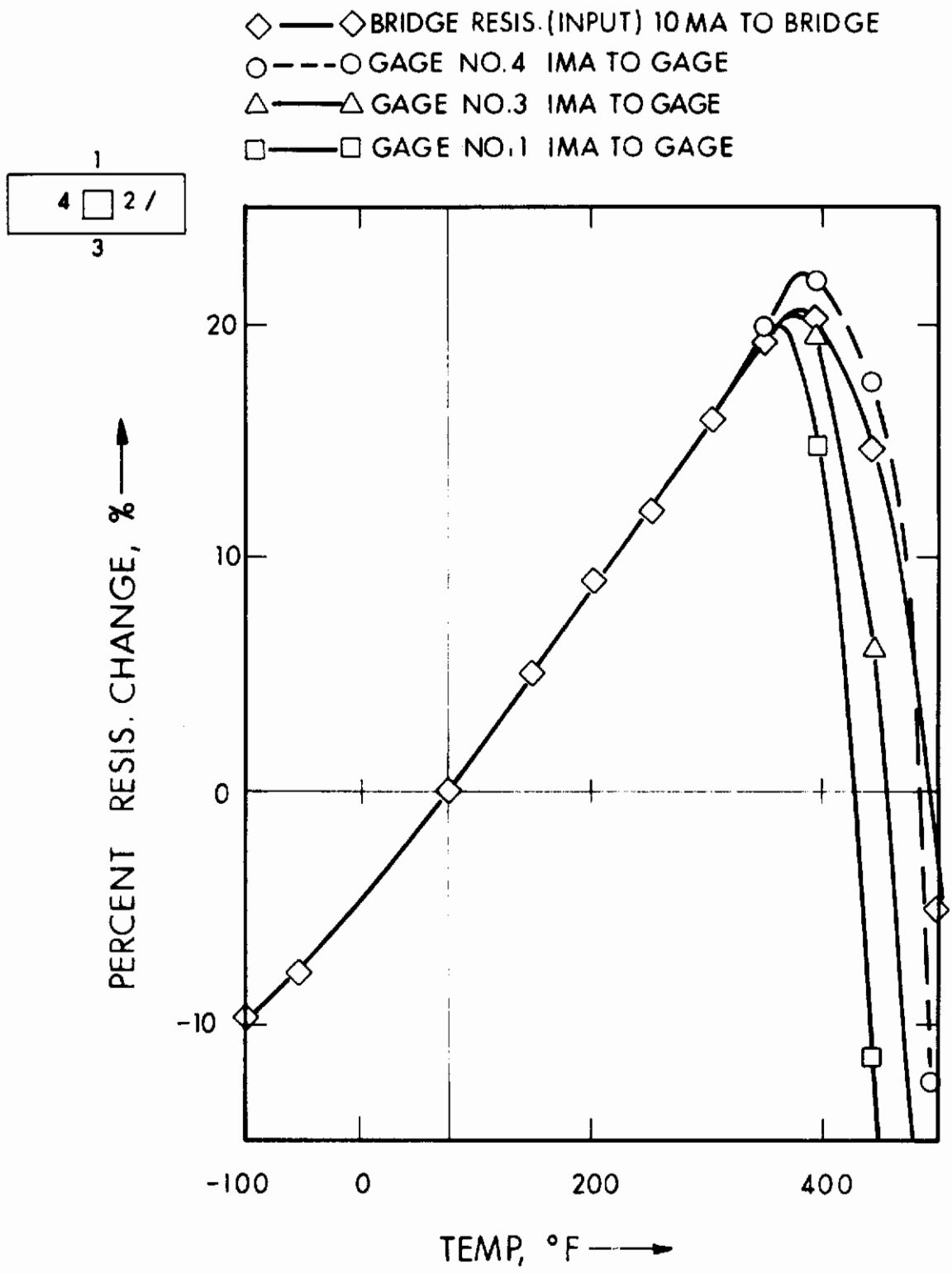

FIG. 15 RELATIVE RESISTANCE CHANGE VERSUS TEMPERATURE (SP5B Strain Gage)

Figure 16 shows the breakdown voltage versus temperature. The breakdown voltage of most beams is between 6.5V and 9V in both directions at room temperature. One highest breakdown voltage is around 19V in both directions at room temperature.

Figure 17 shows the self-heating effect on test beams with various bridge input currents for beam both unmounted and mounted. Notice the first large temperature rise on the mounted beam. An attempt was made to determine the cause of initial temperature rise, but this was unsuccessful. It is believed that the cause was some instrumentation problem.

Figure 18 shows also the self-heating effect of bridge resistance with the bridge input current. It should be noted that a 1 percent increase in resistance corresponds to 0.1 watt dissipation.

It can be seen from Fig. 19 that the zero shift with temperature is flat at temperatures up to 300°F.

The leakage current at ±5V between sensor and bridge is widespread from 0 to 10 μa up to temperature of 300°F, then the current increases rapidly up to 4 mA at 500°F.

Also leakage current is dependent on lighting condition (light sensitive). Leakage current of some beams was one order of magnitude less current when light was excluded.

Bridge gage factor is approximately 42 when strain is a 500με tension at center of bridge. This corresponds to 0.1696 lb load at free end of beam. The apparent gage factor of transverse gage nearest the point of applied force is approximately 34.6 and gage factor of transverse gage farthest from point of applied force is approximately 53.6 when strain is a 500με tension at center of bridge. Average gage factor of transverse gages is 44 at 500με tension. The 34.6 and 53.6 values are due to lower and higher strains, respectively, at the gage locations. The gage factor of longitudinal gage is approximately 43.6 at a 500με tension.

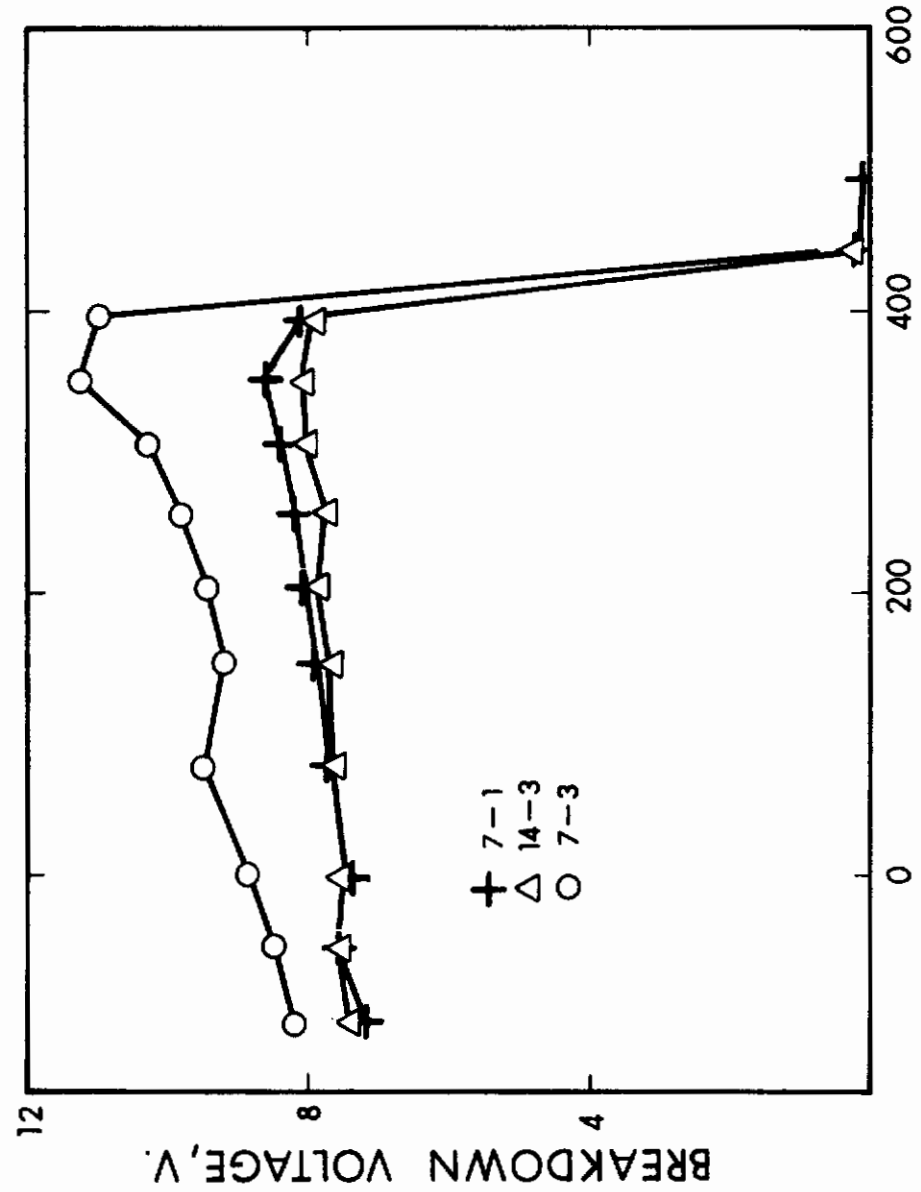

FIG. 16 BREAKDOWN VOLTAGE VS TEMPERATURE (SP5B)

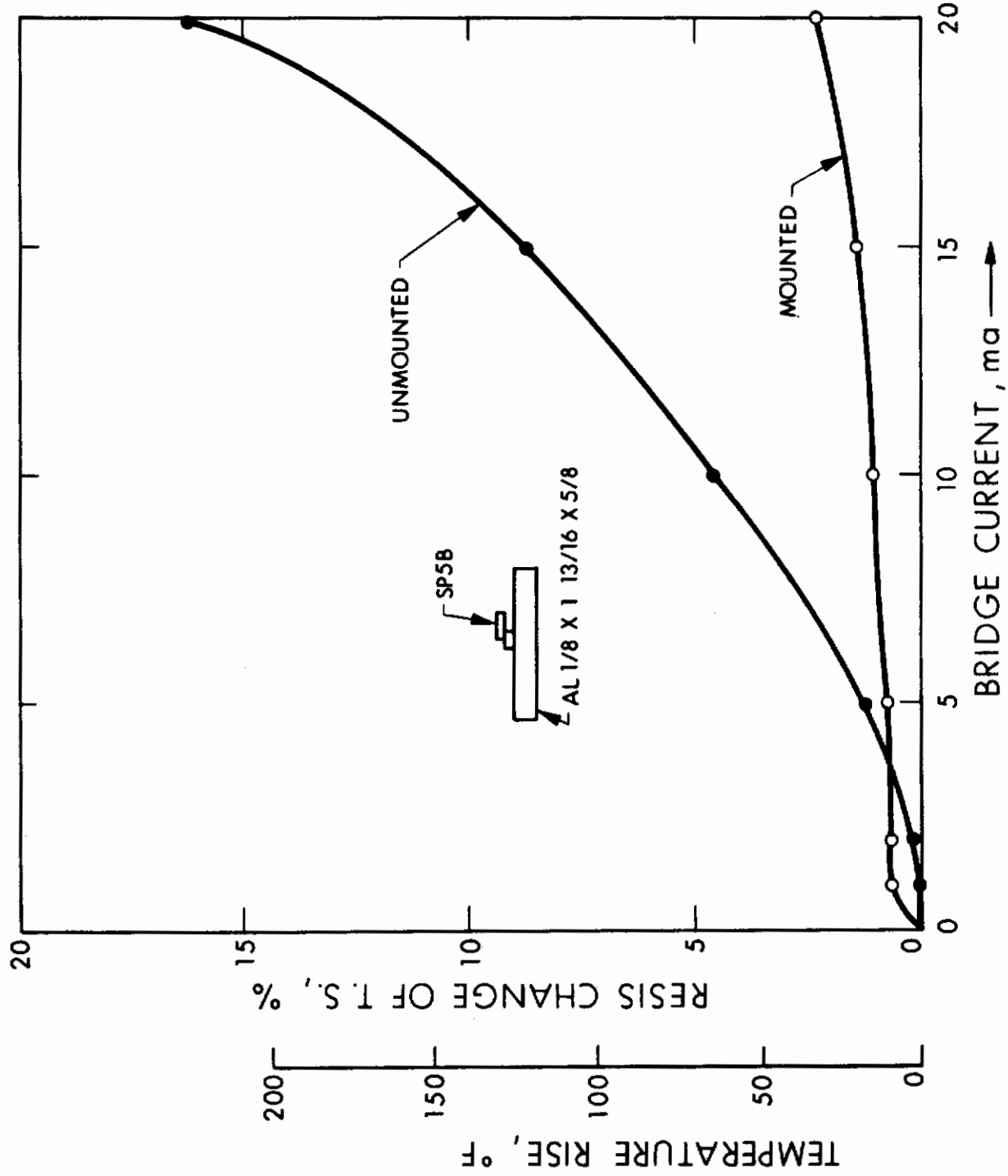

FIG. 17 RESISTANCE CHANGE OF TEMPERATURE SENSOR VS BRIDGE CURRENT (Strain Gage SP5B)

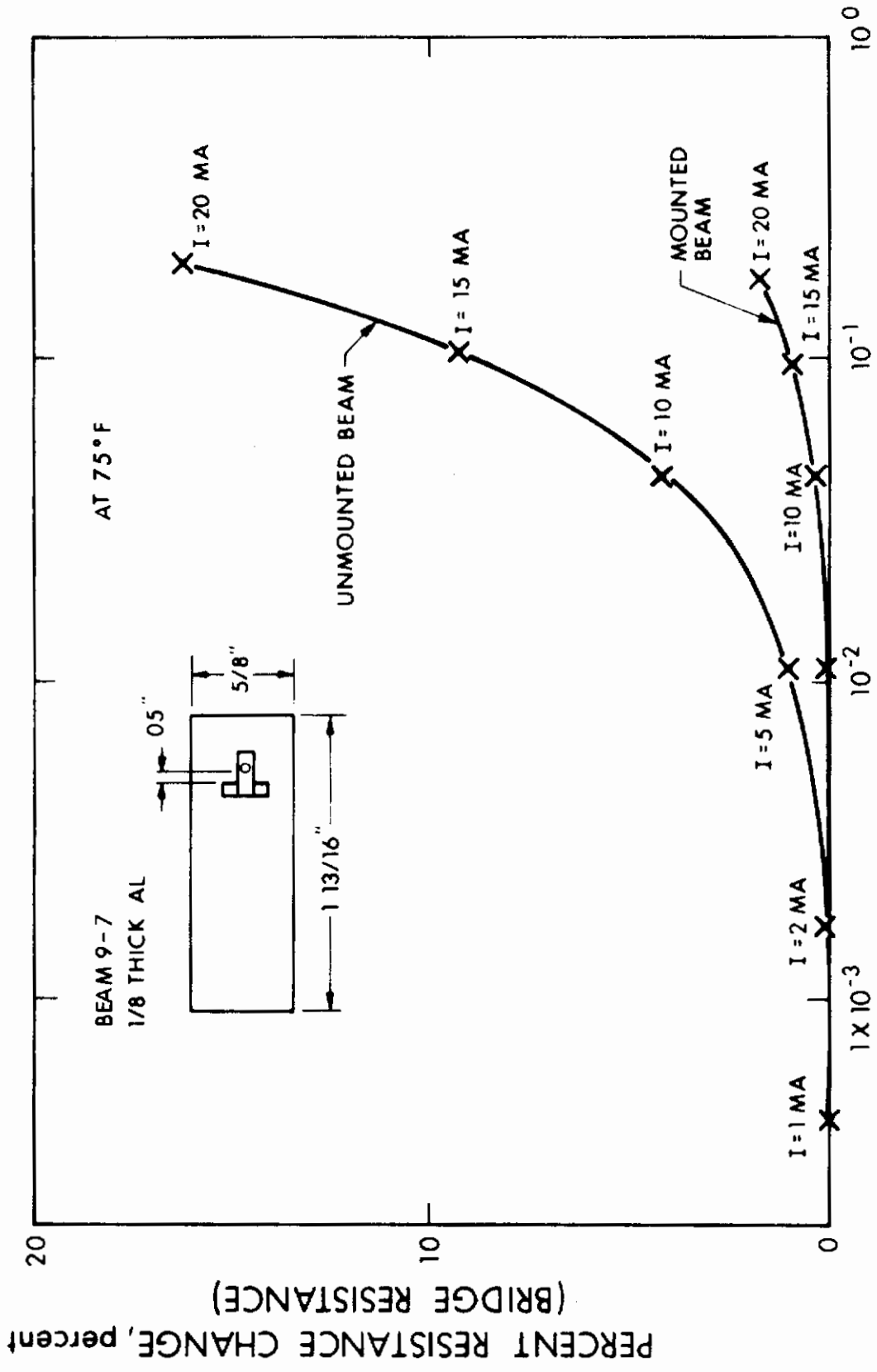

FIG. 18 RELATIVE RESISTANCE CHANGE VERSUS POWER (SP5B)

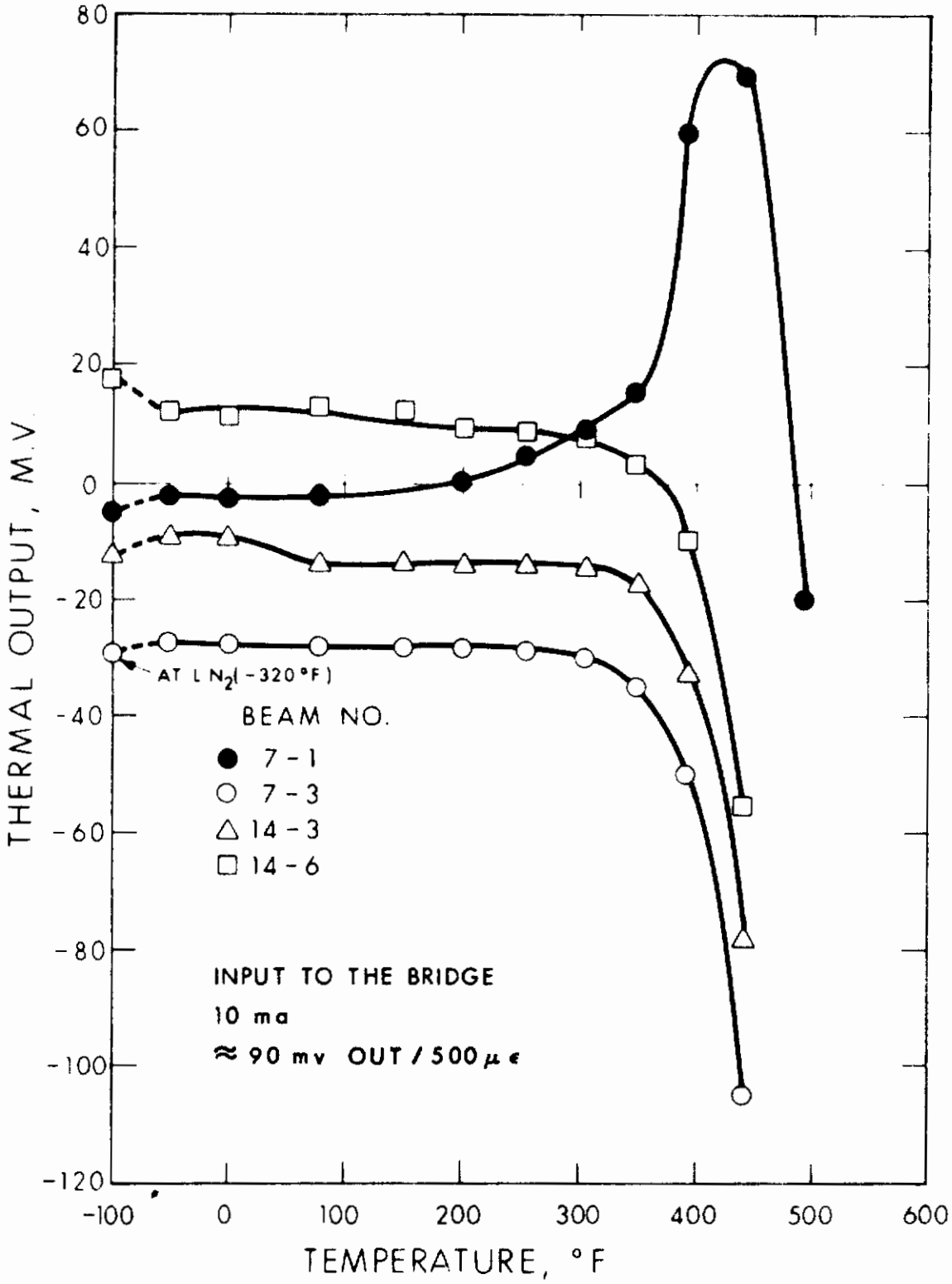

FIG. 19 ZERO SHIFT VS TEMPERATURE

Figures 20 and 21 show input voltage change with time and zero shift with time. The output shift corresponds to bridge unbalance and is a measure of stability. The input shift corresponds to change in absolute bridge resistance. It is felt that the latter was caused by temperature change.

3.1.4 Conclusion and Recommendation

There appears to be no particular problem at temperature up to 300°F with the SP5B silicon beams, but not over 300°F. It is to be noted that this is limited information for few of SP5B beams. Data have not been taken to determine gage factor with temperature and gage characteristic with temperature lower than -100°F.

The beam stability appears quite good. It is recommended that means of extending the temperature limit of voltage breakdown be investigated.

3.2 Examination of High Temperature Epoxy Adhesives

The purpose of this evaluation is to determine the performance of three high temperature epoxy adhesives for semiconductor strain gage application at high temperature. The results show that one of the three epoxies appears good for strain gage application up to 500°F.

3.2.1 Test Objectives

This evaluation test was to study the three types of high temperature epoxy adhesives for bonding semiconductor strain gages to be used at elevated temperature. The following points were determined:

1. Gage factor change with temperature (see Fig. 22).
2. Creep (see Fig. 25).
3. Insulation resistance to ground with temperature (see Fig. 26).

3.2.2 Test Method

The following specimens were used for this experiment:

1. Epoxylite No. 5523 (short time 600°F adhesive).

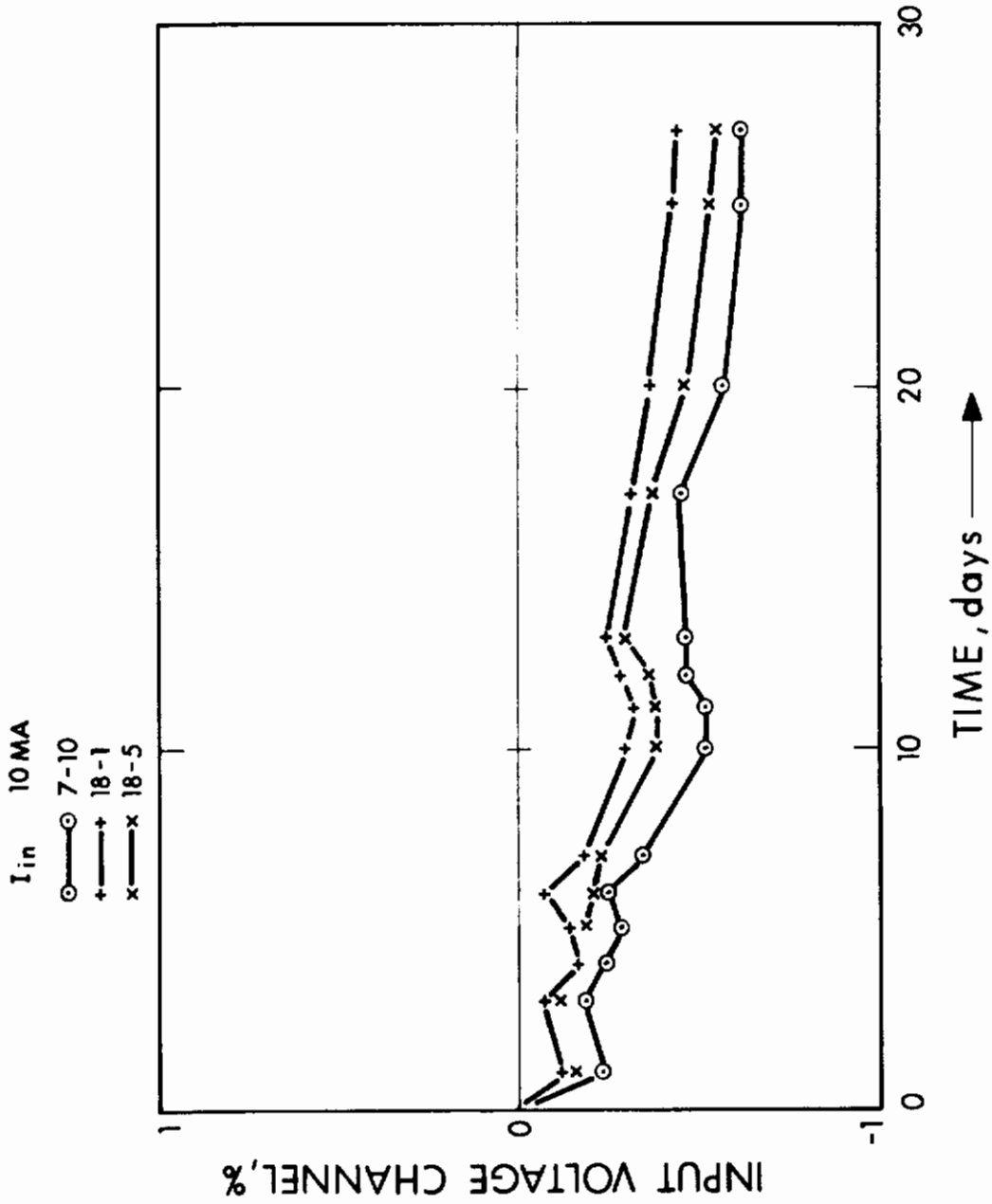

FIG. 20 INPUT VOLTAGE CHANGE VS TIME (SP5B)

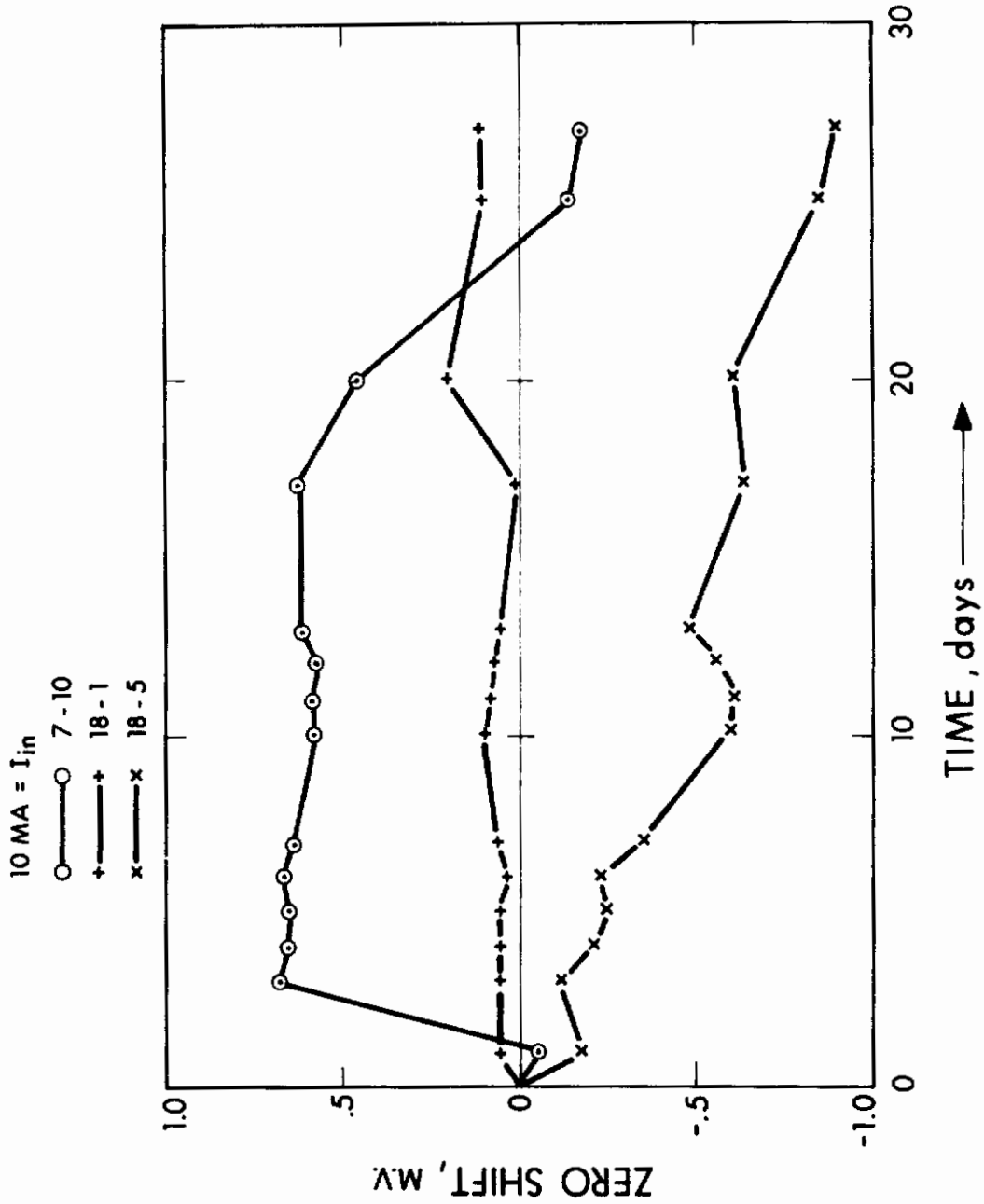

FIG. 21 ZERO SHIFT VS TIME (SP5B)

2. Epoxylite No. 5524 (high temperature adhesive).
3. Epoxylite No. 8831 (strain gage adhesive).
4. Constant stress bending beam (17-4).
5. Strain gages 311-500 (MSI) bulk "P" type resistivity silicon
6. Strain gages SP-2 (diffused gage, EOS).*

Epoxy No. 5523 and No. 5524 were mixed according to the manufacturer's technical bulletins corresponding to each epoxy. Then epoxies were applied to the test beam for base-coat and cured for two hours at +250°F. Epoxy No. 8831 was also mixed according to the bulletin. Then it was applied to the test beam and cured base-coat at room temperature overnight.

Four 311-500 gages and four SP2 gages were bonded to each of the three epoxy base-coated areas, using the same epoxy as the base-coat. The epoxies were all cured using the following schedule:

1. Four hours at +250°F.
2. Eight hours at +350°F.
3. Twenty-four hours at +400°F.
4. Twenty-four hours at +500°F.

The measurements of gage resistance at zero and 500 microstrain in tension and the insulation resistance to ground at 100V dc applied were made at the following temperatures: room temperature, +200°F, +400°F, +450°F, +500°F, and +550°F.

The creep measurements were made at 500 microstrain at the temperatures of +400°F, +500°F, and +550°F for four-hour time at each temperature.

Also the same creep test was performed for twenty-four hours time period at each temperature.

3.2.3 Test Results

1. Application Characteristics. All three epoxies of this test are two-component systems. The thickness of all the epoxy

*Thin layer of "P" type silicon diffused on "N" type silicon substrate.

base-coats was 0.0010 to 0.0013 inch, as measured with a micrometer.

Epoxy No. 5523 is made up of a heavy brown paste (Part A) and a white powder (Part B). It is noted that the white powder, Part B, is much finer than 5524's. This epoxy was hard to mix, even when warmed to +150°F, because of heavy consistency of Part A. The application of a thin base coat of this epoxy to the test beam was somewhat difficult. This epoxy cannot be recommended for a strain gage bonding agent.

Epoxy No. 5524 is made up of an amber liquid (Part A) and a gray powder (Part B). There were no problems in the mixing of this compound. The gray powder, Part B, contains the aluminum filler. It was difficult to apply a thin base coat to the test beam. Also it was difficult to obtain good insulation resistance to ground due to aluminum filler. It was noted that this epoxy No. 5524 lost its adhesion after the first temperature measurement run. It is not recommended that epoxy No. 5524 be used for strain gage application.

Epoxy No. 8831 is made up of an amber liquid (Part A) and a yellow liquid (Part B). Fifty percent of the Part B is crystallized at room temperature. It was necessary to warm Part B up to about +150°F to liquify prior to mixing the compound. There were no particular application problems in using the epoxy No. 8831.

2. Gage Factor Tests. Figure 22 shows the gage factor change with temperature for first temperature measurement run. The gage factor changes of 311-500 gages with temperature are similar for both the 5523 and 8831 adhesives up to +440°F. The gage factor of 311-500 gages with 5523 adhesive decreases rapidly in temperatures above +450°F. It may be due to recuring the epoxy at this temperature. The gage factor

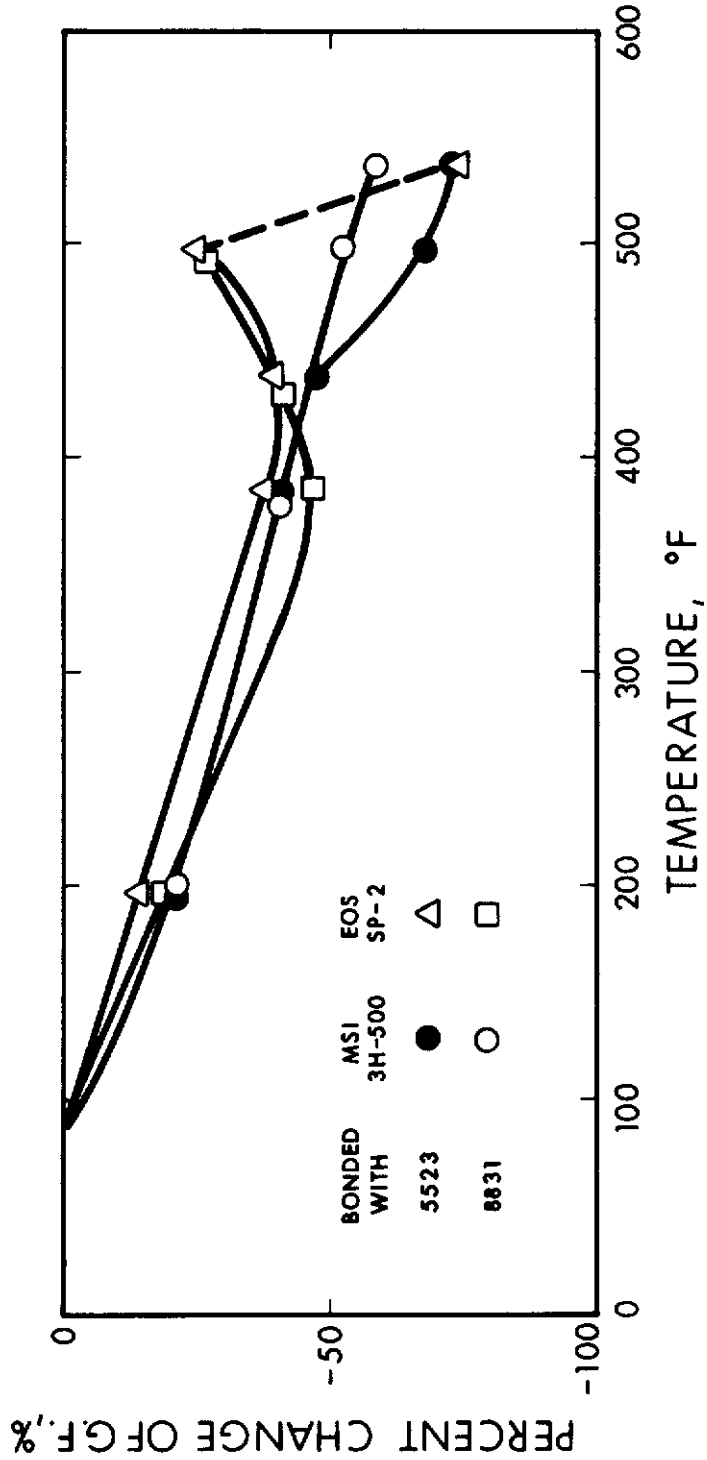

FIG. 22 GAGE FACTOR CHANGE VS TEMPERATURE

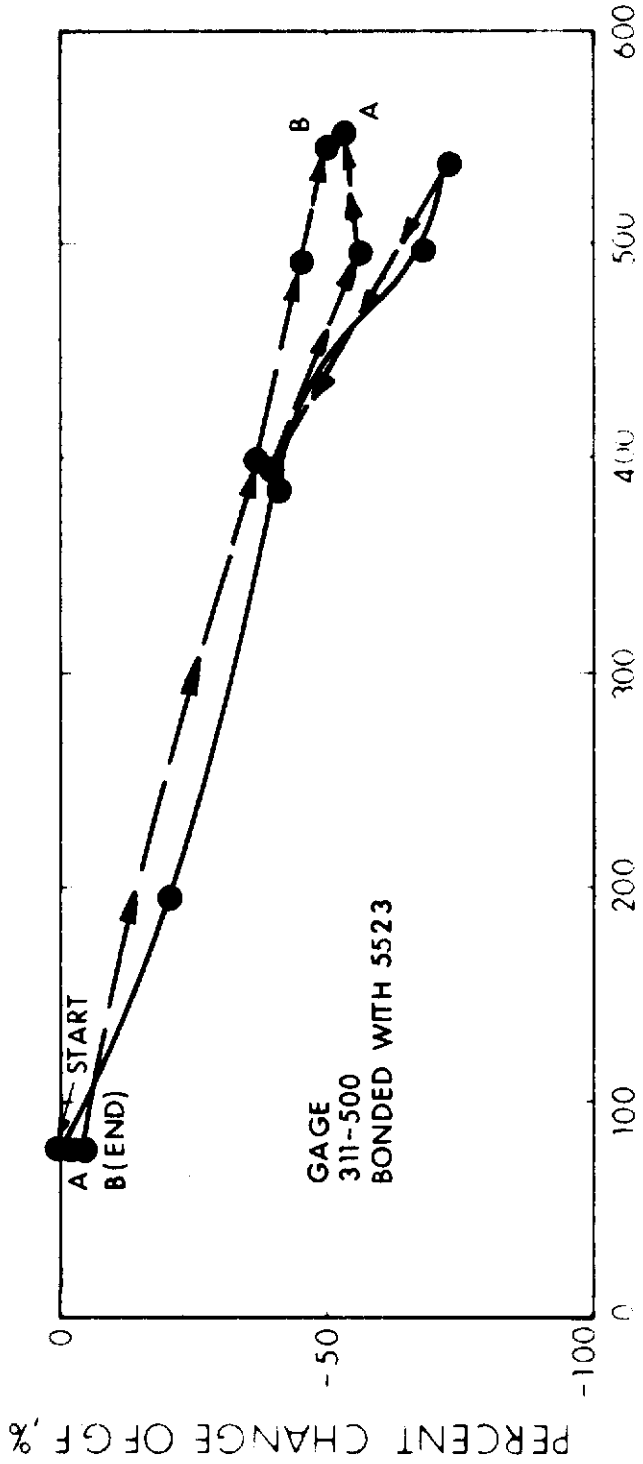

FIG. 23 GAGE FACTOR CHANGE VS TEMPERATURE

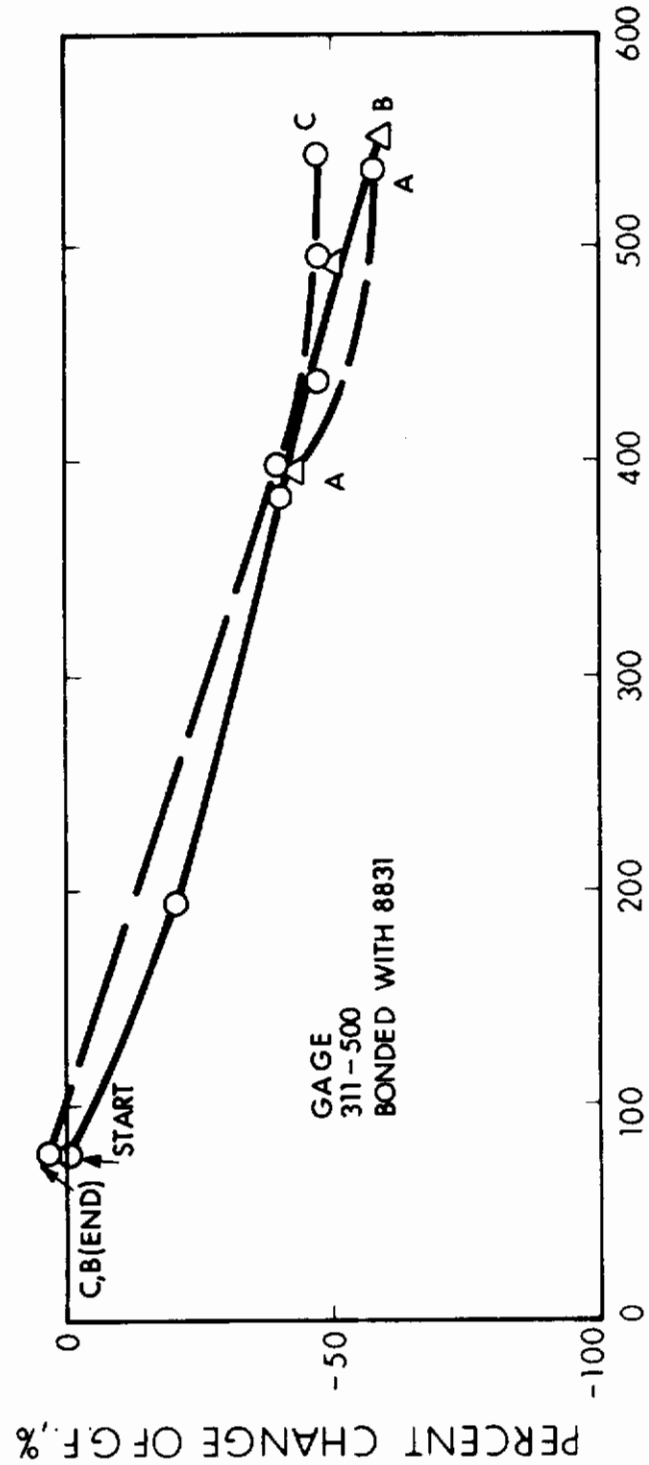

FIG. 24 GAGE FACTOR CHANGE VS TEMPERATURE

data with 5524 adhesive were not obtained due to poor insulation resistance to ground.

It can be seen that the gage factor change of SP-2 with temperature is irregular at elevated temperature due to its P-N junction breakdown.

Figures 23 and 24 also show the gage factor change with temperature. It can be seen that the gage factor of 311-500 gages using 8831 adhesive repeats better than the gage factor of 311-500 gages using 5523 adhesive.

3. Creep Tests. Figure 25 shows the creep versus time. It can be seen that the resistance of gages increases over twenty-four hour time periods at +400°F. It is believed that the cause was due to releasing the previous prestress. It is noted that the resistance change with time is similar for both the 5523 and 8831 adhesives.

4. Insulation Resistance Tests. Figure 26 shows the insulation resistance to ground with temperature. The insulation resistance of both epoxy 5523 and 8831 were greater than 200 K megohms at room temperature and +200°F.

   The insulation resistance of epoxy 5524 was very low. There were only 200 K ohms at room temperature, 1800 ohms at +200°F, and 230 ohms at +400°F.

5. Resistance Tests. Figures 27 and 28 show the resistance change of gages with temperature. The resistance of gages was changed after the first temperature measurement run. It is believed that the shift of gage resistance was due to recure the epoxy at higher temperature. It can be seen that the gage resistance shift using 8831 adhesive is smaller than the resistance shift using 5523 at elevated temperature. Figure 29 shows resistance change of SP-2.

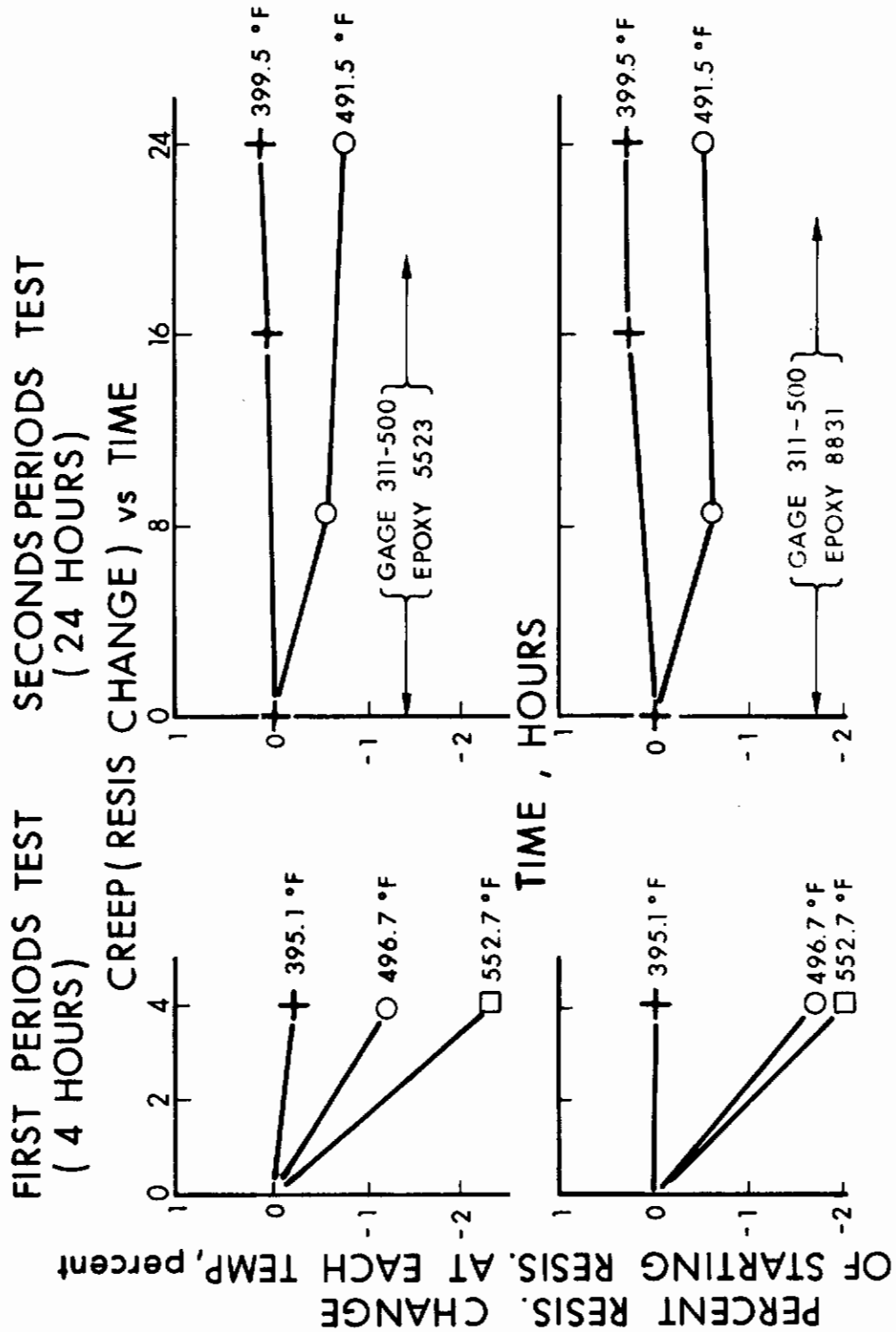

FIG. 25 CREEP (Resistance Change) VERSUS TIME

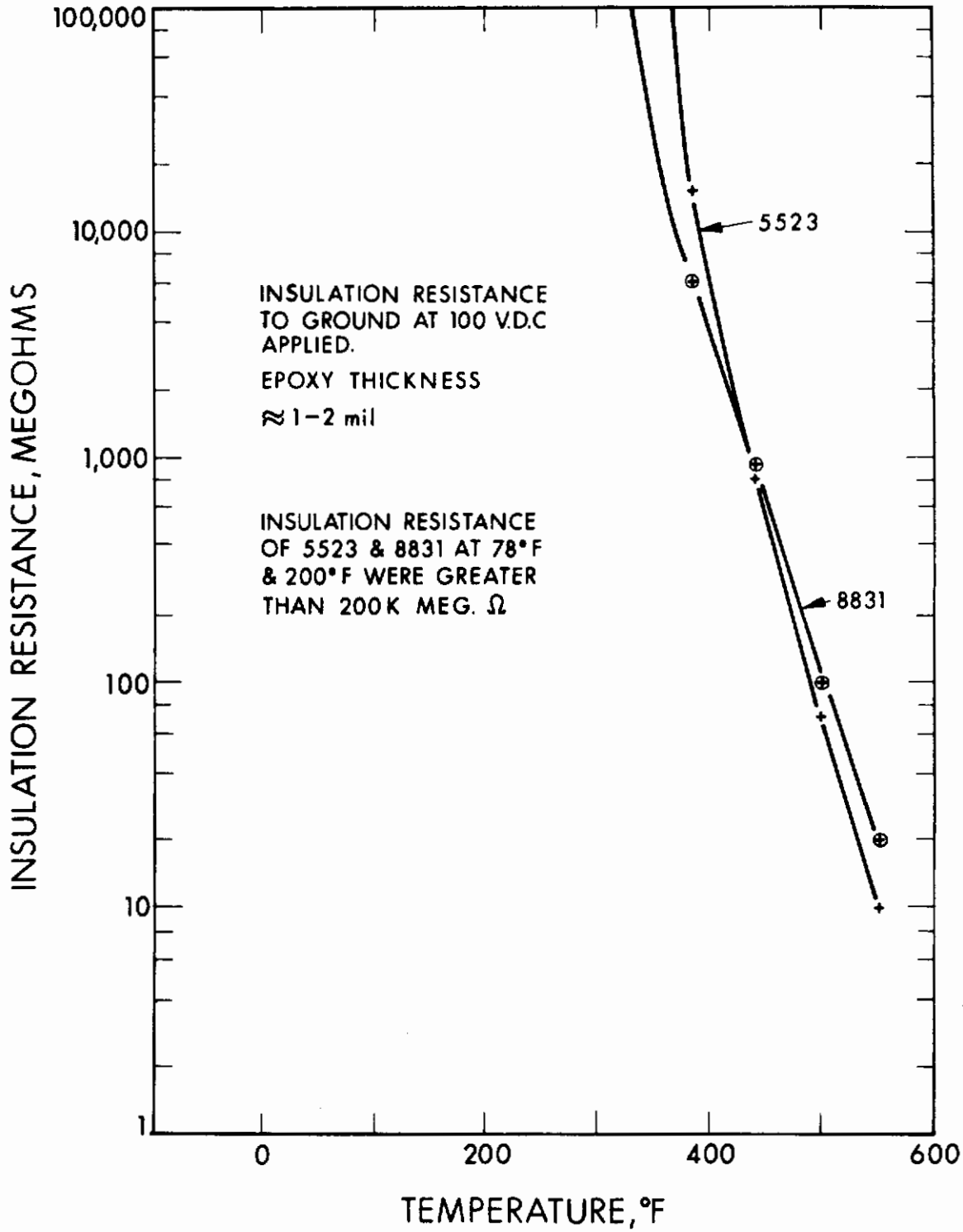

FIG. 26 INSULATION RESISTANCE VS TEMPERATURE

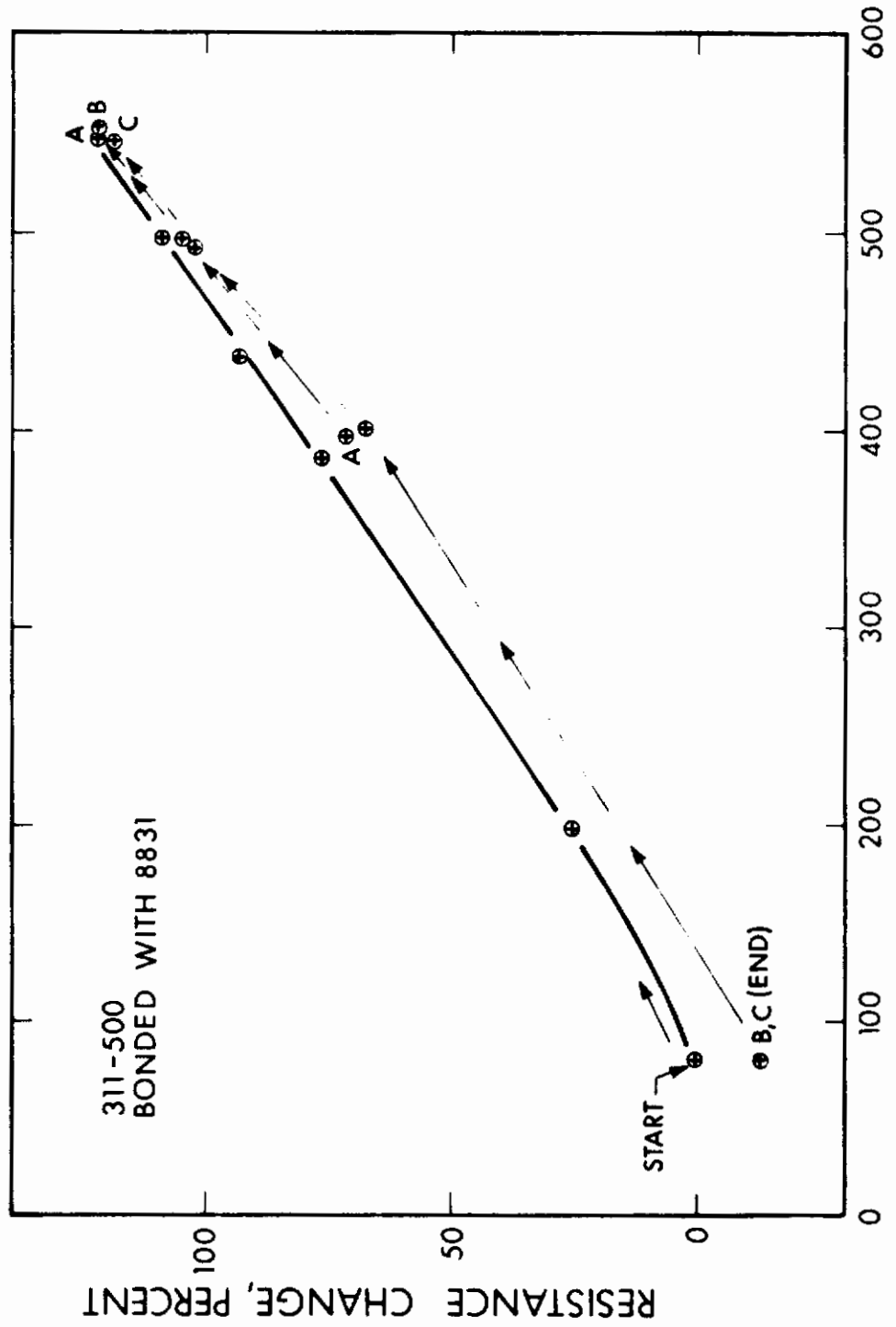

FIG. 27 RESISTANCE CHANGE VERSUS TEMPERATURE

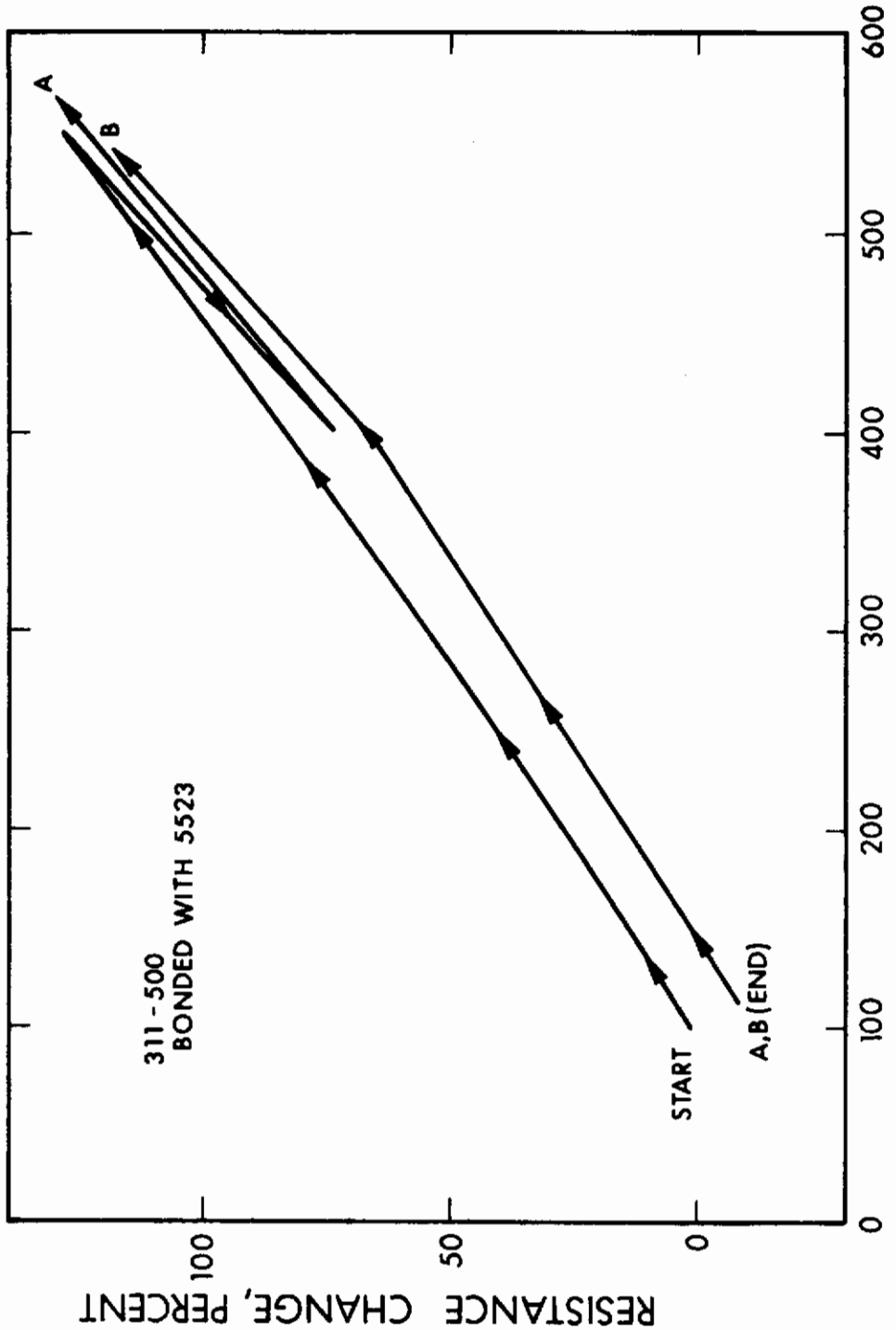

FIG. 28 RESISTANCE CHANGE VS TEMPERATURE

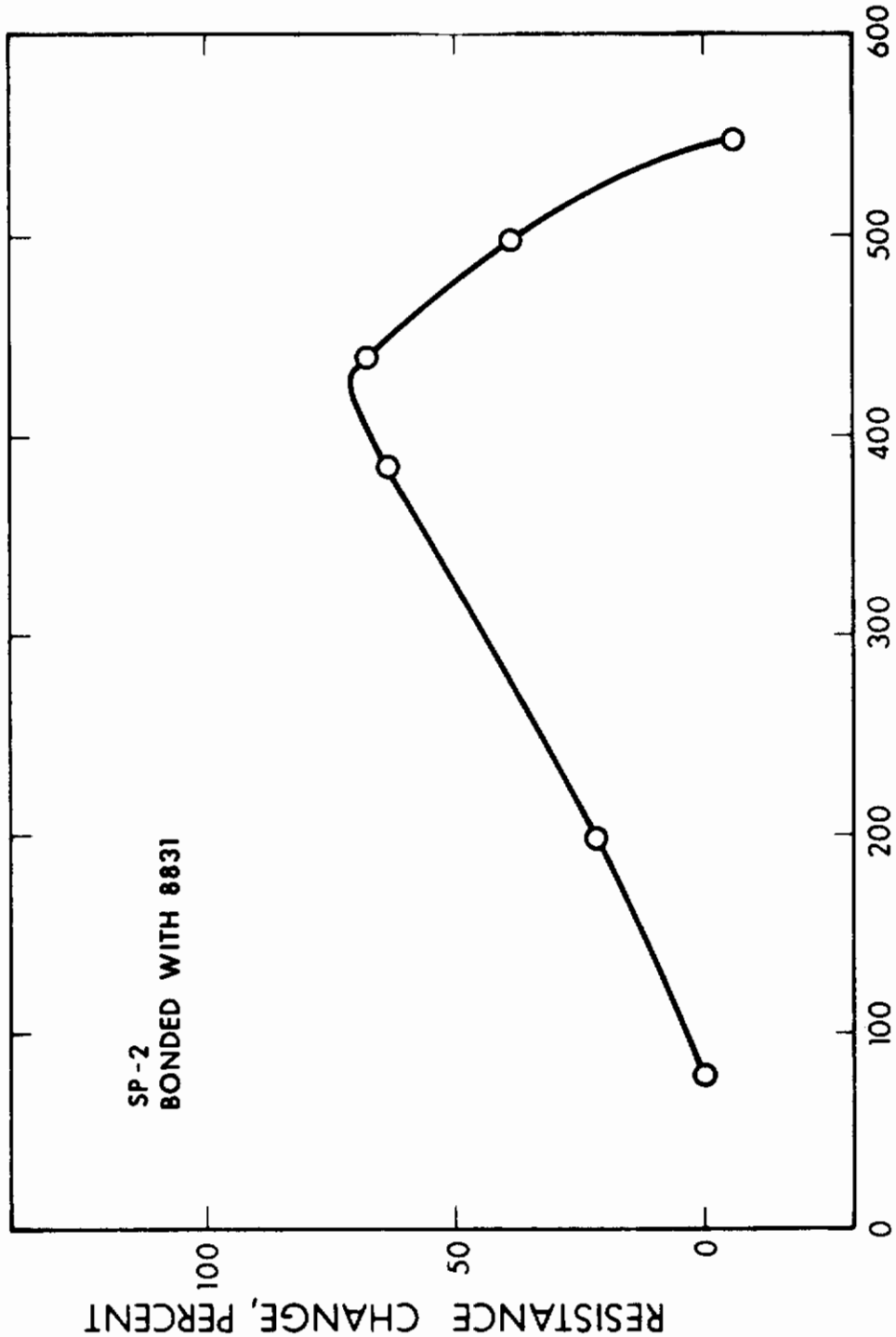

FIG. 29 RESISTANCE CHANGE VS TEMPERATURE

3.2.4 Conclusions and Recommendations

The epoxy 5523 has somewhat poorer characteristics than the epoxy 8831. Also, there are some handling problems in using this epoxy. This epoxy cannot be recommended for the strain gage application because of difficulty in handling. The epoxy 5524 is not suitable for the strain gage application because of its poor insulation resistance and its poor adhesion.

The epoxy 8831 has better characteristics than the epoxies 5523 and 5524. There are no particular problems of application with this epoxy, and its properties make it suitable for this particular usage.

It is recommended that the epoxy 8831 be evaluated for use at cryogenic temperature. Also, it is recommended that the epoxy 8831 be compared to the epoxy 6203 now being used.

Epoxy 8831 is suitable for use as an adhesive for semiconductor strain gages in environmental temperatures up to +500°F.

3.3 Diaphragm Forming

A process of major importance used in the production of these transducers was the diaphragm forming. The advantage of the system used is the fact that the diaphragm exactly matches the stop-plate when it is manufactured by this method. The stop-plate (shown in Fig. 30) is actually used as the die in the forming process.

The diaphragm sheet stock is first carefully welded to a holding ring in a flat but unstretched condition. This ring with its diaphragm is fitted into position over the transducer and located by means of pins in two holes. Forming then takes place and the diaphragm, which is numbered corresponding to its matching stop, is removed together with its holding ring. The correct clearance is then machined from the stop face. The diaphragm is then correctly located onto its transducer body by means of the pins and holes and the two attaching seam-welds are made. The holding ring is now cut free and the excess diaphragm stock is dressed off. This is shown in Fig.31.

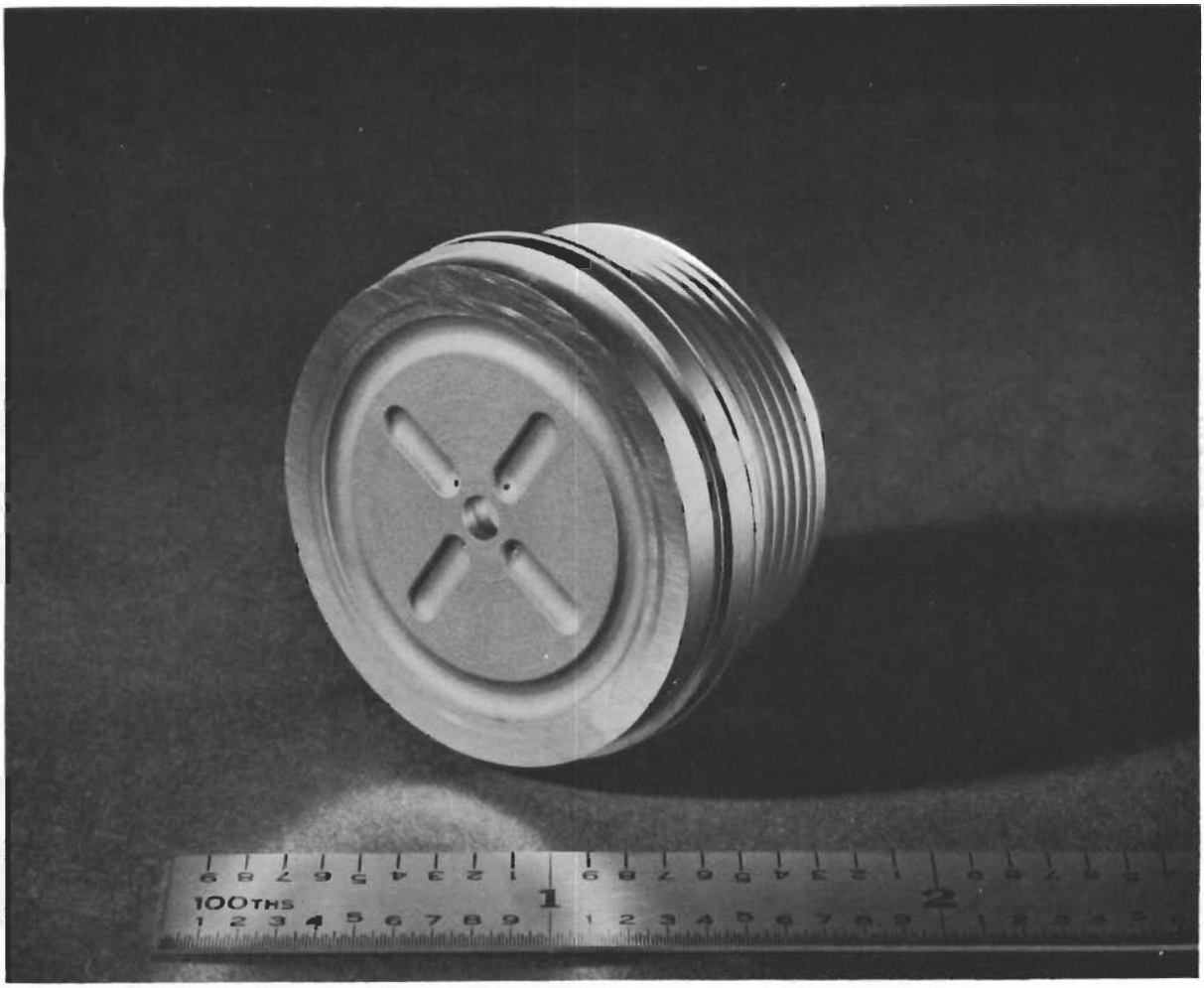

FIG. 30 STOP-PLATE

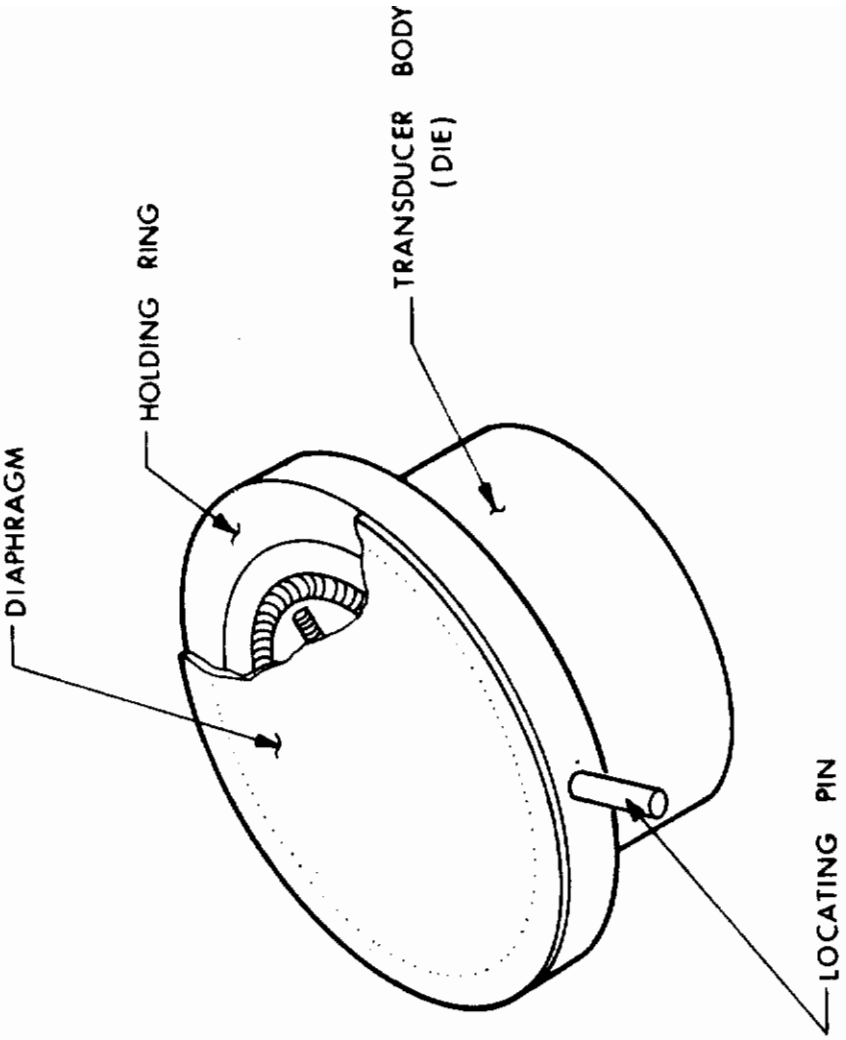

FIG. 31 IMPROVED METHOD OF DIAPHRAGM MANUFACTURE

Forming is effected by high energy rate forming. In the process used, a shock wave is generated by exploding a wire under water and the water conducts the shock-wave to the part to be formed. The wire is exploded by discharging, through high voltage, from a capacitor bank. The forming tool and power unit is shown in Fig. 32 and a diaphragm, before and after forming, is shown in Fig. 33.

FIG. 32 POWER UNIT AND FORMING TOOL

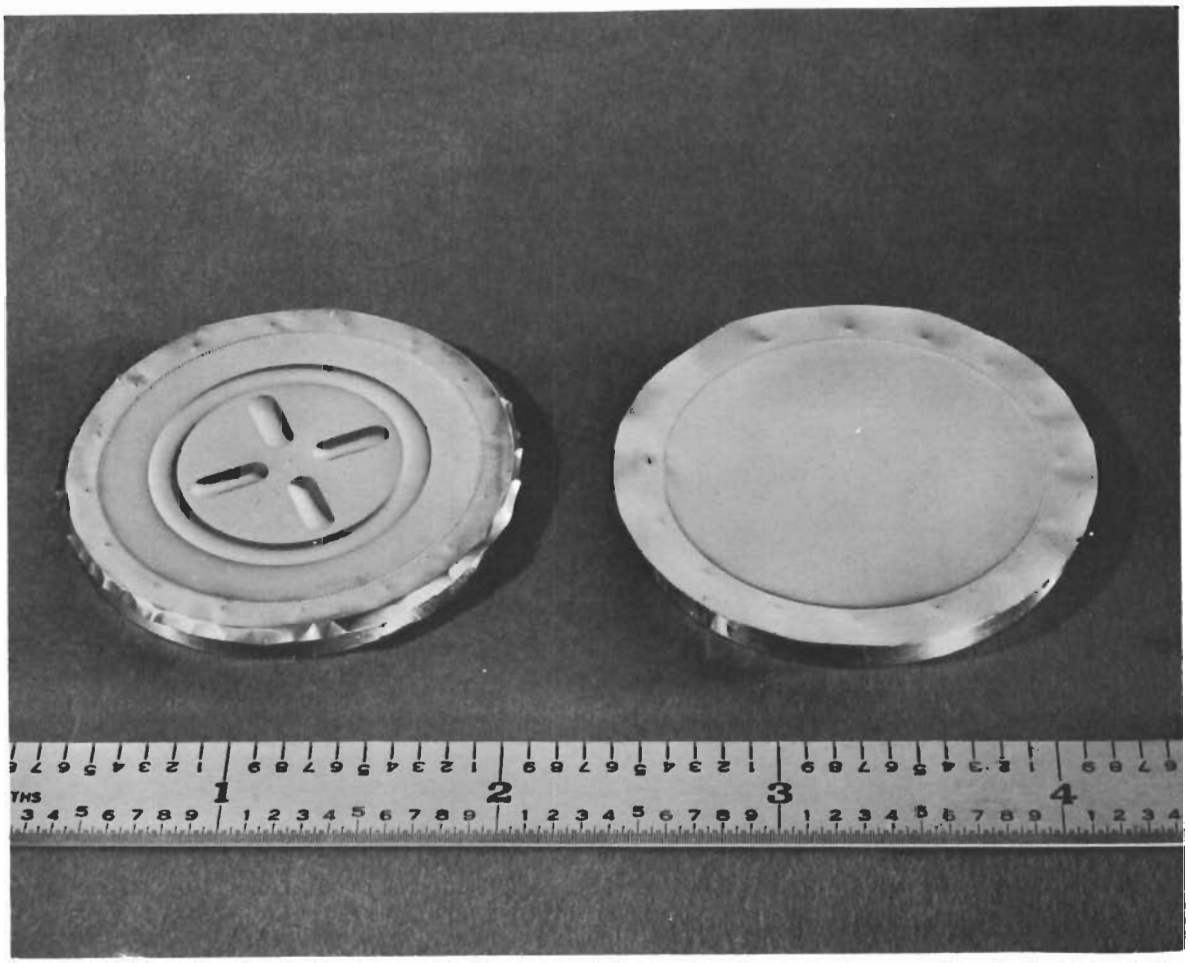

FIG. 33 DIAPHRAGM (After and Before Forming)

APPENDIX I

PRESSURE TRANSDUCER
ROOM AMBIENT TEST DATA

SERIAL No. X-102* DATE: 25 August 1964

INPUT TO BRIDGE 3.158 VOLTS	TYPE OF BRIDGE FULL VOLTS	INPUT TO AMPLIFIER N/A VOLTS	1000Ω SHUNT

PRESSURE psig	OUTPUT	IDEAL STRAIGHT LINE
0	0	0
0.02	16.8	16.28
0.04	33.4	37.56
0.06	49.2	48.84
0.08	64.8	65.12
1.00	81.4	81.40
0.06 Descending	49.7	
0	0	
Full Scale	84.7	
0	-0.1	
Full Scale	84.1	
0	-0.1	
Full Scale	84.7	

LINEARITY	+1.03 %F.S.
HYSTERESIS**	+0.61 %F.S.

**Hysteresis is the difference between 0.06 psi ascending and descending.

*Experimental model using flat stretched diaphragm, diameter 2.2 in.

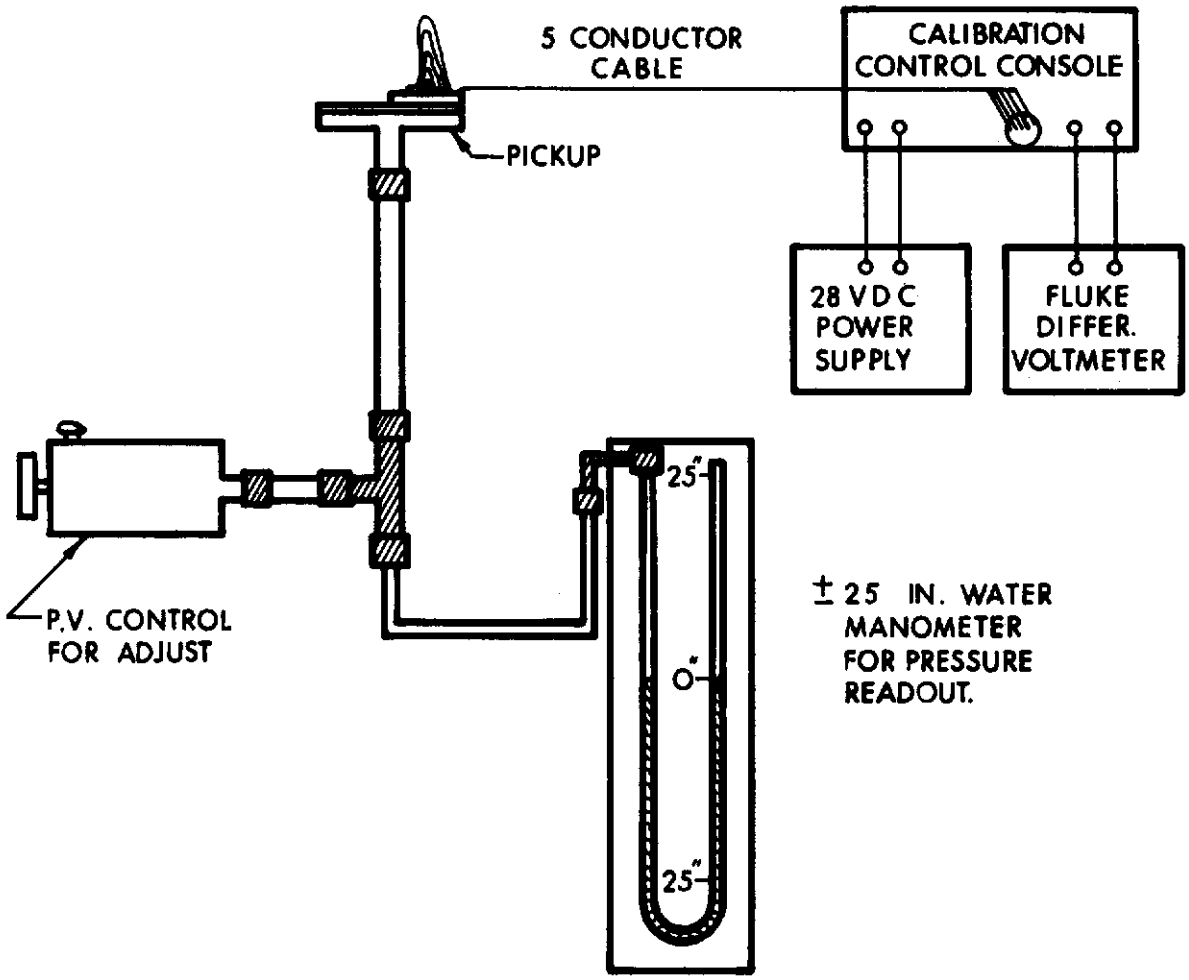

FIG. I-1 TEST SETUP

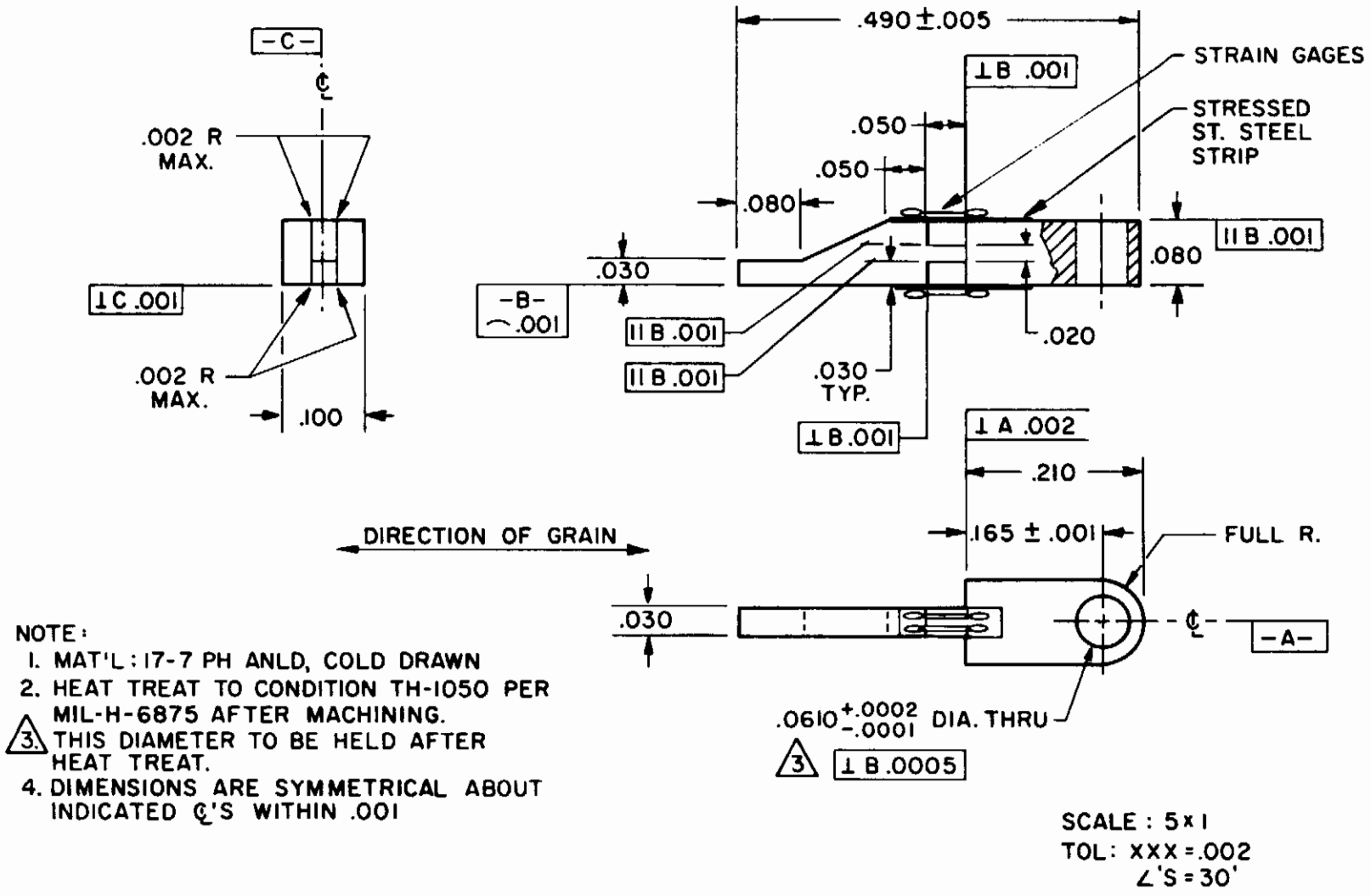

FIG. I-2 EXPERIMENTAL BEAM

TABLE I-1

TEST RESULTS ON CONVOLUTED DIAPHRAGMS

DIAPHRAGM NO. 1 EXPLODED 11/17 ENERGY LEVEL 3.5 kv-1 time DATE 12/1/64

INPUT TO BRIDGE 10 ma at 1. 2. 3.250 vdc WITH 1K SHUNT

		EXPERIMENTAL BEAM				STANDARD BEAM			
Inches of H_2O	PSI	Zero Balance				Zero Balance 21.8Ω LEG 5			
		MV Out	S/L	Dev.	%	MV Out	S/L	Dev.	%
0	0					0 +3.8			
0.5	0.018					27.1	26.47	+0.63	+0.49
1.0	0.036					53.3	52.94	+0.36	
1.5	0.054					79.8	79.41	+0.39	
2.0	0.072					105.9	105.88	+0.42	
2.5	0.090					132.3	132.35	-0.05	
3.0	0.108					158.8	158.8		
0					24.2Ω	0 +7.3			
0.5					LEG 5	28.0	26.7	+1.3	
1.0					Z BAL	54.8	53.4	+1.4	+0.87
1.5						81.2	80.1	+1.1	
2.0						107.8	106.8	+1.0	
2.5						134.4	133.5	0.9	
3.0						160.2	160.2		

REMARKS: Standard beam only.

TABLE I-1 (Con.)

DIAPHRAGM NO. 2 EXPLODED 11/17 ENERGY LEVEL 3.5 kv-1 time DATE 12/1/64

INPUT TO BRIDGE 10 ma at 1. 2. 3.313 vdc WITH 1K SHUNT

Inches of H_2O	PSI	EXPERIMENTAL BEAM Zero Balance MV Out	S/L	Dev.	%	STANDARD BEAM Zero Balance 91.6Ω LEG 5 MV Out	S/L	Dev.	%
0	0					0			
0.5	0.018					34.2	33.1	+1.1	
1.0	0.036					68.0	66.2	+1.8	
1.5	0.054					101.2	99.3	+1.9	0.95
2.0	0.072					134.1	132.4	+1.7	
2.5	0.090					166.4	165.5	+0.9	
3.0	0.108					198.6	198.6	0	
2.5									
2.0									
1.5									
1.0									
0.5									
0									

REMARKS:

TABLE I-1 (Con.)

DIAPHRAGM NO. 3 EXPLODED 11/17 ENERGY LEVEL 4.0 kv and 3.0 kv DATE 12/1/64

INPUT TO BRIDGE 10 ma at 1. 2. 3.240 vdc WITH 1K SHUNT

Inches of H_2O	PSI	EXPERIMENTAL BEAM Zero Balance 42.3Ω LEG 5 MV Out	S/L	Dev.	%	STANDARD BEAM Zero Balance 19.8Ω LEG 5 MV Out	S/L	Dev.	%
0	0	0 1.1				0 +2.2			
0.5	0.018	8.8	8.18	+0.62		25.4	24.2	+1.2	
1.0	0.036	17.0	16.36	+0.64	+1.30	49.8	48.4	+1.4	+0.96
1.5	0.054	25.1	24.54	+0.64		73.5	72.6	+0.9	
2.0	0.072	33.1	32.72	+0.38		97.5	96.8	+0.7	
2.5	0.090	41.0	40.90	+0.10		121.2	121.0	+0.2	
3.0	0.108	49.1	49.1			145.2	145.2		
43.1Ω Z BAL 0		0 -1.9				0 +1.4	0		
0.5		8.2	7.73	+0.47		24.9	24.13	+0.76	
1.0		16.1	15.46	+0.64	+1.38	49.2	48.26	+0.94	+0.65
1.5		23.8	23.19	+0.61		73.2	72.39	+0.81	
2.0		31.4	30.92	+0.48		97.1	96.52	+0.58	
2.5		38.9	38.65	+0.25		121.1	120.65	+0.45	
3.0		46.4	46.4			144.8	144.8		

REMARKS:

TABLE I-1 (Con.)

DIAPHRAGM NO. 4 EXPLODED 11/17 ENERGY LEVEL 3.5 kv -twice DATE 11/30/64

INPUT TO BRIDGE 10 ma at 1. - 3.064 2. - 3.260 vdc WITH 1K SHUNT

		EXPERIMENTAL BEAM				STANDARD BEAM			
Inches of H_2O	PSI	Zero Balance 17.9Ω LEG 5				Zero Balance 1. 4Ω LEG 7 2. 77.9Ω LEG 5			
		MV Out	S/L	Dev.	%	MV Out	S/L	Dev.	%
0	0	0	0	0		1. 0 + 2.8	0		
0.5	0.018	9.6	8.35	+1.25	+2.5	22.4	21.83	+0.57	
1.0	0.036	17.8	16.70	+1.1		44.4	43.66	+0.74	+0.56
1.5	0.054	25.7	25.05	+0.65		66.2	65.49	+0.71	
2.0	0.072	33.8	33.40	+0.40		87.6	87.32	+0.28	
2.5	0.090	42.0	41.75	+0.25		109.1	109.15	-0.05	
3.0	0.108	50.1	50.10	0		131.0 129.8	131.0 129.8		
2.5		42.0	41.75	+0.25		2. 108.2	108.15	+0.05	
2.0		33.8	33.40	+0.40		86.7	86.52	+0.18	
1.5		25.7	25.05	+0.65		65.5	64.89	+0.61	
1.0		17.5	16.70	+0.80		44.2	43.26	+0.94	+0.72
5		9.4	8.35	+1.05	+2.07	22.4	21.63	+0.77	
0		-0.1	0			0 +3.9	0		

REMARKS:

TABLE I-1 (Con.)

DIAPHRAGM NO. 6 EXPLODED 11/17/64 ENERGY LEVEL 3.5 kv-3 tms DATE 12/1/64

INPUT TO BRIDGE 10 ma at 3.244 vdc WITH 1 K SHUNT

		EXPERIMENTAL BEAM				STANDARD BEAM			
Inches of H_2O	PSI	Zero Balance				Zero Balance 6 Ω leg. 5			
		MV Out	S/L	Dev.	%	MV Out	S/L	Dev.	%
0	0					.0			
.5	0.018					23.7	23.2	+ .5	
1.0	0.036					47.4	46.4	+1.0	+ .72
1.5	0.054					70.1	69.6	+ .5	
2.0	0.072					93.2	92.8	+ .4	
2.5	0.090					116.5	116.0	+ .5	
3.0	0.108					139.2	139.2		
0					Z Bal. 10.7 Ω	0			
.5					LEM 5	23.8	23.26	+ .54	
1.0						47.7	46.52	+1.18	+ .84
1.5						70.5	69.78	+ .72	
2.0						93.7	93.04	+ .66	
2.5						116.7	116.30	+ .40	
3.0						139.6	139.6		

REMARKS: Standard beam only

TABLE I-1 (Con.)

DIAPHRAGM NO. 7 EXPLODED 11/16 ENERGY LEVEL 3.5 kv-1 time DATE 12/1/64

INPUT TO BRIDGE 10 ma at 1. 2. 3.2364 vdc WITH 1K SHUNT

		EXPERIMENTAL BEAM				STANDARD BEAM			
Inches of H_2O	PSI	Zero Balance				Zero Balance 23.7Ω LEG 5			
		MV Out	S/L	Dev.	%	MV Out	S/L	Dev.	%
0	0					0			
0.5	0.018					22.0	21.9	+0.1	
1.0	0.036					44.0	43.8	+0.2	
1.5	0.054					66.9	65.9	+1.2	0.98
2.0	0.072					88.0	87.6	+0.4	
2.5	0.090					109.9	109.9	0	
3.0	0.108					131.8	131.8	0	
2.5									
2.0									
1.5									
1.0									
0.5									
0									

REMARKS: 0 return reading 24.1Ω

APPENDIX II

OPTIMUM CONFIGURATION OF STRAIN GAGE PRESSURE TRANSDUCER

1. THEORY

The proposed strain gage pressure transducer is illustrated in Fig. II-1. It consists basically of two parts: (1) cantilever beam, (2) circular diaphragm. The pressure P, that is to be measured, is incident on the underside of the diaphragm. The extension of the beam touching the diaphragm is then forced upward, causing the main body of the beam to undergo bending. The two strain gages placed at the top and bottom of the beam, at the intersection of the beam and the rigid wall, measure the amount of strain experienced by the beam - both tension (bottom of beam), and compression (top of beam). In the figure, L = length of beam, R = radius of diaphragm, h = thickness of diaphragm, t = thickness of beam, b = width of beam. These five quantities establish the configuration of the transducer. We wish to determine a functional relationship between L, R, h, t, b, which satisfies the condition that the strain measured by the strain gages is a maximum, for a given applied pressure, P.

If the diaphragm is placed under an initial tension of N lbs/in., then the deflection w_o of the center of the diaphragm under a uniform pressure P is

$$w_o = \frac{PR^4}{64\,D} \cdot \frac{1}{1+\alpha} \qquad (1)$$

where, $D = Eh^3/12(1-\nu^2)$, $\alpha = NR^2/14.68\,D$. Here, E and ν are Young's Modulus and Poisson's ratio, respectively, of the material contained in the diaphragm and beam. The deflected diaphragm is shown in Fig. II-2.

The amount of bending shown in the figure is exaggerated, since, in reality, the deflection w_o will be of the order of magnitude of the diaphragm thickness, h. The initial tension per unit length, N, is given by

$$N = \frac{Eh}{1 - \nu} \epsilon_r \tag{2}$$

where, ϵ_r is the radial strain in the diaphragm due to N. The quantity ϵ_r can be measured by the strain gage. Since the diaphragm does not have a hole at its center, the strain ϵ_r will be constant over the surface. Hence, the measured value of ϵ_r should be independent of the location of the strain gage on the diaphragm surface.

Consider a single force F to be applied perpendicular to the diaphragm at its center. Refer to Fig. II-3. The deflection w_o of the center of the diaphragm will then be

$$w_o = \frac{FR^2}{16\pi D} \cdot \frac{1}{1 + \alpha} \tag{3}$$

By equating w_o as given by Eq. (3) to w_o in Eq. (1), we obtain

$$F = \frac{PR^2\pi}{4} = \frac{PA}{4} \tag{4}$$

which represents the single force, applied at the center of the diaphragm, that is equivalent to the uniform pressure, P.

Fig. II-4 shows the bending (exaggerated) of the cantilever beam and diaphragm under the action of the uniform pressure P. The equivalent force F is opposed by the restoring force F_d of the diaphragm and the restoring force F_B of the beam. Since the deflection of the tip end of a cantilever beam acted on by a normal force F at the end of the beam is given by $w_o = FL^3/3EI$, where I is the "moment of inertia" of the cross section of the beam ($I = bt^3/12$), we see that

$$F_B = \frac{3EI}{L^3} w_o$$

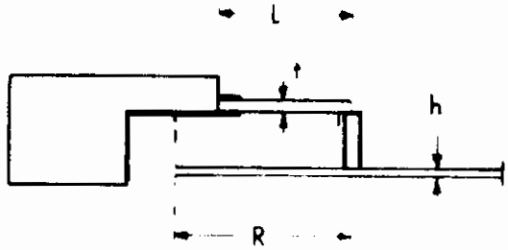

FIG. II-1 STRAIN GAGE PRESSURE TRANSDUCER

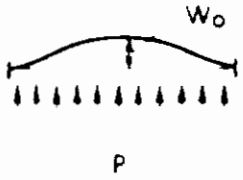

FIG. II-2 DEFLECTED DIAPHRAGM

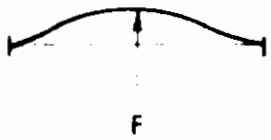

FIG. II-3 APPLIED PERPENDICULARLY

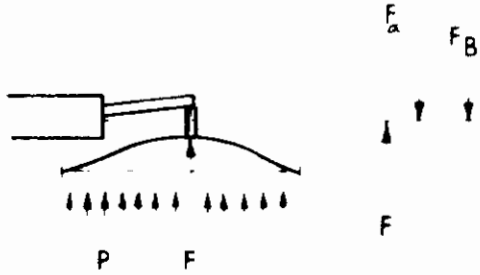

FIG. II-4 BENDING OF THE CANTILEVER BEAM

Also, from Eq. (3), we have

$$F_d = \frac{16\pi D}{R^2} (1 + \alpha) w_o$$

Hence, if the system is in equilibrium, then

$$\frac{PA}{4} = F_B + F_d = \frac{3EI}{L^3} w_o + \frac{16\pi D}{R^2} (1 + \alpha) w_o \qquad (5)$$

The stress at the top or bottom of the beam, adjacent to the rigid support (at the location of the strain gages - refer to Fig. II-1) is given by $\sigma = F_B Lt/2I$. The corresponding strain is $\epsilon = \sigma/E$. Combining this latter equation with the above equation defining F_B, we get

$$\epsilon = \frac{3t}{2L^2} w_o \qquad (6)$$

Eliminating w_o from Eqs. (5) and (6) we then have

$$\epsilon = \frac{\frac{3}{8} \pi R^2 PLt}{\frac{Ebt^3}{4} + \frac{4 \pi E}{3(1-\nu^2)} \left[\frac{h^3}{R^2} + 0.82(1 + \nu) \epsilon_r h \right] L^3} \qquad (7)$$

Eq. (7) gives the strain in the beam, at the location of the strain gages (Fig. II-1), as a function of L, R, h, t, b. From Eq. (7) we see immediately that the strain ϵ is <u>increased</u> by making the beam width b and diaphragm thickness h as small as possible, and by making the diaphragm radius R as large as possible. We also see that the beam length L and beam thickness t each provide ϵ with a relative maximum. It should then be possible to maximize ϵ with respect to either L or t. For brevity, let

$$A = 3/8\ \pi R^2 P, \quad B = \frac{Eb}{4}, \quad C = \frac{4\pi E}{3(1-\nu^2)}\left[\frac{h^3}{R^2} + 0.82(1+\nu)\,\epsilon_r h\right]$$

Then, treating L as constant and solving $d\epsilon/dt = 0$ for t, we find the value t' at which ϵ is a maximum,

$$t' = \left(\frac{C}{2B}\right)^{1/3} L \tag{8}$$

Substituting t' in Eq. (7) then gives the maximum strain, ϵ_{max}, for any value L:

$$\epsilon_{max} = \frac{A}{3}\left(\frac{4}{BC^2}\right)^{1/3} \frac{1}{L} \tag{9}$$

Note that ϵ_{max} increases with decreasing values of L. Also, for small b and h, B and C are small, making ϵ_{max} large, and that for large R, A and C are large and small, respectively, making ϵ_{max} large.

If we treat t as constant and solve $d\epsilon/dL = 0$ for L, we obtain the value L' which makes ϵ a maximum,

$$L' = \left(\frac{B}{2C}\right)^{1/3} t \tag{10}$$

and so

$$\epsilon_{max} = \frac{A}{3}\left(\frac{4}{B^2C}\right)^{1/3} \frac{1}{t} \tag{11}$$

Note that ϵ_{max} varies inversely with t, and also that ϵ_{max} will be large for small b and h and large R.

In determining the optimum configuration of the transducer, either the set of equations (8), (9), or the set (10), (11) may be employed. In both cases, maximum strain is achieved by assigning the smallest practical values to h and b, and the largest practical value to R. Also, if Eq. (9) is used to compute ϵ_{max}, then a minimum practical value should be assigned to L, and if Eq. (11) is used, then a minimum practical value should be assigned to t.

2. EXPERIMENT

Of particular interest is the transducer configuration required to measure pressures as low as 0.1 psi. For the type of transducer shown in Fig. II-1, the smallest practical values of beam width and diaphragm thickness are, respectively b = 0.02" and h = 0.001". The diaphragm radius consistent with that used in the transducers which measure pressures up to 7 psi is R = 0.35". We shall assign a value to L and compute the optimum beam thickness from Eq. (8) and the maximum strain from Eq. (9). The smallest practical beam length is L = 0.238". Since the beam and diaphragm are made of 17-7PH, therefore Young's Modulus and Poisson's ratio are, respectively, $E = 29 \times 10^6$ lbs/in^2, $\nu = 0.28$. Finally, according to experiments performed in the laboratory, the initial strain in the diaphragm is $\epsilon_r = 208 \times 10^{-6}$. Letting P = 0.1, we then get $A = 1.44 \times 10^{-2}$ lbs, $B = 1.45 \times 10^5$ lbs/in, C = 29.8 lbs/in. From Eq. (8), t' = 0.0111", and from Eq. (9) the maximum strain is $\epsilon_{max} = 63.5 \times 10^{-6}$. The value t' = 0.0111" is a practical size for the beam thickness, but the computed maximum strain is one tenth the strain that is desirable for the low pressure transducer. The only practical way to increase the value of ϵ_{max} is to increase the value of R.

We shall let $\epsilon_{max} = 635.0 \times 10^{-6}$, the desired maximum strain, and employ Eq. (9) to solve for the appropriate diaphragm radius, R. Having obtained R we shall then determine the beam thickness from Eq. (8). After a little algebraic manipulation, Eq. (9) becomes

$$R^5 - 1.304\, R^2 - 5.98 \times 10^{-3} = 0$$

Solving the above graphically, we find the root to be R = 1.095". With this value of R, C = 28.9, so that Eq. (8) yields, t' = 0.011", which is very close to the previously calculated value of t'.

To summarize the foregoing, in order to achieve a strain of 635.0×10^{-6} in the transducer beam, for an applied pressure of 0.1 psi, the dimensions of the transducer should be, h = 0.001", b = 0.02", L = 0.238" and, R = 1.095", t = 0.011".

APPENDIX III

OPTIMUM CONFIGURATION OF STRAIN GAGE PRESSURE TRANSDUCER WITH CONVOLUTED DIAPHRAGM SURFACE

In an effort to increase the sensitivity of the low pressure, strain gage pressure transducer, a convolution has been built into the (circular) diaphragm surface. Refer to Fig. III-1. Thus, under an applied pressure P, the deformation of the diaphragm occurs principally in the bending of the convolution, rather than in the bending of the entire diaphragm surface, thereby permitting a greater deflection of the diaphragm center.

The first step in determining the optimum configuration of the transducer is to derive a relationship between the force acting on the diaphragm, under an applied pressure P, and the corresponding deflection of the diaphragm. In order to simplify the derivation, we shall assume that the initially flat portion of the diaphragm remains undistorted during the deflection, i.e., that the deformation occurs entirely in the convolution (Fig. III-1(b)). Figure III-2 shows the (undistorted) convolution in more detail. Note that it is not a complete semi-circle. If we think of the convoluted surface as being formed by a large number of narrow, adjacent strips, each having a width w (where, $w \ll C$, C = circumference of diaphragm) and a thickness h, where h = thickness of diaphragm, then we can regard the cross section shown in Fig. III-2 as a curved beam, having a width w and a thickness h, where, $w \sim h$. Thus, we shall determine the deformation of the convoluted surface, and hence the deflection of the central part of the diaphragm, by examining the bending of a single, initially curved beam. In Fig. III-2 we regard one end of the beam as being rigidly supported and consider the other end to be acted on by a force F_1. We shall determine the displacement, δ, of the end of the beam in the

direction of the applied force, F_1. The strain energy, U, of bending is given by

$$U = \int \frac{M^2 ds}{2EI_1} = \int_0^{\pi - 2\alpha} \frac{M^2 r d\varphi}{2EI_1} \tag{1}$$

where, E = Young's Modulus, $I_1 = wh^3/12$, r and φ are the polar coordinates of a cross section of the beam, and M is the bending moment at this cross section. Here,

$$M = F_1 d = r[\cos \alpha - \cos(\varphi + \alpha)] \tag{2}$$

The displacement is given by

$$\delta = \frac{\partial U}{\partial F_1} \tag{3}$$

Substituting Eq. 2 in Eq. 1 gives

$$U = \frac{6 F_1^2 r^3}{E w h^3} \mu$$

where

$$\mu = (\cos^2 \alpha + \tfrac{1}{2})(\pi - 2\alpha) - \tfrac{1}{2} \sin 2\alpha$$

Hence, Eq. 3 yields

$$\delta = \frac{12 F_1 r^3}{E w h^3} \mu \tag{4}$$

Since we have assumed that the unconvoluted portion of the diaphragm remains undistorted, i.e., rigid, under the pressure P, it then follows that $F_1 = F_d/N$, where F_d = force acting on diaphragm due to the applied pressure P, and N is the total number of individual curved beams (of width w) contained in the convoluted surface. (The equation, $F_1 = F_d/N$, is not exactly correct if the force of gravity has a component perpendicular to the diaphragm; it is correct, however, if the pressure transducer is in free-fall, or if we consider the diaphragm to be massless.) Then,

since $N = 2\pi R/w$, where R is the radius of the unconvoluted surface - refer to Fig. III-3, we have $F_1 = F_d w/2\pi R$. Substituting in Eq. 4 we finally get

$$F_d = \frac{\pi E R}{6\mu}\left(\frac{h}{r}\right)^3 \delta \qquad (5)$$

Figure III-4 shows the complete pressure transducer, consisting of the convoluted diaphragm and the beam containing the strain gages. The force on the beam, F_B, causing the displacement δ is given by

$$F_B = \frac{3EI}{L^3}\,\delta \qquad (6)$$

where, L = length of beam, and $I = bt^3/12$. Here, b = width of beam and t = thickness of beam. In order for equilibrium to exist, it must be true that

$$PA = F_d + F_B$$

where, A = area of unconvoluted surface = πR^2. Thus,

$$\pi R^2 P = \frac{\pi E R}{6\mu}\left(\frac{h}{r}\right)^3 \delta + \frac{Ebt^3}{4L^3}\,\delta$$

The strain, ϵ, measured by the strain gages at the base of the beam is given by

$$\epsilon = \frac{3t}{2L^2}\,\delta$$

Eliminating δ from the above two equations then gives

$$\epsilon = \frac{3\pi R t L P}{E\left(\frac{bt^3}{2R} + \frac{\pi L^3}{3\mu}\frac{h^3}{r^3}\right)} \qquad (7)$$

From Eq. 7 we see that the strain ϵ can be increased by making R and r (= radius of curvature of convolution) as large as possible, and by making b, h and α (μ is a function of α) as small as possible. We also see that L and t each provide ϵ with a relative maximum. Hence, we can maximize ϵ with respect to either L or t. Treating L as a constant and solving $d\epsilon/dt = 0$ for t, we find the value t' at which ϵ is a maximum,

$$t' = \left(\frac{\pi R}{3b\mu}\right)^{\frac{1}{3}} \frac{Lh}{r} \tag{8}$$

Substituting t' in Eq. 7 then gives the maximum strain, ϵ_{max}, for any value of L:

$$\epsilon_{max} = 6 \frac{P}{E} \frac{Rr^2}{Lh^2} \left(\frac{\pi R\mu^2}{3b}\right)^{\frac{1}{3}} \tag{9}$$

The convolution dimensions presently being considered at EOS for a low pressure ($P = 0.10$ lbs/in^2) transducer are $\alpha = 25^\circ 5'$ ($\mu = 2.606$) and $r = 0.0607$". For this same transducer, $h = 0.001$", $b = 0.02$", $E = 29 \times 10^6$ lbs/in^2. By assigning a value to ϵ_{max}, namely, $\epsilon_{max} = 635 \times 10^{-6}$, we can determine the optimum functional relationships L(R) and t(R). These will prove helpful in completing the design of the transducer. Substituting the foregoing values in Eq. 9 yields

$$L = 0.850\, R^{\frac{4}{3}}$$

Substituting the above in Eq. 8 yields

$$t = 0.0380\, R^{\frac{5}{3}}$$

Figure III-5 shows L and t plotted as a function of R.

FIG: III-1 CROSS-SECTIONAL VIEW OF DIAPHRAGM SURFACE

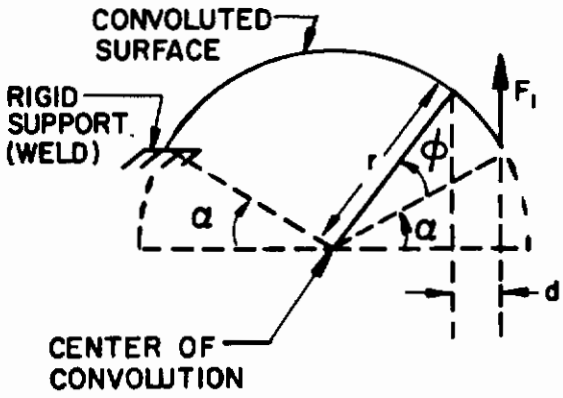

FIG. III-2 GEOMETRY OF CONVOLUTION

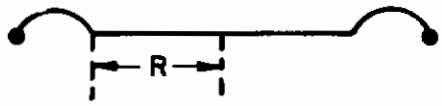

FIG. III-3 DEFINITION OF R

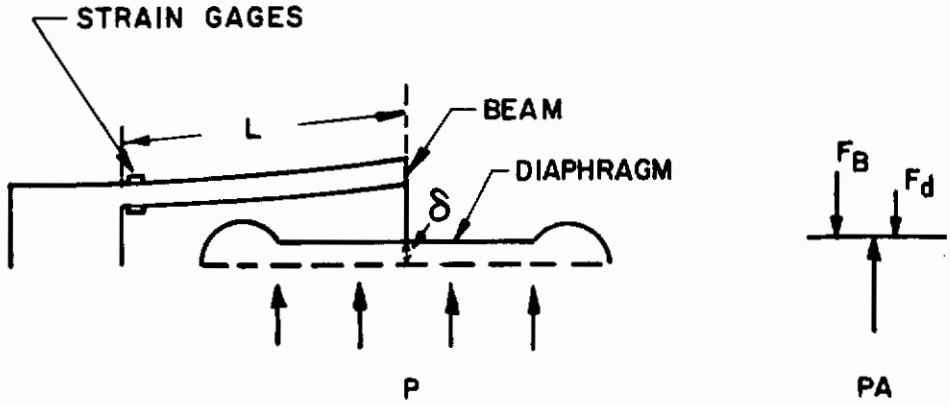

FIG. III-4 STRAIN GAGE PRESSURE TRANSDUCER

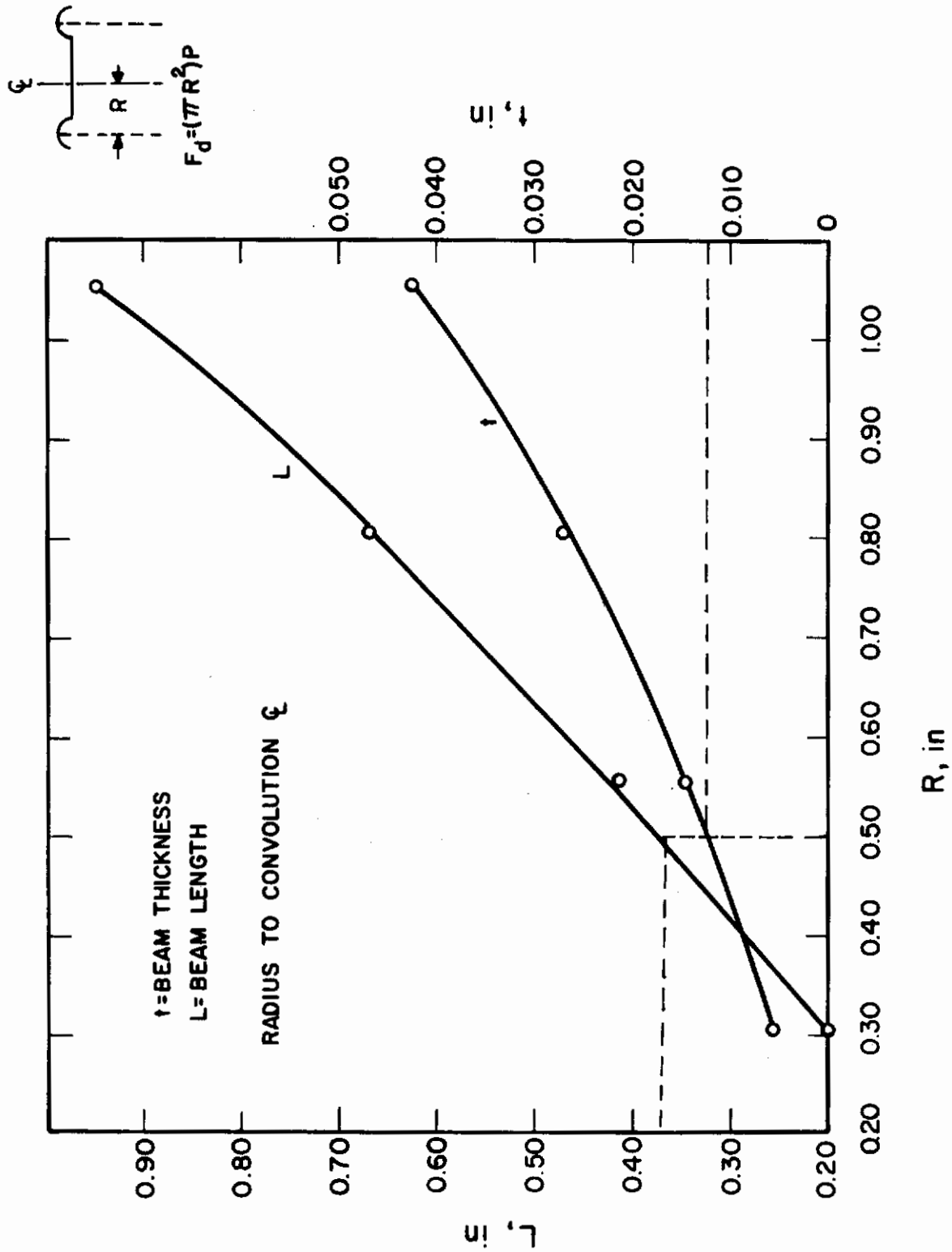

FIG. III-5 DIAPHRAGM DESIGN CHART

APPENDIX IV

SIGNAL CONDITIONING PACKAGE

The strain gage bridge sensor requires an electrical signal conditioner to meet the typical aerospace requirements of regulation, isolation, 0 to 5 vdc output, and low-output impedance.

There are several methods available to the designer for achieving the required high output (5 volts) level. This section discusses the advantages to the MSI approach of using a high-output level (0 mv) pickup feeding a low-gain (16.7X) direct-coupled amplifier.

There are two major types of strain gages available in which conversion from mechanical strain to an electrical parameter may occur: the foil or wire gage and the silicon sensor. The normal output level of the wire gage transducer is about 30 mv. Relatively high input voltages are required to produce this output voltage, and output voltage is usually limited by gage power dissipation. The resultant 30 mv signal is processed through an amplifier of 167X dc gain. The upper limit of simple (and reliable) dc amplifier design is around 125X gain. For gains in excess of 125X a disproportionately high open-loop gain (before beedback) is essential for the required stable sensitivity; thus, closely-matched transistors are required for the initial amplifier stages in order that reasonable offset stability be achieved through time and temperature. In aerospace telemetry applications, electrical isolation is a common requirement, so the transducer pickup and signal conditioning electronics must be supplied through a dc-dc converter. The noise spikes generated by the converter's chopper appear on the output proportional to amplifier gain. In the MSI unit, a low-gain-differential amplifier is used with an attendant decrease in spikes, inherent rejection of noise, and reduced size.

In order to fulfill the requirements for excitation/output dc isolation, a transformer is used to couple excitation power into the secondary circuits. In the Model 1025, a voltage regulator ahead of the dc-dc converter assures excellent preregulation of power supply dc fluctuations and ac ripple and noise. In addition, the differential amplifier and current regulator of the secondary circuits are inherently self-regulating for supply voltage variations, thus the overall transducer regulation is greatly improved over other designs currently being supplied-change in output voltage (% full scale) per unit change in input voltage is 0.0018%/v.

It should be noted that this signal conditioner will accept an excitation voltage from 20 to 50 vdc with regulation of the output better than 0.05% full scale.

APPENDIX V
THE EOS MICROMANOMETER

1. DESCRIPTION

The EOS micromanometer is a mercury "U" tube manometer, having a range of 2 inches of mercury, full scale. It consists of two glass tubes of 1 1/2 inches diameter, connected at the bottom by a stainless steel "U" tube. Two barrel micrometers are mounted at the tops of the tubes so that their shafts can be adjusted to touch the respective miniscus. Each shaft is ground to a conical point, thereby making the sensing quite simple and accurate. The micrometers are calibrated in 0.001-inch steps. Accurate spirit levels are mounted on the base-plate. A photograph of the manometer is shown in Fig. V-1.

2. ACCURACY

The manometer is theoretically capable of discriminating 0 inch of mercury (±0.0001 psia). The true accuracy of the manometer can only be determined after the manometer is set up in the position where it will be used. Also, the correctness of the readings obtained is controlled by the skill and experience of the operator.

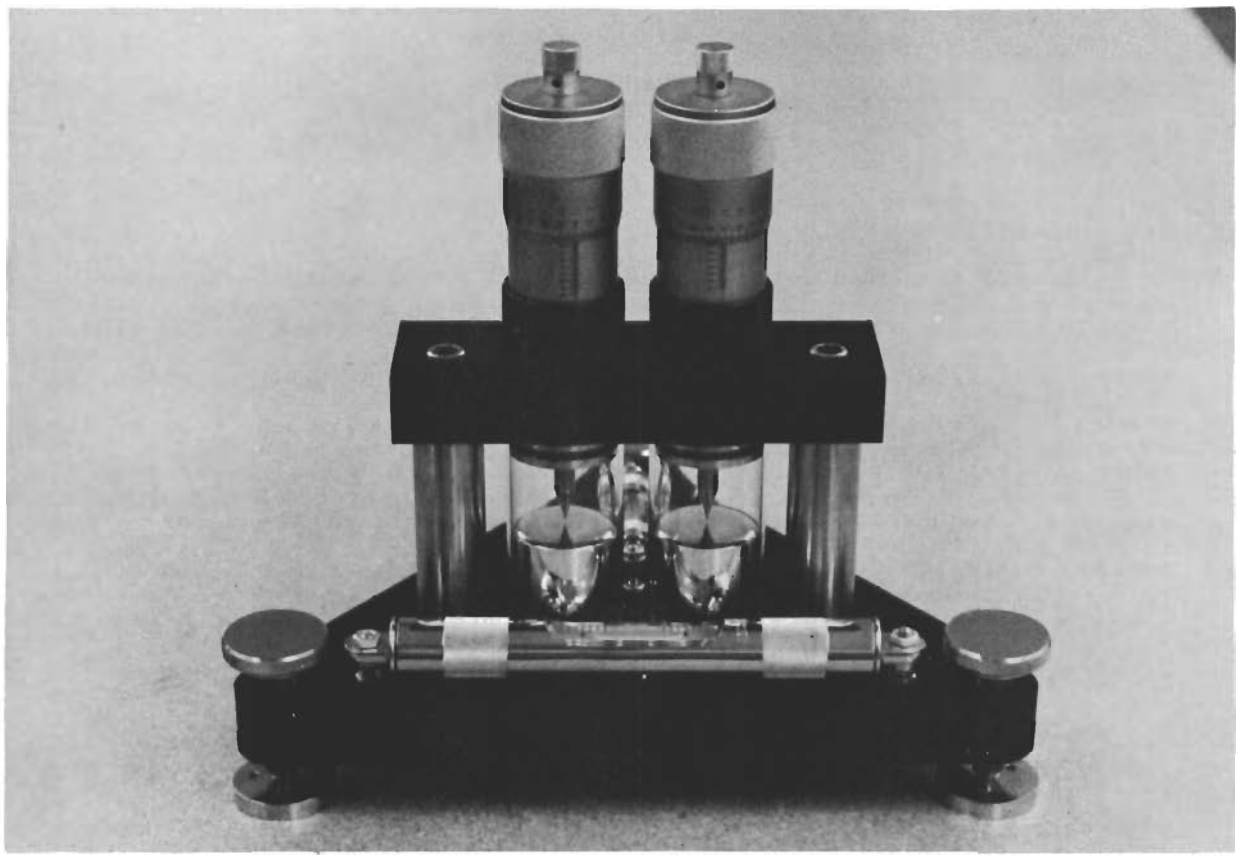

FIG. V-1 EOS MICROMANOMETER

APPENDIX VI

ABSOLUTE PRESSURE CALIBRATION SYSTEM

1. DESCRIPTION

Volumetrics Model ATC Absolute Pressure Calibration System provides within a single mobile console, a self-contained system for the precise calibration of pressure instruments in the range 0.01 psia, to one atmosphere. The unit houses its own vacuum source and provides means of accurately controlling the level of system pressures. In addition, lighted indicators and switches are provided to signal at all times system status and proper functioning of all system valving.

2. PRINCIPLE OF OPERATION

The Model ATC utilizes the Knudsen principle of transfer volumes to provide its capability of developing extremely low absolute pressures with a potential for accuracy beyond that of McLeod primary standards. Basically, the Knudsen principle is a paraphrase of Boyle's law, wherein it is demonstrated that a pressure (P) enclosed in a static volume (V) will change in inverse proportion to a change in the volume (V). That is, if V is doubled, P will be halved; conversely, if V is halved, P will be doubled.

NOTE

This technique was first evaluated and is presently recognized as valid by the National Bureau of Standards with the reservation that at submicronic absolute pressure levels, where the mean free path of the residual gas molecules can approach the internal dimensions of V, pressure discontinuities can exist within a closed static volume.

As utilized in the ATC System, the principle is applied as follows: A "minor volume" is provided whose volume is small compared to that of a major volume. A realistic pressure can, therefore, be established in the minor volume with a potential for accuracy as great as 0.01 percent of reading. If this minor volume is then vented into the major volume whose internal volume could be 999 times that of the minor volume, a resultant incremental rise in pressure in the major volume will result whose magnitude will be only 1/1000 of the minor volume set pressure. Since the volumetric ratio can be readily calibrated to within 0.015 percent of ratio accuracy, the overall system accuracy can be as great as 0.025 percent of reading (with external accessories). The procedure can be repeated to provide incremental calibration of any pressure instrument within the pressure range of the system.

Functionally, the system consists, essentially, of three volumes whose volumetric relationships are capable of precise calibration. These volumes are referred to as the (1) Minor, (2) Major, and (3) Hysteresis Volumes. These volumes are interconnected with one another and with the vacuum and pressure systems, indicators, controls and TEST manifold through solenoid valves. These valves are controlled by front-panel programming switches.

Volumetric relationships are first calibrated for the number of incremental pressure steps to be performed and for the full-scale range of the instrument undergoing calibration. For instance, if a 0.1 psia full-scale transducer is to be calibrated and 10 percent increments are desired, the volume of the major volume (plus the TEST manifold) would be adjusted to 999 times that of the minor volume. The hysteresis volume would then be adjusted to exactly equal that of the major volume (plus TEST manifold).

NOTE

The ratio of 999:1 is arbitrarily used here because it permits a minor volume pressure of 10 psid to be

utilized, which can be readily and precisely read and controlled. Any other combination of volumetric ratio and minor volume pressurization that would yield a pressure step of 0.01 psia could, alternatively, be utilized.

The major and hysteresis volume are then evacuated to an absolute pressure of 10 microns Hg or less by the integral vacuum system and the two volumes are isolated from one another and from the system. A pressure of 10 psid is then set in the minor volume with the reference level equivalent to that of the major volume. The minor volume is then isolated from its source of pressure. The minor volume is then coupled to the major volume through a special valve whose internal volume is the same whether open or closed. Major and minor volume pressures equalize at a level 1/1000 of the minor volume set pressure higher than the original zero absolute reference level or 0.001 x 10 = 0.01 psia.

The connecting valve is then closed and the source valve opened and the minor volume pressure is again set to 10 psid (always using the existing major volume pressure as the reference) The source valve is then closed and the connecting valve again opened Resultant equalization provides a further incremental 0.01 psi pressure step to 0.02 psia. This procedure is repeated until the 100 percent point, or 0.1 psia, is attained. A valve connecting the major volume to the hysteresis volume is then opened. Since the hysteresis volume was still held at the reference zero level, and its volume is identical to that of the major volume (plus TEST manifold), equalization results in halving of the major volume pressure generating a mid-point hysteresis calibration. The system is then vented to atmospheric pressure and the test is complete.

The wide range of adjustment of volumetric ratio coupled with the range of control over minor volume pressure level permit system utilization of 10 point calibrations over the pressure range of 0.01 to one atmosphere.

3. OPERATING FEATURES

All valving is electrically or electropneumatically operated, permitting use of simple rotary switches for programming system operation for semi-automatic operation.

Only one adjustment is made at each incremental pressure step: minor volume pressure level. A Volumetrics Model V-I Pressure-Volume Control is panel mounted for this purpose and permits control to within 0.0005 psi.

System accuracy is almost entirely controlled by the accuracy of the minor volume pressure gauge, permitting upgrading without system redesign. If a primary standard is utilized in place of this gauge, the system becomes a primary standard.

APPENDIX VII

TEST PROCEDURE AND TEST DATA ON DELIVERED UNITS

1. SCOPE

This test procedure covers the method of testing the 0.1 psia transducers for Contract AF 33(615)-1838 to ensure that the transducers meet all requirements for acceptance.

2. APPLICABLE DOCUMENTS

1. Contract AF 33(615)-1838
2. EOS WA 5430-01-00
3. Proposal 63-586, EOS

3. TEST EQUIPMENT

Low Pressure Calibrator (Volumetrics)
Differential Voltmeter (Fluke Model 825A)
Power Supply (Power Designs Model 4005)
EOS Calibration Control Console
Vibration System (MB Electronics C-50)
Centrifuge (Genisco "G" Accelerator Model 1220-1)
Oscilloscope -(Tektronics 53A)

4. TEST PROCEDURE

4.1 Configuration

The transducers will be inspected for overall length and diameter. The length inclusive will not exceed 5 inches nor will the diameter exceed 1.5 inches, including pressure fitting and electrical receptacle, and excluding mounting lugs.

4.2 Linearity, Hysteresis, and Repeatability

4.2.1 Connect the transducer to the test equipment as shown in Fig. 1.

4.2.2 Adjust the power supply for 28 Vdc ± 0.1 Vdc input to the transducer.

4.2.3 Apply 0 psia (approximately 50 microns) to the transducer. Record output reading on differential voltmeter.

4.2.4 With the transducer at 0 psia, increase the input pressure in successive steps of 0.01 psia. Record the output reading at each successive increase in pressure until full scale pressure is obtained.

4.2.5 Reduce the applied pressure to 0.05 psia, and record the output.

4.2.6 Reduce pressure to 0 psia, and record the output.

4.2.7 Repeat step 4.2.4.

4.2.8 Linearity is the maximum deviation between the curve recorded in paragraph 4.2.4 and a straight line drawn between the zero psia point and the full-scale psia point expressed as a percentage of the full-scale output.

Repeatability is the maximum deviation between the curve recorded in paragraph 4.2.4 and the one recorded in paragraph 4.2.7 expressed as a percentage of full-scale output.

Hysteresis is the difference in output at 50 percent full-scale pressure obtained in paragraph 4.2.4 and that obtained in paragraph 4.2.5 expressed as a percentage of full-scale output.

Combined linearity hysteresis and repeatability errors must not exceed ± 1 percent of full-scale output.

4.3 Regulation

4.3.1 Set power supply for 28 Vdc ± 0.1 Vdc.

4.3.2 Apply 0.1 psia. Note and record output.

4.3.3 Decrease power supply voltage to 24 vdc + -0.1 vdc. Record output.

4.3.4 Compute change in output from 28 vdc to 24 vdc. The change should be less than 1 percent full scale.

4.3.5 Increase power supply voltage to 32 vdc + 0.1, -0 vdc. Record output.

4.3.6 Compute change in output from 28 vdc to 32 vdc. The change should be less than 1 percent full scale.

4.4 Temperature Test

4.4.1 Connect the transducer as shown in Fig. VII-1, setting the power supply at 28 Vdc ± 0.1 Vdc.

4.4.2 At ambient temperature (+ 75°F ± 4°F), record the output readings at 0 psia (approximately 50 microns) and at full scale pressure 0.1 psia. Compute sensitivity by subtracting the 0 psia reading from the full scale reading and record.

4.4.3 Decrease temperature in the test chamber to 0°F. Stabilize at this temperature for 1 hour. Record output readings at 0 and full scale pressures. Compute sensitivity and record.

4.4.4 Increase temperature in test chamber to + 250°F. Stabilize at this temperature for 1 hour. Record output readings at 0 and full scale pressures. Compute sensitivity and record.

4.4.5 Express the difference between zero readings recorded at 0°F and + 250°F as a percentage of full scale output at 75°F. These values of zero deviation will not exceed ± 3 percent from the 75°F value.

4.4.6 Express the difference in sensitivity readings recorded at 0°F and + 250°F as a percentage of full scale output at

+ 75°F. These values of sensitivity deviation will not exceed ± 3 percent from the + 75°F value.

4.5 Overload Test

4.5.1 Record the output readings at 0.0 psia and full scale pressures. Compute and record sensitivity.

4.5.2 Remove transducer from pressure source.

4.5.3 Connect transducer to pressure source and apply 0.0 psia pressure.

4.5.4 Repeat steps 4.5.2 and 4.5.3 ten times. In this manner, repeated overloads of 15 psia will be applied to the transducer.

4.5.5 After completion of 10 overload cycles, record 0 and full scale output readings.

4.5.6 Note and record changes in output from step 1 of Subsection 4.7 of 0.0 and full scale, computing sensitivity changes.

4.5.7 Compute percentage change of full scale for 0 and sensitivity.

NOTE

These percentages must be less than 1 percent of full scale.

4.6 Vibration

4.6.1 Complete test setup as shown in Fig. VII-2, with evacuation fixture connected to head of exciter with cabling and plumbing installed for the performance of the test as required.

4.6.2 Adjust power supply to 28 vdc ± 0.1 vdc.

4.6.3 Apply 0.0 psia (approximately 50 microns) to the transducer and record the output voltage before vibration.

4.6.4 Specifications for Vibration

Frequency range of 5 to 2400 cps with crossover at 20 cps. From 5 to 20 cps displacement will be 1/2 inch double amplitude.

From 20 to 2400 cps acceleration will be ± 10 g. Time duration will be 5 minutes from 5 cps to 2400 cps and back to 5 cps.

4.6.5 Commence vibration run.

4.6.6 Note and record all resonances exhibiting amplification factors greater than 1.5.

4.6.7 Repeat vibration run for three orthogonal directions.

4.7 Acceleration Test

4.7.1 Complete test setup as shown in Fig. VII-3, with transducer connected to the centrifuge and with cabling installed for the performance of the test as required. The transducer will have been brought to 0.0 psia with a device which will be leakproof.

4.7.2 Adjust power supply to 28 vdc ± 0.1 vdc.

4.7.3 Record the output voltage before acceleration test.

4.7.4 Commence acceleration test, bringing centrifuge to 10 g for two minutes.

4.7.5 Note and record change in output at acceleration.

4.7.6 Repeat steps 4.7.3, 4.7.4, and 4.7.5 for plus and minus acceleration in three orthogonal axes.

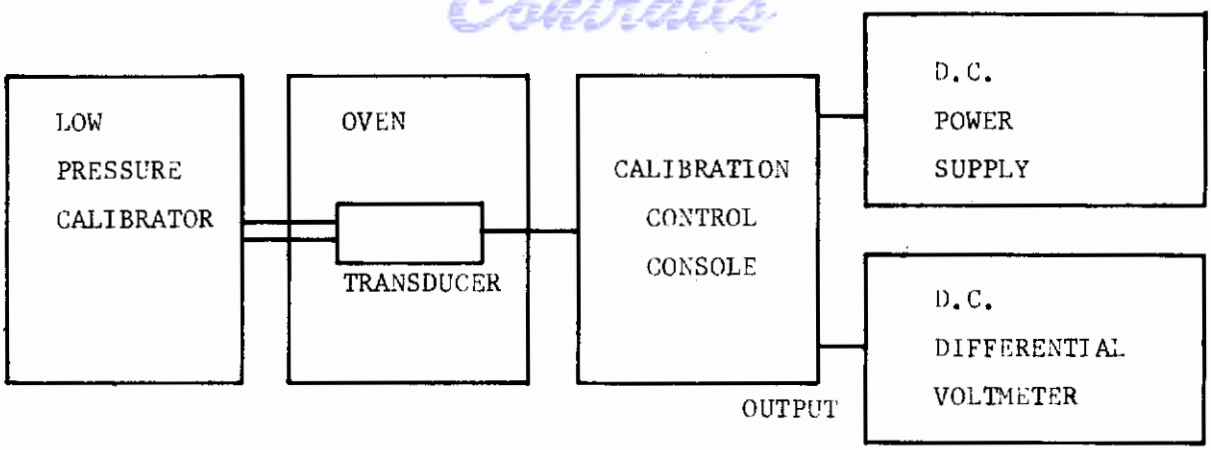

FIG. VII-1 TEMPERATURE TEST SETUP

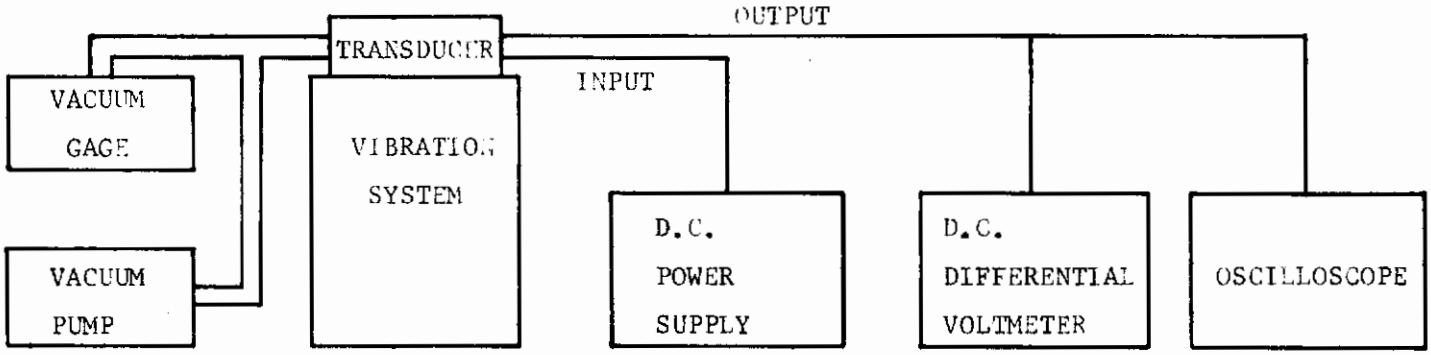

FIG. VII-2 VIBRATION TEST SETUP

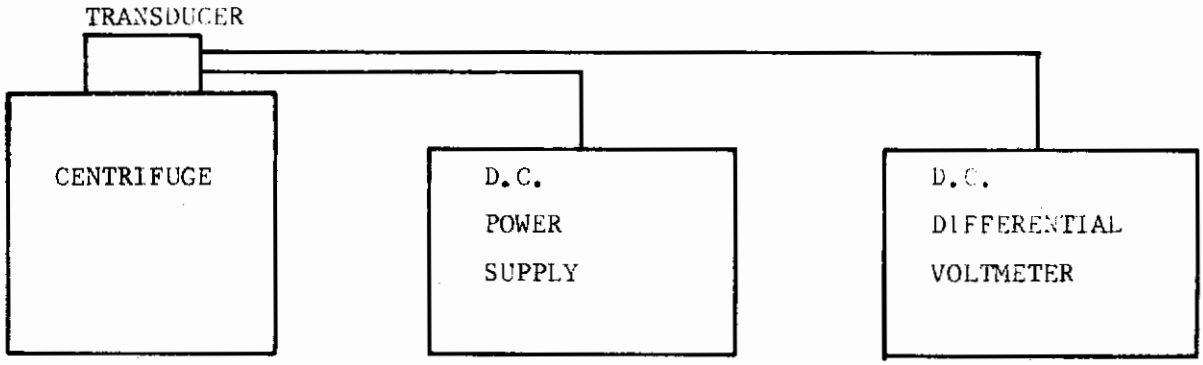

FIG. VII-3 ACCELERATION TEST SETUP

5. TEST DATA

5.1 The following test data was obtained during the testing of the first prototype of Model 5431-1, Serial No. .002. It will be noticed that the transducer experienced a severe change in output at zero psia during the second transient high temperature test. The transducer was repaired and recalibrated and the testing resumed.

Initial Calibration at Room Temperature, 12 April 1965

5 Point Run Taken to Expedite Test

First Run		Second Run	
psia	output	psia	output
0	- .040 vdc	0	- .037 vdc
.02	+ .942	.02	+ .940
.04	1.927	.04	1.925
.06	2.915	.06	2.912
.08	3.903	.08	3.903
.10	4.893	.10	4.891

Ambient temperature increased from +75°F to +400°F in 10 minutes. The largest change of zero output during this test was from -.040 vdc to -.260 vdc.

The temperature was held at 400°F for 5 minutes during which time the zero output changed to +.020 volts dc.

The ambient temperature was then reduced to 250°F in 5 minutes and held at this temperature for 11 minutes. The zero psia output changed to -.103 vdc and the following test run was made:

psia	output
0	- .103 vdc
.02	+ .945
.04	1.850
.06	2.789
.08	3.809
.10	5.030

The ambient temperature was held at +250°F for 1 hour and the following test run made:

psia	output (vdc)
0	- .325
.02	+ .799
.04	1.653
.06	2.593
.08	3.625
.10	4.630

The ambient temperature was then returned to +75°F and after 1 hour the following test run made:

psia	output (vdc)
0	-.115
.02	+.870
.04	1.857
.06	2.841
.08	3.829
.10	4.815

To obtain 10 point calibration data the high temperature transient test was repeated with results as follows:

Serial No. .002 Final Temperature Test, conducted 13 April 1965

Run #1 - 75°F

psia	output (mv)
0	- 34.0
.01	472
.02	972
.03	1465
.04	1964
.05	2459
.06	2954
.07	3452
.08	3948
.09	4444
.10	4937

Run #2 - 75°F

psia	output (mv)
0	- 34.0
.01	471
.02	970
.03	1465
.04	1962
.05	2457
.06	2952
.07	3450
.08	3947
.09	4443
.10	4937

Run #3 - 0°F

psia	output (mv)
0	+ 28 mV
.02	984
.04	1942
.06	2900
.08	3864
.10	4825

Run #4 - 400°F

psia	output (mv)
0	+ 600
.02	1500
.06	2320
.08	*
.10	

*At this point severe output voltage drift was recorded. Testing was discontinued

After this failure the transducer was repaired and recalibrated and data obtained as follows:

15 April 1965, Zero Reset. Temperature Compensation - None.
34 ohms in Leg 7, Gain Resistance 328 ohms, Shunt 10K

Room Temperature Run 3:03 P.M.

psia	output			psia	output		
0	- .0345			0	- .0334		
.01	+ .4051			.01	+ .427		
.02	.9150			.02	.932		
.03	1.426			.03	1.445		
.04	1.940			.04	1.961		
.05	2.455	.05	2.438	.05	2.475	.05	2.455
.06	2.968			.06	2.987		
.07	3.484			.07	3.499		
.08	3.999			.08	4.011		
.09	4.510			.09	4.523		
.10	5.023			.10	5.035		

Up to 250°F Start 3:15 P.M. Peak at 235°F - .538V at 3:25 P.M.

psia	output		
0	- .4105		
.01	- .385		
.02	+ .122		
.03	.699		
.04	1.140		
.05	1.60	.05	1.452
.06	2.10		
.07	2.603		
.08	3.132		
.09	3.633		
.10	4.155		

It was necessary to readjust the zero temperature compensation at this point.

16 April 1965, Changed zero balance to 249 ohms

Changed Balco from 0 to 250 ohms in Leg 7

Room Temperature Run (75°F) - Commenced at 8:10 AM

First Run psia	First Run output			Second Run psia	Second Run output			Corrected Curve	Ideal St. Line
0	+ .010			0	+ .009			.510	.507
.01	.514			.01	.519			1.014	1.014
.02	1.020			.02	1.023			1.518	1.521
.03	1.524			.03	1.527			2.024	2.028
.04	2.031			.04	2.033			2.531	2.534
.05	2.537	.05	2.512	.05	2.540	.05	2.521	3.038	3.041
.06	3.041			.06	3.047			3.544	3.548
.07	3.546			.07	3.553			4.053	4.055
.08	4.049			.08	4.062			4.558	4.562
.09	4.553			.09	4.567			5.069	5.069
.10	5.055			.10	5.070				

Commenced Heating, 8:25 AM

Drift Peak - 127 mV at 230°F, 8:33 AM

250°F at 9:20 AM

First Run psia	First Run output			Second Run psia	Second Run output			Corrected Curve	Ideal St. Line
0	+ .200			0	+ .159			.548	.495
.01	.747			.01	.707			1.031	.991
.02	1.220			.02	1.190			1.481	1.486
.03	1.684			.03	1.640			1.956	1.981
.04	2.155			.04	2.115			2.454	2.476
.05	2.659	.05	2.550	.05	2.613	.05	2.504	2.970	2.972
.06	3.176			.06	3.129			3.465	3.467
.07	3.676			.07	3.624			3.966	3.962
.08	4.183			.08	4.125			4.461	4.458
.09	4.680			.09	4.620			4.953	4.953
.10	5.156			.10	5.112				

Commenced Cold 9:45 AM

Drift Peak - 35 mV 0°F, 9:55 AM

0°F at 10:35 AM

First Run psia	First Run output			Second Run psia	Second Run output			Corrected Curve	Ideal St. Line
0	- .030			0	- .031			.491	.492
01	+ .470			.01	+ .460			.985	.984
.02	.961			.02	.954			1.479	1.476
.03	1.448			.03	1.448			1.968	1.968
.04	1.939			.04	1.937			2.462	2.460
.05	2.426	.05	2.403	.05	2.431	.05	2.415	2.953	2.952
.06	2.919			.06	2.922			3.443	3.444
.07	3.407			.07	3.412			3.937	3.936
.08	3.897			.08	3.905			4.425	4.428
.09	4.390			.09	4.394			4.920	4.920
.10	4.879			.10	4.887				

Room Temperature 11:40 AM

First Run psia	output		Second Run psia	output		Corrected Curve	Ideal St. Line
0	- .029 vdc		0	- .030 vdc		.510	.505
.01	+ .480		.01	+ .480		1.014	1.009
.02	.983		.02	.984		1.516	1.514
.03	1.488		.03	1.486		2.021	2.018
.04	1.993		.04	1.991		2.525	2.523
.05	2.498	2.488	.05	2.495	2.475	3.032	3.028
.06	3.004		.06	3.002		3.534	3.532
.07	3.509		.07	3.504		4.040	4.037
.08	4.015		.08	4.010		4.545	4.541
.09	4.520		.09	4.515		5.046	5.046
.10	5.026		.10	5.016			

Voltage stability test at full scale 22-32 vdc change on power supply caused 1 mv change in output at 5.026 volts.

The acceleration test was carried out and data obtained as follows:

Acceleration Run at 0.02 psia, ±10 g, 3 axes

	dc-mv Output	
	Y+	Y-
Before Run	+934.4 mv	+1058 mv
After 10 g	911.0	1050
After Run	934.7	1059
	Z+	Z-
Before Run	+1080 mv	+1069 mv
At 10 g	1063	1025
After Run	1075	1069
	X+	X-
Before Run	+1066 mv	+1066 mv
At 10 g	1359	729
After Run	1066	1064

S/N .002 Vibration Test 4/19/65, conducted by D. P. Torgerson.
(ac background 3 mv, 20 to 2000 cps ±10 gs)

	ac mv (rms)		
cps	Y Axis	X Axis	Z Axis
20	7	13	240
100	12	10	192
200	10	13	126
300	10	9	94
400	7	3	76
500	5	3	66
600	7	6	58
700	14	8	50
800	23	15	48
900	35	25	44
1000	22	11	45
1100	20	11	46
1200	19	12	52
1300	22	16	62
1400	35	25	74
1500	35	320	70
1600	25	15	45
1700	18	10	40
1800	17	10	37
1900	16	6	34
2000	14	8	35

Resonant Frequency: 1420 cps

Y Axis Sub-Harmonic (870 cps) - 45 mv
Z Axis Sub-Harmonic (250 cps) - 32 mv
Z Axis Sub-Harmonic (850 cps) - 30 mv

5.2 Test data pertinent to serial numbers 003, 004, and 005 follow on subsequent pages of this appendix.

PRESSURE TRANSDUCER

RANGE: 0 to 0.1 psia

MODEL NO: 5431-1

SERIAL NO: 003

OUTPUT IN MILLIVOLTS

INPUT PRESSURE PSIA	+75°F		0°F		+250°F		+75°F	
	RUN 1	RUN 2	RUN 1	RUN 2	RUN 1	RUN 2	RUN 1	RUN 2
0	+29	+32	-39	-31	+47	+42	-1	+4
0.01	500	500	421	421	534	525	467	468
0.02	993	992	904	903	1043	1035	958	958
0.03	1491	1490	1391	1390	1553	1546	1450	1452
0.04	2001	2000	1889	1889	2069	2062	1957	1959
0.05	2510	2510	2390	2389	2587	2581	2464	2466
0.06	3021	3020	2892	2891	3105	3101	2974	2976
0.07	3531	3529	3396	3393	3625	3622	3482	3484
0.08	4041	4039	3898	3895	4142	4139	3992	3993
0.09	4550	4546	4398	4395	4652	4649	4499	4498
0.10	5050	5045	4895	4892	5141	5141	4999	4995
SENSITIVITY	5021	5013	4934	4923	5094	5099	5000	4991
0.05	2481	2481	2363	2363	2542	2541	2436	2436

LINEARITY: -0.88%

HYSTERESIS: -0.38%

REPEATABILITY: 0

TEMPERATURE TEST:

0°F - **ZERO:** -1.35%
- **SENSITIVITY:** -1.73%

250°F - **ZERO:** +0.36%
- **SENSITIVITY:** +1.65%

VOLTAGE REGULATION

24 vdc: 4990 mv
32 vdc: 4992 mv

OVERLOAD TEST

BEFORE **ZERO:** +4 mv
SENSITIVITY: 4980 mv

AFTER ZERO: +2 mv
SENSITIVITY: 4989 mv

DIFF. ZERO: -2 mv
SENSIVITY: +9 mv

VIBRATION

X AXIS: 2% OFF.S.
Y AXIS: 0.6% OFF.S.
Z AXIS: 1.4% OFF.S.

ACCELERATION

X AXIS: +5.7% OFF.S.
-6.4% OFF.S.
Y AXIS: +0.05% OFF.S.
-0.15% OFF.S.
Z AXIS: +0.2% OFF.S.
-0.25% OFF.S.

CONFIGURATION

LENGTH: 4.160 inches
DIAMETER: 1.500 inches

PRESSURE TRANSDUCER

VIBRATION ACCEPTANCE TEST

RANGE: 0 to 0.1 psia

MODEL NO: 5431-1

SERIAL NO: 003

CPS	X AXIS AC-MV RMS		Y AXIS AC-MV RMS		Z AXIS AC-MV RMS	
	UP	DOWN	UP	DOWN	UP	DOWN
0	1.5		2	2	7	
5	10		2	2	7	7
20	94		5	4	14	13
100	87		4	4	12	10
200	76		4	3	10	9
300	61		2	4	9	8
400	50		3	3	8	8
500	43		2	3	8	8
600	37		3	4	8	12
700	33		5	5	10	7
800	30		14	14	7	7
900	28		11	9	13	9
1000	27		5	5	10	10
1100	28		3.5	4	12	12
1200	30		6	7	17	15
1300	45		32	32	28	20
1400	70		5	5	70	18
1500	100		5	5	14	13
1600	16		5	5	13	11
1700	14		6	6	11	12
1800	13		7	7	9	13
1900	12		8	8	9	15
2000	11		7	10	10	14
2100	10		3.5	8	10	10
2200	5		2.5	2.5	10	9
2300	3		2	2	10	8
2400	2.5		2	2	8	8
RESONANCE at CPS	1450		1320		1380	
AC-MV RMS	1V rms		60 mv		280 mv	

PRESSURE TRANSDUCER

ANGE: 0 to 0.1 psia

MODEL NO: 5431-1

SERIAL NO: 004

OUTPUT IN MILLIVOLTS

INPUT PRESSURE (PSIA)	+75°F		0°F		+250°F		+75°F	
	RUN 1	RUN 2	RUN 1	RUN 2	RUN 1	RUN 2	RUN 1	RUN 2
0	+40	+43	-48	-42	-9	-13	+40	+41
0.01	532	530	435	442	481	473	536	535
0.02	1034	1034	934	939	974	969	1036	1038
0.03	1538	1540	1434	1436	1469	1465	1539	1542
0.04	2043	2047	1934	1934	1964	1961	2042	2045
0.05	2548	2553	2434	2433	2460	2457	2544	2547
0.06	3056	3061	2935	2931	2956	2953	3047	3051
0.07	3563	3568	3434	3429	3452	3450	3550	3554
0.08	4073	4078	3932	3928	3948	3945	4053	4058
0.09	4573	4578	4430	4426	4443	4440	4555	4559
0.10	5076	5078	4926	4922	4933	4930	5054	5057
ENSITIVITY	5036	5035	4974	4964	4942	4943	5014	5016
0.05	2552	2555	2439	2440	2457	2453	2546	2548

LINEARITY: -0.33%

HYSTERESIS: +0.08%

REPEATABILITY: +0.10%

TEMPERATURE TEST:

0°F - ZERO: -1.79%

- SENSITIVITY: -1.41%

250°F - ZERO: -1.10%

- SENSITIVITY: -1.85%

VOLTAGE REGULATION

24 vdc: -0.02%

32 vdc: -0.04%

OVERLOAD TEST

ZERO: +0.02%

SENSITIVITY: -0.12%

VIBRATION

X AXIS:

Y AXIS: (see Vibration Sheet)

Z AXIS:

ACCELERATION

X AXIS:

Y AXIS: (see Acceleration Sheet)

Z AXIS:

CONFIGURATION

LENGTH: 4.155 inches

DIAMETER: 1.500 inches

PRESSURE TRANSDUCER

VIBRATION ACCEPTANCE TEST

RANGE: 0 to 0.1 psia

MODEL NO: 5431-1

SERIAL NO: 004

CPS	X AXIS		Y AXIS		Z AXIS	
	AC-MV RMS		AC-MV RMS		AC-MV RMS	
	UP	DOWN	UP	DOWN	UP	DOWN
0	0.7	0.7	0.5	0.5	0.6	0.6
5	12	12	0.7	0.7	0.9	1.5
20	200	215	11	11	15	16
100	170	160	15	12	24	18
200	105	100	1	2	3	35
300	72	70	0.9	0.9	3	3.5
400	55	55	0.8	0.8	4	4
500	46	42	0.1	0.9	4.5	5
600	37	35	0.8	1.5	7	7
700	33	33	9	1.5	9	12
800	28	35	2.5	12	150	200
900	24	24	10	10	35	40
1000	22	22	1.3	0.8	2	2
1100	20	21	1	1	4	4
1200	20	20	1	1.2	7	7
1300	19	20	0.9	1	10	11
1400	19	20	2	1.5	15	14
1500	20	20	4	4	20	15
1600	35	32	9	10	35	20
1700	250	320	50	10	40	35
1800	30	20	30	5	250	300
1900	17	16	4	5	17	15
2000	15	14	3	4	12	13
2100	11	11	1	1	10	12
2200	15	15	2	2	8	9
2300	9	10	2	2	7	8
2400	7	7	1	1	5	5
RESONANCE at CPS AC-MV RMS	1670 cps 900 mv		1690 cps 100 mv		850 cps 1V	1620 cps 1.5V

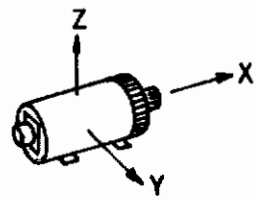

PRESSURE TRANSDUCER

ACCELERATION ACCEPTANCE TEST

RANGE: 0 to 0.1 psia

MODEL NO: 5431-1

SERIAL NO: 004

	OUTPUT VDC					
	X AXIS		Y AXIS		Z AXIS	
	POS.+	NEG.-	POS.+	NEG.-	POS.+	NEG.-
	②	⑤	④	③	①	⑥
BEFORE	2.200	2.283	2.203	2.250	2.200	2.359
DURING	2.477	1.964	2.211	2.249	2.158	2.346
AFTER	2.202	2.287	2.210	2.754	2.192	2.362

Encircled Number Designates Run Sequence

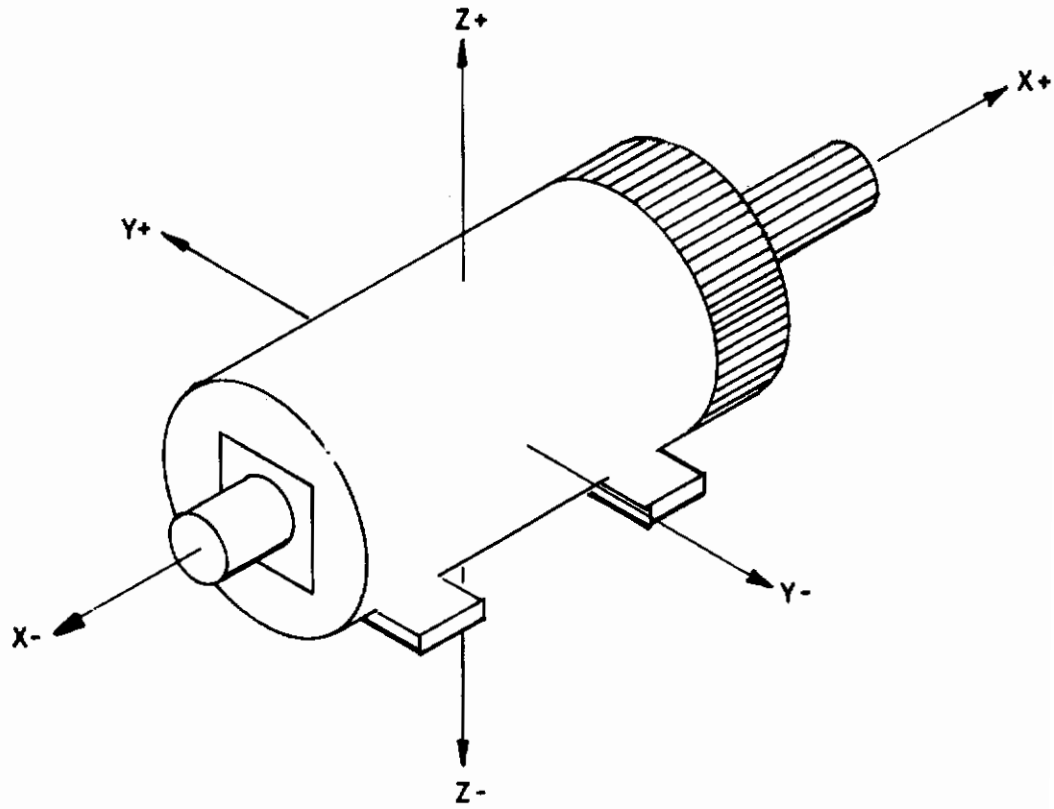

PRESSURE TRANSDUCER

RANGE: 0 to 0.1 psia

MODEL NO: 5431-1

SERIAL NO: 005

OUTPUT IN MILLIVOLTS

INPUT PRESSURE (PSIA)	+75°F		0°F		+250°F		+75°F	
	RUN 1	RUN 2	RUN 1	RUN 2	RUN 1	RUN 2	RUN 1	RUN 2
0	+2	+4	+46	+52	+114	+93	-21	-17
0.01	489	488	529	532	590	567	467	469
0.02	988	988	1028	1028	1077	1058	963	966
0.03	1488	1489	1528	1528	1565	1548	1461	1466
0.04	1992	1993	2032	2026	2056	2040	1964	1967
0.05	2498	2500	2533	2528	2548	2535	2465	2467
0.06	3003	3005	3038	3027	3040	3030	2967	2970
0.07	3507	3511	3540	3527	3533	3524	3469	3471
0.08	4017	4017	4044	4036	4028	4024	3973	3975
0.09	4525	4525	4547	4539	4521	4517	4480	4480
0.10	5033	5028	5050	5044	5012	5007	4988	4985
SENSITIVITY	5031	5024	5004	4992	4898	4914	5009	5002
0.05	2500	2501	2536	2534	2539	2528	2469	2472

LINEARITY: -0.46%

HYSTERESIS: +0.04%

REPEATABILITY: +0.04%

TEMPERATURE TEST:

0°F - ZERO: +0.98%
- SENSITIVITY: -0.77%

250°F - ZERO: +2.22%
- SENSITIVITY: -2.64%

VOLTAGE REGULATION

24 vdc: -0.02%
32 vdc: +0.04%

OVERLOAD TEST

ZERO: +0.04%
SENSITIVITY: -0.38%

VIBRATION

X AXIS:
Y AXIS: (see Vibration Sheet)
Z AXIS:

ACCELERATION

X AXIS:
Y AXIS: (see Acceleration Sheet
Z AXIS:

CONFIGURATION

LENGTH: 4.155 inches
DIAMETER: 1.500 inches

PRESSURE TRANSDUCER

VIBRATION ACCEPTANCE TEST

RANGE: 0 to 0.1 psia

MODEL NO: 5431-1

SERIAL NO: 005

CPS	X AXIS		Y AXIS		Z AXIS	
	AC-MV RMS		AC-MV RMS		AC-MV RMS	
	UP	DOWN	UP	DOWN	UP	DOWN
0	0.65	0.65	0.6	0.6	0.7	0.7
5	10.5	14	0.65	0.7	0.88	0.9
20	200	205	11	7	7	7
100	93	88	5	3	2.5	2.1
200	42	45	1	0.8	1.3	1.2
300	33	31	0.6	0.6	0.78	0.7
400	26	25	0.6	0.6	0.7	0.8
500	21	21	0.6	0.6	0.7	0.7
600	19	18	0.6	0.6	0.7	0.8
700	17	17	0.7	0.7	3.5	1.1
800	17	16	0.7	1	4	5
900	15	15	3.5	3	6	7
1000	17	17	0.9	8	1	1.1
1100	19	19	0.7	0.8	1.8	1.7
1200	25	25	0.8	3	5	4
1300	38	30	15	15	32	32
1400	40	17	1	0.7	5	4.5
1500	13	13	0.7	0.7	3.5	3.4
1600	12	12	0.7	0.7	3.6	3.5
1700	14	15	0.6	0.6	4	3.5
1800	8	4	0.6	0.6	5	4
1900	1	1.5	0.6	0.6	3	3
2000	1	1.1	0.7	0.7	3	3
2100	1	1.1	0.8	0.7	2	2
2200	1.3	1.3	0.9	0.8	1.7	1.3
2300	1.4	1	9	0.9	1	0.8
2400	1	1	8	8	8	0.8
RESONANCE at CPS AC-MV RMS	1310 cps 48 mv		1280 cps 20 mv		1310 cps 64 mv	

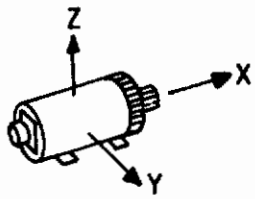

PRESSURE TRANSDUCER

ACCELERATION ACCEPTANCE TEST

RANGE: 0 to 0.1 psia

MODEL NO: 5431-1

SERIAL NO: 005

	OUTPUT VDC					
	X AXIS		Y AXIS		Z AXIS	
	POS.+	NEG.-	POS.+	NEG.-	POS.+	NEG.-
	⑤	④	③	②	⑥	①
BEFORE	2.521	2.435	2.396	2.372	2.545	2.266
DURING	2.823	2.090	2.378	2.360	2.521	2.259
AFTER	2.521	2.440	2.400	2.378	2.551	2.274

Encircled Number Designates Run Sequence

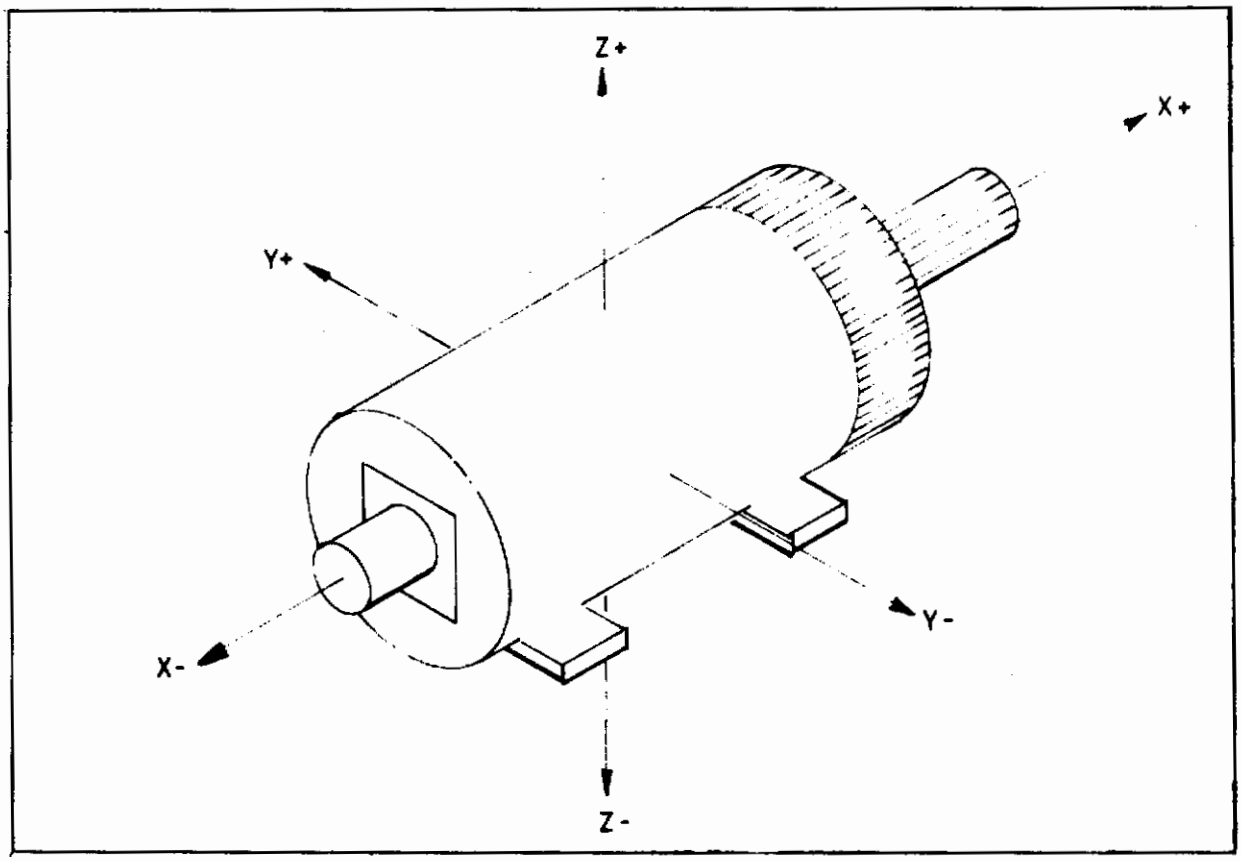

UNCLASSIFIED

Security Classification

DOCUMENT CONTROL DATA - R&D

(Security classification of title, body of abstract and indexing annotation must be entered when the overall report is classified)

1. ORIGINATING ACTIVITY *(Corporate author)*
Electro-Optical Systems, Inc.
300 N. Halstead Street
Pasadena, California 91100

2a. REPORT SECURITY CLASSIFICATION
Unclassified

2b. GROUP

3. REPORT TITLE

LOW PRESSURE MEASUREMENT TECHNIQUES

4. DESCRIPTIVE NOTES *(Type of report and inclusive dates)*
Final Technical Report, 12 June 1964 to 31 December 1965

5. AUTHOR(S) *(Last name, first name, initial)*

Painter, Herbert A.

6. REPORT DATE	7a. TOTAL NO. OF PAGES	7b. NO. OF REFS
July 1966	111	0

8a. CONTRACT OR GRANT NO.	9a. ORIGINATOR'S REPORT NUMBER(S)
AF 33(615)-1838	AFFDL-TR-66-11
b. PROJECT NO. 1469	
c. 146907	9b. OTHER REPORT NO(S) *(Any other numbers that may be assigned this report)*
d.	

10. AVAILABILITY/LIMITATION NOTICES This document is subject to special export controls and each transmittal to foreign governments or foreign nationals may be made only with prior approval of AF Flight Dynamics Laboratory, Wright-Patterson Air Force Base, Ohio 45433

11. SUPPLEMENTARY NOTES	12. SPONSORING MILITARY ACTIVITY
	Research and Technology Division Wright-Patterson Air Force Base, Ohio 45433

13. ABSTRACT

This project was initiated to develop four prototype pressure transducers in the range of 0.0 to 0.1 psia for Wright-Patterson AFB. The design selected makes use of a convoluted diaphragm force collector to drive a cantilever beam. A semiconductor strain gage bridge bonded to the beam converts the force to an electrical signal which is amplified to provide a 0 to 5V dc output. The results presented demonstrate achievement of essentially all requirements, save high-temperature transient performance. It is apparent from the results of this project that an accurate 0.0 to 0.1 psia transducer of low weight and reasonably high natural frequency can be produced. Achievement of higher operating temperature and natural frequency is possible. Further work to accomplish this is recommended.

DD FORM 1 JAN 64 1473

UNCLASSIFIED

Security Classification

14. KEY WORDS	LINK A		LINK B		LINK C	
	ROLE	WT	ROLE	WT	ROLE	WT
Pressure Transducer **Strain Gage Configuration** **Flat Diaphragm** **Convoluted Diaphragm** **Thermal Compensation** **Gage Factors**						

INSTRUCTIONS

1. ORIGINATING ACTIVITY: Enter the name and address of the contractor, subcontractor, grantee, Department of Defense activity or other organization *(corporate author)* issuing the report.

2*a*. REPORT SECURITY CLASSIFICATION: Enter the overall security classification of the report. Indicate whether "Restricted Data" is included. Marking is to be in accordance with appropriate security regulations.

2*b*. GROUP: Automatic downgrading is specified in DoD Directive 5200.10 and Armed Forces Industrial Manual. Enter the group number. Also, when applicable, show that optional markings have been used for Group 3 and Group 4 as authorized.

3. REPORT TITLE: Enter the complete report title in all capital letters. Titles in all cases should be unclassified. If a meaningful title cannot be selected without classification, show title classification in all capitals in parenthesis immediately following the title.

4. DESCRIPTIVE NOTES: If appropriate, enter the type of report, e.g., interim, progress, summary, annual, or final. Give the inclusive dates when a specific reporting period is covered.

5. AUTHOR(S): Enter the name(s) of author(s) as shown on or in the report. Enter last name, first name, middle initial. If military, show rank and branch of service. The name of the principal author is an absolute minimum requirement.

6. REPORT DATE: Enter the date of the report as day, month, year; or month, year. If more than one date appears on the report, use date of publication.

7*a*. TOTAL NUMBER OF PAGES: The total page count should follow normal pagination procedures, i.e., enter the number of pages containing information.

7*b*. NUMBER OF REFERENCES: Enter the total number of references cited in the report.

8*a*. CONTRACT OR GRANT NUMBER: If appropriate, enter the applicable number of the contract or grant under which the report was written.

8*b*, 8*c*, & 8*d*. PROJECT NUMBER: Enter the appropriate military department identification, such as project number, subproject number, system numbers, task number, etc.

9*a*. ORIGINATOR'S REPORT NUMBER(S): Enter the official report number by which the document will be identified and controlled by the originating activity. This number must be unique to this report.

9*b*. OTHER REPORT NUMBER(S): If the report has been assigned any other report numbers *(either by the originator or by the sponsor)*, also enter this number(s).

10. AVAILABILITY/LIMITATION NOTICES: Enter any limitations on further dissemination of the report, other than those imposed by security classification, using standard statements such as:

(1) "Qualified requesters may obtain copies of this report from DDC."

(2) "Foreign announcement and dissemination of this report by DDC is not authorized."

(3) "U. S. Government agencies may obtain copies of this report directly from DDC. Other qualified DDC users shall request through _____."

(4) "U. S. military agencies may obtain copies of this report directly from DDC. Other qualified users shall request through _____."

(5) "All distribution of this report is controlled. Qualified DDC users shall request through _____."

If the report has been furnished to the Office of Technical Services, Department of Commerce, for sale to the public, indicate this fact and enter the price, if known.

11. SUPPLEMENTARY NOTES: Use for additional explanatory notes.

12. SPONSORING MILITARY ACTIVITY: Enter the name of the departmental project office or laboratory sponsoring *(paying for)* the research and development. Include address.

13. ABSTRACT: Enter an abstract giving a brief and factual summary of the document indicative of the report, even though it may also appear elsewhere in the body of the technical report. If additional space is required, a continuation sheet shall be attached.

It is highly desirable that the abstract of classified reports be unclassified. Each paragraph of the abstract shall end with an indication of the military security classification of the information in the paragraph, represented as *(TS)*, *(S)*, *(C)*, or *(U)*.

There is no limitation on the length of the abstract. However, the suggested length is from 150 to 225 words.

14. KEY WORDS: Key words are technically meaningful terms or short phrases that characterize a report and may be used as index entries for cataloging the report. Key words must be selected so that no security classification is required. Identifiers, such as equipment model designation, trade name, military project code name, geographic location, may be used as key words but will be followed by an indication of technical context. The assignment of links, rules, and weights is optional.